(12) INTERNATIONAL APPLICATION PUBLISHED UNDER THE PATENT COOPERATION TREATY (PCT)

(19) World Intellectual Property Organization
International Bureau

(43) International Publication Date
03 March 2022 (03.03.2022)

WIPO | PCT

(10) International Publication Number
WO 2022/047294 A1

(51) International Patent Classification:
A61K 31/437 (2006.01) *C07H 21/04* (2006.01)
A61K 31/713 (2006.01) *C12N 15/113* (2010.01)
A61P 35/00 (2006.01)

(21) International Application Number:
PCT/US2021/048208

(22) International Filing Date:
30 August 2021 (30.08.2021)

(25) Filing Language: English

(26) Publication Language: English

(30) Priority Data:
63/071,457 28 August 2020 (28.08.2020) US

(71) Applicant: **THE REGENTS OF THE UNIVERSITY OF CALIFORNIA** [US/US]; 1111 Franklin Street, 5th Floor, Oakland, California 94607 (US).

(72) Inventors: **YEO, Eugene**; c/o UC San Diego, 9500 Gilman Drive, Mail Code 0910, La Jolla, California 92093 (US). **EINSTEIN, Jaclyn**; c/o UC San Diego, 9500 Gilman Drive, Mail Code 0910, La Jolla, California 92093 (US).

(74) Agent: **YOON, Sohee Kim** et al.; Fish & Richardson P.C., PO Box 1022, Minneapolis, Minnesota 55440 (US).

(81) Designated States *(unless otherwise indicated, for every kind of national protection available)*: AE, AG, AL, AM, AO, AT, AU, AZ, BA, BB, BG, BH, BN, BR, BW, BY, BZ, CA, CH, CL, CN, CO, CR, CU, CZ, DE, DJ, DK, DM, DO, DZ, EC, EE, EG, ES, FI, GB, GD, GE, GH, GM, GT, HN, HR, HU, ID, IL, IN, IR, IS, IT, JO, JP, KE, KG, KH, KN, KP, KR, KW, KZ, LA, LC, LK, LR, LS, LU, LY, MA, MD, ME, MG, MK, MN, MW, MX, MY, MZ, NA, NG, NI, NO, NZ, OM, PA, PE, PG, PH, PL, PT, QA, RO, RS, RU, RW, SA, SC, SD, SE, SG, SK, SL, ST, SV, SY, TH, TJ, TM, TN, TR, TT, TZ, UA, UG, US, UZ, VC, VN, WS, ZA, ZM, ZW.

(84) Designated States *(unless otherwise indicated, for every kind of regional protection available)*: ARIPO (BW, GH, GM, KE, LR, LS, MW, MZ, NA, RW, SD, SL, ST, SZ, TZ, UG, ZM, ZW), Eurasian (AM, AZ, BY, KG, KZ, RU, TJ, TM), European (AL, AT, BE, BG, CH, CY, CZ, DE, DK, EE, ES, FI, FR, GB, GR, HR, HU, IE, IS, IT, LT, LU, LV, MC, MK, MT, NL, NO, PL, PT, RO, RS, SE, SI, SK, SM, TR), OAPI (BF, BJ, CF, CG, CI, CM, GA, GN, GQ, GW, KM, ML, MR, NE, SN, TD, TG).

Declarations under Rule 4.17:
— *as to applicant's entitlement to apply for and be granted a patent (Rule 4.17(ii))*

(54) **Title:** METHODS FOR MYC-DEPENDENT CANCER THERAPY

(57) **Abstract:** Methods for Myc-dependent cancer therapy are described, wherein the methods include administering an shRNA containing lentiviral vector, wherein the shRNA is directed to an identified RNA-binding protein. The identified RNA-binding protein can, in some cases, be YTH N-6 Methyladenosine RNA Binding Protein 2 (YTHDF2).

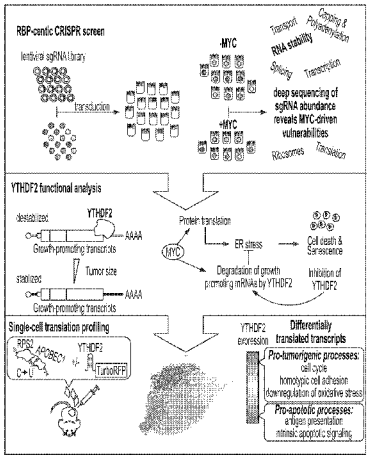


FIG. 9

WO 2022/047294 A1

[Continued on next page]

Published:

— *with international search report (Art. 21(3))*

— *before the expiration of the time limit for amending the claims and to be republished in the event of receipt of amendments (Rule 48.2(h))*

METHODS FOR MYC-DEPENDENT CANCER THERAPY

TECHNICAL FIELD

The present disclosure relates to methods for Myc-dependent cancer therapy. More particularly, the present disclosure relates to methods of inhibiting the interaction between a RNA binding protein and a RNA.

BACKGROUND

Changes in cellular growth rate and identity that occur during cancer progression are driven by specific gene expression signatures programmed by the activity of DNA-binding transcription factors (TFs) and RNA-binding proteins (RBPs). To support high oncogenic growth rates, cancer cells generally require increased levels of transcription and global pre-RNA synthesis controlled by TFs, consequently increasing the cell's dependence on post-transcriptional processing by RBPs. Although TF mutations have been studied for decades, RBPs have been overlooked as drivers of disease and as therapeutically relevant targets. RBPs determine the fate of transcribed RNAs by regulating their splicing, polyadenylation, translation, subcellular localization, and turnover. Somatic mutations, as well as epigenetic and post-translational modifications, can cause aberrant RBP expression in cancer cells, which can promote cell division, cell survival, metastasis, angiogenesis, and host immune evasion. However, RBPs remain largely unexplored as drug targets because their systematic evaluation has been limited by the lack of sensitive and efficient assays for phenotypic interrogation of individual RBPs.

C-MYC (MYC) was among one of the earliest described human oncogenes identified and is now recognized as the primary driver in oncogenic transformation and maintenance of cancer gene expression programs in a broad spectrum of cancer types where cells become "addicted" and dependent on *MYC* for survival. *MYC* transcript stability is coordinately regulated by RNA-binding proteins (RBPs) that both positively and negatively affect its half-life. Several RBPs interacting with m^6A-modified RNA become upregulated in cancer, and are required for cellular growth, survival, and invasion of cancer cells. Thus, Myc regulates cellular function and survival in part by modulating RNA metabolism and is itself controlled posttranscriptionally by RBPs.

There have been conflicting findings regarding the function of the YTH N-6 Methyladenosine RNA binding protein 2 (YTHDF2) protein in cancer. YTHDF2 selectively binds m^6A modified sites on RNA and localizes target transcripts to mRNA decay sites for

degradation by the CCR4-NOT deadenylase complex. For example, loss of YTHDF2 sensitizes acute myeloid leukemia (AML) cells to TNF-induced apoptosis, while overexpression of YTHDF2 in hepatocellular carcinoma (HCC) represses cell proliferation and growth by destabilizing EGFR mRNA. Moreover, the direct YTHDF2 target RNAs have yet to be defined in the mammary epithelial or in human breast cancer.

Serine protease 23 (PRSS23) has been shown to signal through the eIF2 pathway as well as the Notch-TGF-β-Snail pathway by initiating endothelial to mesenchymal transition (EndoMT), however, it is unknown how the stability of *PRSS23* mRNA is regulated. *PRSS23* is not normally expressed in adult breast tissue, and its known functions include tissue remodeling in the developing fetus and in adult ovaries. PRSS23 has not been studied in the context of Myc-dependent cancers as described herein.

SUMMARY

Provided herein are methods of Myc-dependent cancer therapy. More particularly, provided herein are methods of inhibiting the interaction between a RNA binding protein and a RNA.

Provided herein are methods of treating a Myc-dependent cancer in a subject in need thereof, the method comprising administering a therapeutically effective amount of a nucleic acid targeting YTH N-6 Methyladenosine RNA Binding Protein 2 (YTHDF2), thereby treating a Myc-dependent cancer in a subject in need thereof.

Also provided herein are methods of treating a Myc-dependent cancer in a subject in need thereof, the method comprising: (a) determining that the subject has a Myc-dependent cancer; and (b) administering to the subject a therapeutically effective amount of a nucleic acid targeting YTH N-6 Methyladenosine RNA Binding Protein 2 (YTHDF2), wherein administering the agent treats a Myc-dependent cancer in a subject in need thereof.

Also provided herein are in vitro methods of inducing apoptosis in a Myc-dependent cancer cell, the method comprising administering a therapeutically effective amount of a nucleic acid targeting YTH N-6 Methyladenosine RNA Binding Protein 2 (YTHDF2), thereby inducing apoptosis in a Myc-dependent cancer cell.

Also provided herein are methods of weakening triple negative breast cancer cells, the method comprising administering to the triple negative breast cancer cells a therapeutically effective amount of a nucleic acid targeting YTH N-6 Methyladenosine RNA Binding Protein 2 (YTHDF2), thereby weakening triple negative breast cancer cells.

In some embodiments, the nucleic acid comprises RNA, DNA, or combinations thereof. In some embodiments, the RNA comprises shRNA, miRNA, siRNA, or combinations thereof. In some embodiments, the RNA comprises shRNA. In some embodiments, the shRNA further comprises a lentiviral vector. In some embodiments, the lentiviral vector comprises The RNAi Consortium (TRC) lentiviral shRNA vector YTHDF2. In some embodiments, the shRNA further comprises an adenoviral vector (AAV).

In some embodiments, the Myc-dependent cancer comprises ovarian cancer, breast cancer, colorectal cancer, pancreatic cancer, gastric cancer, uterine cancer, leukemia, or combinations thereof. In some embodiments, the Myc-dependent cancer cell is a Myc-dependent breast cancer cell.

In some embodiments, the administration of a nucleic acid targeting N-6 Methyladenosine RNA Binding Protein 2 (YTHDF2) induces unfolded protein accumulation in a Myc-dependent cancer cell. In some embodiments, the administration of a nucleic acid targeting N-6 Methyladenosine RNA Binding Protein 2 (YTHDF2) induces apoptosis in a Myc-dependent cancer cell.

DESCRIPTION OF DRAWINGS

FIGs. 1A-1J show that RBP CRISPR screen identifies mRNA decay as a vulnerability in MYC-driven cancer. **FIG. 1A** is an exemplary schematic describing the generation and implementation of the RBP-targeted CRISPR screen in MYC-ER HMECs. **FIG. 1B** shows cumulative distribution of normalized read counts for sgRNAs in each sample. Each condition is representative of two independent replicates. Two-sided Kolmogorov-Smirnov tests compared with day 0. **FIG. 1C** shows comparison of β score replicates on day 16. Inset highlights synthetic lethal candidate RBPs, and genes enriched for ‘‘negative regulation of macromolecule

metabolic process’’ are labeled. **FIG. 1D** is an exemplary schematic describing the function of RBP candidates identified in **FIG. 1C**. RBPs in bold are significantly upregulated in basal-like TNBC tumors compared with ER/PR/HER2-positive tumors from TCGA data portal. **FIG. 1E** shows a boxplot comparing mRNA expression levels for MYC and YTHDF2 between TNBC and ER/PR/HER2-positive tumors from TCGA data portal. **FIG. 1F** shows a western blot confirming shRNA-mediated knockdown in MYC-ER HMECs. **FIG. 1G** shows quantification of Annexin V staining in MYC-ER HMECs with indicated knockdowns with and without 24 h of MYC induction. **FIG. 1H** shows quantification of propidium iodide (PI)

staining in MYC-ER HMECs with indicated knockdowns with and without 24 h of MYC induction. **FIG. 1I** shows quantification of cell cycle phase using PI in MYC-ER HMECs with indicated knockdowns with and without 3 days of MYC induction. **FIG. 1J** shows cell proliferation of shYTHDF2 cells compared with non-targeting control (NTC) over time in TNBC, HR+, and HER2+ breast cancer cell lines.

FIGs. 2A-2I show that depletion of YTHDF2 in TNBC cells suppresses tumor growth in vivo. **FIG. 2A** shows an exemplary schematic of pooled shRNA screen conducted in MDA-MB-231-LM2 cells in vitro and in vivo. **FIGs. 2B–2D** show dot plots quantifying shRNA normalized abundance following doxycycline (DOX)-induced knockdown of MDA-MB-231-LM2 cells (**FIG. 2B**) in vitro (n = 4 independent replicates) and (**FIG. 2C** and **FIG. 2D**) in vivo. Dots represent individual tumor samples. Bars are median ± quartile. T0 is the tumor composition when DOX was introduced. _DOX, n = 16 mice; +DOX, n = 10 mice. **FIG. 2E** shows average tumor volume over time of DOX-induced, YTHDF2-depleted xenografted mice compared with vehicle controls. **FIG. 2F** shows images of mice 35 days following DOX induction compared with vehicle controls. **FIG. 2G** shows tumor volumes 35 days following DOX induction compared with vehicle controls. _DOX, n = 9 mice; +DOX, n = 6 mice. **FIG. 2H** shows qRT-PCR analysis relative to Gapdh of mRNA extracted from final tumors, 35 days following DOX induction. **FIG. 2I** shows immunohistochemical staining of DOX-treated and vehicle control tumor sections, 35 days following DOX induction.

FIGs. 3A-3F show eCLIP and m^{6}A-seq identify MAPK/ERK pathway transcripts that are regulated by YTHDF2. **FIG. 3A** shows metagene profiles of filtered and unfiltered eCLIP and m^{6}A-seq peak enrichment. **FIG. 3B** shows motif analysis of unfiltered eCLIP (top) and m^{6}A-seq (bottom) data. Representative of two independent replicates. **FIG. 3C** shows Venn diagram overlaps of high-confidence m^{6}A-seq peak and gene enrichment. **FIG. 3D** shows four-way Venn diagram of overlapping, high-confidence YTHDF2 target genes among TNBC, HR+, and HER2+ breast cancer cell lines. Genes overlapping in TNBC cell lines are outlined. **FIG. 3E** shows a hierarchical cluster map illustrating expression levels of overlapping YTHDF2 target genes outlined in **FIG. 3D**. Gene clusters are depicted in the dendrogram. **FIG. 3F** shows Gene Ontology (GO) enrichment of genes in dendrogram clusters from **FIG. 3E**.

FIGs. 4A-4H show depletion of YTHDF2 triggers activation of EMT. **FIG. 4A** shows cumulative distribution of the fold change in mRNA expression of shYTHDF2 cells over non-targeting control (NTC) in MYC-induced HMECs. Two-sided Kolmogorov-Smirnov test

compared with non-targets. n = 4 replicates (2 hairpins × 2 biological replicates). **FIG. 4B** shows a Volcano plot describing the upregulated and downregulated genes in shYTHDF2 cells compared with NTC in MYC-induced HMECs. **FIG. 4C** shows Gene Ontology (GO) enrichment of differentially expressed genes in shYTHDF2 cells compared with NTC in MYC-induced HMECs. **FIG. 4D** shows immunofluorescent staining in TNBC cell lines. Arrowheads indicate cell projections. **FIG. 4E** is an exemplary schematic displaying upstream signaling pathways that induce ERK1/2 signaling and EMT in breast cancer. Overlapping YTHDF2 targets in TNBC cell lines are listed. **FIG. 4F** shows western blot analysis of cell lysates from NTC and shYTHDF2 TNBC, HR+, and HER2+ breast cancer cell lines of EMT transcription factor protein expression. **FIG. 4G** shows western blot analysis of cell lysates from NTC and shYTHDF2 TNBC, HR+, and HER2+ breast cancer cell lines of ERK1/2 pathway activation and downstream effectors. **FIG. 4H** shows qRT-PCR analysis relative to GAPDH of mRNA extracted from shYTHDF2 cells compared with NTC in TNBC, HR+, and HER2+ breast cancer cell lines.

FIGs. 5A-5I show that YTHDF2-depleted TNBC cells initiate apoptosis from intrinsic mitochondrial stress. **FIG. 5A** shows and exemplary schematic describing the pathways that contribute to extrinsic versus intrinsic apoptosis. **FIG. 5B** shows western blot analysis of cell lysates from non-targeting control (NTC) and shYTHDF2 TNBC, HR+, and HER2+ breast cancer cell lines assessing activation of the terminal unfolded protein response pathway. **FIG. 5C** shows Genome Browser tracks (hg19) depicting YTHDF2 eCLIP peaks over size-matched (SM) input and m^6A methylation peaks over input on the PRSS23 transcript. **FIG. 5D** shows boxplot displaying mRNA expression levels for MYC and PRSS23 in TNBC and ER/PR/HER2-positive tumors from TCGA data portal. **FIG. 5E** shows cell proliferation of shYTHDF2 and YTHDF2/PRSS23 co-depleted TNBC cells. **FIG. 5F** shows western blot analysis of cell lysates from shYTHDF2 and YTHDF2/PRSS23 co-depleted TNBC cells assessing protein expression of UPR pathway genes and translation initiation factors. **FIG. 5G** shows cumulative distribution of the fold change in mRNA expression of shYTHDF2 cells over NTC in MYC-induced HMECs. Describes direct TCF12 targets (ENCSR000BUN) or non-targets. **FIG. 5H** shows Venn diagram describing the overlap of TCF12 targets determined in **FIG. 5G** with high-confidence YTHDF2 target genes and differentially upregulated genes in shYTHDF2 MYC-induced HMECs. **FIG. 5I** shows quantification of reactive oxygen species (ROS) in shYTHDF2 and YTHDF2/PRSS23 co-depleted MDA-MB-231-LM2 cells compared with NTC.

FIGs. 6A-6K show analysis of single cells within tumors reveals increased translation rates in YTHDF2-depleted, TurboRFP-tagged cells. **FIG. 6A** is an exemplary schematic describing experimental workflow for generating cell lines, engrafting mice and dissociating tumors followed by single cell RNA-seq (scRNA) to profile the translatome within tumors. **FIG. 6B** shows uniform manifold approximation and projection (UMAP) analysis of mRNA expression of merged cells from wild-type (WT) control-STAMP cells, WT RPS2-STAMP cells, shYTHDF2 control-STAMP cells, and shYTHDF2 RPS2-STAMP cells. Experiments performed in MDA-MB-231-LM2 cells. **FIG. 6C** shows UMAP analysis of mRNA expression from merged cells from all samples. Outline indicates the cluster of highest TurboRFP expressing cells. **FIG. 6D** shows UMAP analysis of mRNA expression from merged cells from all samples colored by expression score of differentially upregulated genes from in vitro bulk RNAseq in shYTHDF2 MYC-induced HMECs (**FIG. 4B**; upregulated). Outline indicates the cluster of highest TurboRFP-expressing cells. **FIG. 6E** shows UMAP analysis of mRNA expression from merged cells. Outline indicates the cluster of highest TurboRFP expressing cells. **FIG. 6F** shows a bar chart describing the fraction of each mRNA expression Louvain cluster in TurboRFP low-expressing (n = 21,464) or high-expressing (n = 3,992) populations. TurboRFP high fraction defined as cells with TurboRFP Z score > 0. **FIG. 6G** shows clustered heatmaps of enriched Gene Ontology (GO) terms extracted from differentially expressed genes belonging to each mRNA expression Louvain cluster ($p < 0.05$). **FIG. 6H** shows UMAP analysis of unfiltered EPKM of merged cells indicated by sample. **FIG. 6I** shows UMAP analysis of unfiltered EPKM of merged cells indicated by average EPKM per cell. **FIG. 6J** shows UMAP analysis of unfiltered EPKM of merged cells indicated by EPKM Louvain clustering. Cells filtered on the basis of assignment to control- or RPS2-STAMP cluster. Bar chart describes the fraction of each cluster contained in each sample. **FIG. 6K** shows distribution of control-STAMP filtered, average EPKM per cell for TurboRFP low- and high-expressing populations.

FIGs. 7A-7F show that scRibo-STAMP identifies unique changes in the translatome of single cells clustering with TurboRFP-expressing populations. **FIG. 7A** shows uniform manifold approximation and projection (UMAP) analysis of control-STAMP filtered EPKM of merged cells from RPS2-STAMP conditions indicated by mRNA expression Louvain clustering. Outline indicates the cluster of highest TurboRFP-expressing cells. Bar chart describes the fraction of each mRNA expression Louvain cluster in each EPKM Louvain cluster. **FIG. 7B** shows UMAP analysis of control-STAMP filtered EPKM of merged cells

from RPS2-STAMP samples indicated by EPKM Louvain clustering. Outline indicates the cluster of highest TurboRFP-expressing cells. Bar chart describes the fraction of each EPKM Louvain cluster contained in TurboRFP high-expressing (n = 1,696) and low-expressing (n = 6,389) populations. **FIG. 7C** shows clustered heatmaps of enriched Gene Ontology (GO) terms extracted from differentially edited genes from each EPKM Louvain cluster ($p < 0.05$). **FIG. 7D** shows Venn diagram overlaps of differentially edited genes between EPKM Louvain clusters A and C (top). Violin plots summarizing the normalized EPKM of differentially edited genes in EPKM Louvain cluster A (CST3), EPKM Louvain cluster C (CFL1) or both (RPL24). Cluster A, n = 3,656; cluster C, n = 1,823. **FIG. 7E** shows heatmap of normalized EPKM signatures for merged RPS2-STAMP cells for the top seven differentially edited genes per EPKM Louvain cluster. **FIG. 7F** shows boxplot comparing protein expression levels for CST3, RPL24, and CFL1 between TNBC and ER/PR/HER2-positive tumors downloaded from TCGA's Cancer Proteome Study of Breast Tissue.

FIGs. 8A-8B show that exemplary expression of PRSS23 in Myc-dependent cancer cells is lethal. **FIG. 8A** is an exemplary schematic depicting function of YTHDF2 in control cells. **FIG. 8B** is an exemplary schematic showing mechanism of programmed cell death with loss of YTHDF2 in Myc-dependent breast cancer cells.

FIG. 9 shows an exemplary schematic of a workflow of screening RBPs for therapeutic targets. RNA-binding proteins (RBPs) are aberrantly expressed in cancer, but they remain largely unexplored as drug targets. Using RBP-focused CRISPRCas9 screening, an essential and selective role for YTHDF2 is uncovered in MYC-driven breast cancer, highlighting the utility of discovering RBPs as safe and effective therapeutic targets.

DETAILED DESCRIPTION

Detailed herein are methods for Myc-dependent cancer therapy and methods of inhibiting an interaction between an RNA binding protein and an RNA. In some embodiments, a binding interaction between YTH N-6 Methyladenosine RNA Binding Protein 2 (YTHDF2) protein and Serine Protease 23 (PRSS23) transcript is present. For example, the YTHDF2 binds to m^6A modified sites on the 3' untranslated region (UTR) of Prss23. In some embodiments, abolishing the YTHDF2-PRSS23 interaction triggers apoptosis in Myc-dependent breast cancer cells. In some embodiments, the lethality of YTHDF2 knockout was identified by RBP CRISPR/Cas9 screening in isogenic Myc-inducible human mammary epithelial cells and the binding interaction with Prss23 was

identified by overlapping YTHDF2 eCLIP-seq, m^6A-seq, and RNA-seq datasets in several human Myc-dependent breast cancer cell lines.

In some embodiments, the regulation of Prss23 mRNA stability is through reversible m^6A RNA methylation. In some embodiments, Myc-dependent cancer cells maintain low to absent levels of PRSS23 transcript and protein through regulation by YTHDF2. In some embodiments, depletion of YTHDF2 increases translation of PRSS23 and triggers apoptosis in Myc-dependent cells. In some embodiments, PRSS23 transcript is lowly expressed in most adult tissues. In some embodiments, interruption of the binding interaction between YTHDF2 and Prss23 by depletion of YTHDF2 leads to upregulation of PRSS23 translation. In some embodiments, PRSS23 expression induces EMT-like phenotypes including, but not limited to upregulation of SNAIL expression, branching morphogenesis, cap-dependent translation and subsequent Myc expression. In some embodiments, Prss23 signals through the EIF2 pathway by upregulating translation initiation factors and effectively downregulating the PERK/eIF2α arm of the unfolded protein response (UPR). In some embodiments, unfolded proteins accumulate in the endoplasmic reticulum due to toxic levels of translation since amplified Myc expression routinely causes higher levels of transcription and translation. In some embodiments, ER-stress induced apoptosis is activated via the IRE1α/JNK arm of the UPR. In some embodiments, this ER-stress induced apoptosis is activated in Myc-dependent cells. In some embodiments, the YTHDF2 depletion leaves Myc-independent cells unaffected.

Various non-limiting aspects of these methods are described herein, and can be used in any combination without limitation. Additional aspects of various components of methods for treating a Myc-dependent cancer in a patient, or inhibiting an interaction between a RNA binding protein and a RNA are known in the art.

It must be noted that, as used in the specification and the appended claims, the singular forms “a,” “an” and “the” include plural referents unless the context clearly dictates otherwise.

As used herein, the term “administration” can refer to the administration of a composition to a subject or system to achieve delivery of the composition. Those of ordinary skill in the art will be aware of a variety of routes that may, in appropriate circumstances, be utilized for administration to a subject, for example a human. For example, in some embodiments, administration may be ocular, oral, parenteral, or topical. In some

embodiments, administration may be bronchial (e.g., by bronchial instillation), buccal, dermal (which may be or comprise, for example, one or more of topical to the dermis, intradermal, interdermal, or transdermal), enteral, intra-arterial, intradermal, intragastric, intramedullary, intramuscular, intranasal, intraperitoneal, intrathecal, intravenous, intraventricular, within a specific organ (e.g. intrahepatic), mucosal, nasal, oral, rectal, subcutaneous, sublingual, topical, tracheal (e.g., by intratracheal instillation), vaginal, or vitreal. In some embodiments, administration may involve only a single dose. In some embodiments, administration may involve application of a fixed number of doses. In some embodiments, administration may involve dosing that is intermittent (e.g., a plurality of doses separated in time) and/or periodic (e.g., individual doses separated by a common period of time) dosing. In some embodiments, administration may involve continuous dosing (e.g., perfusion) for at least a selected period of time.

As used herein, the term "agent" in general refers to any agent that elicits a desired pharmacological effect when administered to an organism. In some embodiments, an agent is considered to be a therapeutic agent if it demonstrates a statistically significant effect across an appropriate population. In some embodiments, the appropriate population may be a population of model organisms. In some embodiments, an appropriate population may be defined by various criteria, such as a certain age group, gender, genetic background, preexisting clinical conditions, etc. In some embodiments, an agent is a substance that can be used to alleviate, ameliorate, relieve, inhibit, prevent, delay onset of, reduce severity of, and/or reduce incidence of one or more symptoms or features of a disease, disorder, and/or condition. In some embodiments, an agent has been or is required to be approved by a government agency before it can be marketed for administration to humans. In some embodiments, an agent can be an agent for which a medical prescription is required for administration to humans. In some embodiments, an agent does not require a medical prescription. In some embodiments, one or more agents can be used to elicit a desired pharmacological effect. In some embodiments, an agent includes a small molecule. In some embodiments, an agent includes a nucleic acid. In some embodiments, an agent comprises CRISPR/Cas9 components. In some embodiments, an agent comprises a single-guide RNA (sgRNA), wherein the sgRNA is targeted to an individual gene. In some embodiments, an agent comprises a short hairpin RNA (shRNA), wherein the shRNA is targeted to an individual gene.

As used herein, the terms "cancer" or "tumor" refer to cells that exhibit relatively abnormal, uncontrolled, and/or autonomous growth, so that they exhibit an aberrant growth

phenotype characterized by a significant loss of control of cell proliferation. In some embodiments, a tumor may be or comprise cells that are precancerous (e.g., benign), malignant, pre-metastatic, metastatic, and/or non-metastatic. In some embodiments, a relevant cancer may be characterized by a solid tumor. In some embodiments, a relevant cancer may be characterized by a hematologic tumor. In general, examples of different types of cancers known in the art include, for example, hematopoietic cancers including leukemias, lymphomas (Hodgkin's and non-Hodgkin's), myelomas and myeloproliferative disorders; sarcomas, melanomas, adenomas, carcinomas of solid tissue, squamous cell carcinomas of the mouth, throat, larynx, and lung, liver cancer, genitourinary cancers such as prostate, cervical, bladder, uterine, and endometrial cancer and renal cell carcinomas, bone cancer, pancreatic cancer, skin cancer, cutaneous or intraocular melanoma, cancer of the endocrine system, cancer of the thyroid gland, cancer of the parathyroid gland, head and neck cancers, breast cancer, gastro-intestinal cancers and nervous system cancers, benign lesions such as papillomas, and the like. In some embodiments, a cancer is a breast cancer. In some embodiments, a cancer is a Myc-dependent cancer.

As used herein, the term "effective amount" or "therapeutically effective amount" means an amount that is sufficient, when administered to a population suffering from or susceptible to a disease, disorder, and/or condition in accordance with a therapeutic dosing regimen, to treat the disease, disorder, and/or condition. In some embodiments, a therapeutically effective amount is one that reduces the incidence and/or severity of, stabilizes one or more characteristics of, and/or delays onset of, one or more symptoms of the disease, disorder, and/or condition. Those of ordinary skill in the art will appreciate that the term "therapeutically effective amount" does not in fact require successful treatment be achieved in a particular individual. Rather, a therapeutically effective amount may be that amount that provides a particular desired pharmacological response in a significant number of subjects when administered to patients in need of such treatment. For example, in some embodiments, term "therapeutically effective amount", refers to an amount which, when administered to an individual in need thereof in the context of the inventive therapy, will block, stabilize, attenuate, or reverse a cancer-supportive process occurring in said individual, or will enhance or increase a cancer-suppressive process in said individual. In the context of cancer treatment, a "therapeutically effective amount" is an amount which, when administered to an individual diagnosed with a cancer, will prevent, stabilize, inhibit, or reduce the further development of cancer in the individual. A particularly preferred "therapeutically effective amount" of a composition described herein reverses (in a

therapeutic treatment) the development of a malignancy such as a pancreatic carcinoma or helps achieve or prolong remission of a malignancy. A therapeutically effective amount administered to an individual to treat a cancer in that individual may be the same or different from a therapeutically effective amount administered to promote remission or inhibit metastasis. As with most cancer therapies, the therapeutic methods described herein are not to be interpreted as, restricted to, or otherwise limited to a "cure" for cancer; rather the methods of treatment are directed to the use of the described compositions to "treat" a cancer, i.e., to effect a desirable or beneficial change in the health of an individual who has cancer. Such benefits are recognized by skilled healthcare providers in the field of oncology and include, but are not limited to, a stabilization of patient condition, a decrease in tumor size (tumor regression), an improvement in vital functions (e.g., improved function of cancerous tissues or organs), a decrease or inhibition of further metastasis, a decrease in opportunistic infections, an increased survivability, a decrease in pain, improved motor function, improved cognitive function, improved feeling of energy (vitality, decreased malaise), improved feeling of well-being, restoration of normal appetite, restoration of healthy weight gain, and combinations thereof. In addition, regression of a particular tumor in an individual (e.g., as the result of treatments described herein) may also be assessed by taking samples of cancer cells from the site of a tumor such as a pancreatic adenocarcinoma (e.g., over the course of treatment) and testing the cancer cells for the level of metabolic and signaling markers to monitor the status of the cancer cells to verify at the molecular level the regression of the cancer cells to a less malignant phenotype. For example, tumor regression induced by employing the methods of this invention would be indicated by finding a decrease in any of the pro-angiogenic markers discussed above, an increase in anti-angiogenic markers described herein, the normalization (i.e., alteration toward a state found in normal individuals not suffering from cancer) of metabolic pathways, intercellular signaling pathways, or intracellular signaling pathways that exhibit abnormal activity in individuals diagnosed with cancer. Those of ordinary skill in the art will appreciate that, in some embodiments, a therapeutically effective amount may be formulated and/or administered in a single dose. In some embodiments, a therapeutically effective amount may be formulated and/or administered in a plurality of doses, for example, as part of a dosing regimen.

As used herein, the terms "subject" and "patient" are used interchangeably throughout the specification to describe an organism, typically a mammal, human, or non-human, to whom treatment according to the methods of the present disclosure is provided. Veterinary applications are contemplated by the present disclosure. The terms include, but are not

limited to, mammals, e.g., humans, other primates, pigs, hamsters, rats, mice, cows, horses, cats, dogs, sheep, and goats. In some embodiments, a subject is suffering from a relevant disease, disorder, or condition. In some embodiments, a subject displays one or more symptoms or characteristics of a disease, disorder, or condition. In some embodiments, a subject does not display any symptom or characteristic of a disease, disorder, or condition. In some embodiments, a subject is someone with one or more features characteristic of susceptibility to or risk of a disease, disorder, or condition. In some embodiments, a subject is a patient. In some embodiments, a subject is an individual to whom diagnosis and/or therapy is and/or has been administered.

Myc-dependent cancer

MYC is a transcription factor that can regulate the expression of up to 15% of genes in the genome. In the human genome, c-myc is located on chromosome 8 and is believed to regulate expression of genes through binding on enhancer box sequences (E-boxes). Overexpression of MYC is thought to contribute to the pathogenesis of over 50% of human cancers, and the inhibition of MYC has been shown to reverse tumorigenesis in transgenic mouse models. Therefore, therapeutically targeting MYC would have broad clinical impact across multiple cancer types.

The gene encoding MYC encodes the proto-oncogene, which is a nuclear phosphoprotein that plays a role in cell cycle progression, apoptosis, and cellular transformation. The encoded protein forms a heterodimer with the related transcription factor MAX. This complex binds to the E box DNA consensus sequence and regulates the transcription of specific target genes. Amplification of this gene is frequently observed in numerous human cancers. Translocations involving this gene are associated with Burkitt's lymphoma and multiple myeloma in human patients. C-MYC (MYC) is the primary oncogenic driver of cancer gene expression programs in a broad spectrum of cancer types in which cells become ''addicted'' to and dependent on MYC for survival. The MYC oncogene drives the pathogenesis of many hematopoietic malignancies, including Burkitt's lymphoma (BL), Diffuse large B cell lymphoma (DLBCL), and Acute Lymphoblastic Leukemia (ALL).

In some embodiments, a cancer is a hematologic cancer. In some embodiments, a hematologic cancer includes lymphomas (e.g. Non-Hodgkin lymphomas (NHL)), leukemias, and multiple myelomas. In some embodiments, a cancer is a Myc-dependent cancer. In some embodiments, a Myc-dependent cancer can include lymphoma, leukemia, osteosarcoma, hepatocellular carcinoma, squamous carcinoma, and pancreatic carcinoma. In some

embodiments, a Myc-dependent cancer includes ovarian cancer, breast cancer, colorectal cancer, pancreatic cancer, gastric cancer, uterine cancer, leukemia, or combinations thereof. In some embodiments, the Myc-dependent cancer is breast cancer.

RNA Binding Protein (RBP)

As used herein, "RNA binding protein" can refer to a protein that binds to the double or single stranded RNA in cells and participate in forming ribonucleoprotein complexes. RNA binding proteins (RBPs) play a major role in post-transcriptional control of RNAs (e.g., splicing, polyadenylation, mRNA stabilization, mRNA localization, and translation). The term "RNA binding protein" can refer to a protein that interacts with RNA molecules (e.g., mRNA) from synthesis to decay to affect their metabolism, localization, stability, and translation. In some embodiments, an RBP is a nuclear protein. In some embodiments, RBPs can include, but are not limited to, splicing factors, RNA stability factors, histone stem-loop binding proteins, or ribosomes. For example, a eukaryotic ribosome can include a collection of RBPs that can interact directly with mRNA coding sequences. In some embodiments, an RBP is a cytoplasmic protein.

In some embodiments, an RNA binding protein comprises a ribosomal protein, wherein the ribosomal protein binds to a ribosome and an mRNA during translation. In some embodiments, an RNA binding protein comprises a ribosomal protein, wherein the ribosomal protein binds to a ribosome or an mRNA during translation. In some embodiments, the RNA binding protein comprises at least one of: SLTM, ZGPAT, PPARGC1B, PELP1, DCP2, CSTF3, TRA2B, ZNF638, SRSF9, LUC7L2, PTBP3, SF3B3, VCP, HNRNPA2B1, PTBP1, PCBP2, LSM14A, LSM12, DHX15, DDX27, DDX17, DDX21, IPO5, RPL22L1, RPL35, RPSA, MRPS34, NIFK, THUMPD1, RPUSD3, RRBP1, EEFSEC, UBAP2L, PUS7L, EIF4ENIF1, BICC1, EIF4E2, DARS2, TRDMT1, UPF3B, ZFP36L2, YTHDF2, EDC3, HNRNPR, UPF3A, ELAVL1, RBM27, XRN1, FUS, EXOSC7, PSPC1, CNOT7, CNOT6, CNOT4, CNOT3, AGO2, ENDOU, RBFOX1 (A2BP1), RBFOX2 (RBM9), RBFOX3 (NeuN), SLBP, RBM5, RBM6, PRBP1, ACO1, Adat1, PCBP1, PCBP3, PCBP4, RBM3, RBM4, APOBEC1, BTG1, CNOT2, CPSF5, DDX6, EWSR1, FUBP1, hnRNPA0, hnRNPC1/2, MEX3C, NANOS1, NANOS2, NOP56, PARN, PRR3, RBM14, RBM7, RPS6, SAMD4A, SNRPA, SRSF11, TOB1, TOB2, UTP11L, ZC3H18, ZCCHC11, ZFP36, ZFP36L1, ABT1, AC004381.6, AIMP1, ALDH18A1, ANXA2 , APOBEC3F, ASCC1, ATP5C1, BCCIP, BOLL, BYSL, BZW1, CELF5, CLK1, CLK2, CPSF1, DAZ2, DAZ3, DAZ4, DCN, DDX1, DDX19B, DDX20, DDX39A, DMPK, EEF1A1, EIF3G, ERAL1,

XOSC4, FAM46A, FAM98A, FKBP3, FXR2, G3BP2, GLTSCR2, GSPT2, GTF2F1, GTPBP10, HADHB, HDGF, hnRNPE1, HNRPDL, HSPB1, KIAA1324, LARP1, LARP4, LARP4B, LIN28A, LUC7L, MAK16, MATR3, MBNL2, MEPCE, MRPL39, MTDH, NDUFV3, NUFIP2, NUSAP1, PABPC1, PABPC5, PCBP4, PEG10, PPAN, PPIL4, PRPF3, PRPF31, PRRC2B, PTRH1, PUS7, RBM33, RBM38, RBMX2, RPL10A, RPL14, RPL15, RPLP0, RPS20, RPUSD3, RPUSD4, RTN4, SERBP1, SF3A3, SFRS10, SFRS13A, SFRS2IP, SLC7A9, SMN1, SPATS2L, SRSF5, SRSF8, THOC1, TRA2A, TRIM39, TUFM, UBAP2L, UTP23, XPO5, XRN1, YWHAE, or ZRANB2.

RNA-binding proteins (RBPs) have roles in controlling the fate of RNAs including the modulation of pre-mRNA splicing, RNA modification, translation, stability, and localization. RBPs are a group of proteins that interact with RNA using an array of strategies from well-defined RNA-binding domains to disordered regions that recognize RNA sequence and/or secondary structures. As used herein, "RNA-RBP complex" can refer to a ribonucleoprotein complex comprising an RNA-binding protein (RBP) bound to a double or single stranded RNA in a cell.

In some embodiments, an RNA-binding protein is YTH N-6 Methyladenosine RNA Binding Protein 2 (YTHDF2). In some embodiments, the YTHDF2 binds to m^6A modified sites. In some embodiments the m^6A modified sites are on the 3' UTR of an RNA. In some embodiments, the m^6A modified sites are on a PRSS23 transcript. In some embodiments, the m^6A modified sites are on the 3' UTR of a PRSS23 transcript.

YTHDF2

YTH N6-methyladenosine RNA binding protein 2 (YTHDF2) is an RNA binding protein encoded by the YTHDF2 gene. The YTHDF2 gene encodes a member of the YTH (YT521-B homology) superfamily containing YTH domain. The YTH domain is usually located in the middle of the protein sequence and may function in binding to RNA. In addition to a YTH domain, this protein has a proline-rich region which may be involved in signal transduction, and an Alu-rich domain which is thought to be associated with human longevity. Also, reciprocal translocations between this gene and the Runx1 (AML1) gene on chromosome 21 has been observed in patients with acute myeloid leukemia.

Methylation at the *N*6 position of adenosine (m^6A) is the most abundant RNA modification within protein-coding and long noncoding RNAs in eukaryotes and is a reversible process with important biological functions. YTHDF proteins are the readers of m^6A, the binding of which results in the alteration of the translation efficiency and stability of

m^6A-containing RNAs. It has been shown that disrupting YTHDF2-dependent mRNA degradation triggers apoptosis in triple-negative breast cancer (TNBC) cells and tumors (**FIGs. 8A-8B**). eCLIP (enhanced crosslinking and immunoprecipitation) and m^6A sequencing reveal that YTHDF2 interacts with mRNAs encoding proteins in the MAPK pathway that, when stabilized, induce epithelial-to-mesenchymal transition and increase global translation rates. As used herein, "crosslinking and immunoprecipitation (CLIP)" is a method to identify RNA nucleotides that bind proteins of interest. CLIP typically delivers regions up to hundreds of nucleotides in length that are the approximate binding sites of a given protein. Enhanced crosslinking and immunoprecipitation (eCLIP) is a method to profile RNAs bound by an RNA binding protein of interest.

Also, scRibo-STAMP profiling of translating mRNAs reveals unique alterations in the translatome of single cells within YTHDF2-depleted solid tumors, which selectively contribute to endoplasmic reticulum stress-induced apoptosis in triple-negative breast cancer (TNBC) cells. As used herein, "Surveying targets by APOBEC mediated profiling (STAMP)" is a method of efficiently detecting RBP-RNA interaction, and identifying RBP- and cell type-specific RNA-protein interactions, by using a chimeric protein including an RNA binding protein and RNA editing protein. STAMP is an integrated experimental and computational framework which demonstrates the discovery of RBP-RNA binding sites, including isoform-specific binding sites, at single-cell resolution. In some embodiments, STAMP is performed using with ribosome subunits. As used herein, "ribosome-subunit STAMP" (Ribo-STAMP) refers to a chimeric protein, wherein the chimeric protein includes an RNA binding protein, and a ribosome subunit, wherein the ribosome subunit is fused to the RNA editing protein. In some embodiments, ribosome association and gene expression can be examined in a single-cell, in a homologous cell population, or in a heterologous cell population. As used herein, "scRibo-STAMP" refers to profiling of RBP-RNA interaction in single cells with the Ribo-STAMP method. A critical role for YTHDF2 is in counteracting the global increase of mRNA synthesis in MYC-driven breast cancers.

Nucleic Acid

As used herein, "nucleic acid" is used to include any compound and/or substance that comprise a polymer of nucleotides. In some embodiments, a polymer of nucleotides are referred to as polynucleotides. Exemplary nucleic acids or polynucleotides can include, but are not limited to, ribonucleic acids (RNAs), deoxyribonucleic acids (DNAs), threose nucleic acids (TNAs), glycol nucleic acids (GNAs), peptide nucleic acids (PNAs), locked nucleic

acids (LNAs, including LNA having a β-D-ribo configuration, α-LNA having an α-L-ribo configuration (a diastereomer of LNA), 2′-amino-LNA having a 2′-amino functionalization, and 2′-amino-α-LNA having a 2′-amino functionalization) or hybrids thereof. Naturally-occurring nucleic acids generally have a deoxyribose sugar (e.g., found in deoxyribonucleic acid (DNA)) or a ribose sugar (e.g., found in ribonucleic acid (RNA)).

A nucleic acid can contain nucleotides having any of a variety of analogs of these sugar moieties that are known in the art. A deoxyribonucleic acid (DNA) can have one or more bases selected from the group consisting of adenine (A), thymine (T), cytosine (C), or guanine (G), and a ribonucleic acid (RNA) can have one or more bases selected from the group consisting of uracil (U), adenine (A), cytosine (C), or guanine (G).

In some embodiments, disclosed herein are methods of treating a Myc-dependent cancer in a subject in need thereof, the method comprising administering a therapeutically effective amount of a nucleic acid targeting YTH N-6 Methyladenosine RNA Binding Protein 2 (YTHDF2), thereby treating a Myc-dependent cancer in a subject in need thereof. In some embodiments, the nucleic acid comprises RNA, DNA, or combinations thereof. In some embodiments, the nucleic acid is an RNA. In some embodiments, the RNA comprises shRNA, miRNA, siRNA, or combinations thereof. In some embodiments, the nucleic acid is a shRNA, wherein the shRNA induces knock down of a target RNA. As used herein, “small hairpin RNAs (shRNAs)” refer to sequences of RNA, typically about 80 base pairs in length that include a region of internal hybridization that creates a hairpin structure. ShRNA molecules are processed within the cell to form small interfering RNA (siRNA) which in turn knock down gene expression. In some embodiments, shRNA can be incorporated into plasmid vectors and integrated into genomic DNA for longer-term or stable expression, and thus longer knockdown of a target RNA.

Target RNA

In some embodiments, an RNA can be a target RNA. As used herein, a “target RNA” refers to a RNA or RNA motif that is identified with a disease-related function. In some embodiments, various screening approaches and libraries can be used to identify drug-like small molecules with appropriate pharmacological properties. In some embodiments, a target RNA can be a therapeutically relevant target for a Myc-dependent cancer. In some embodiments, a target RNA can encode a RNA binding protein. In some embodiments, a target RNA is a RBP coding gene encoding the YTH N-6 Methyladenosine RNA Binding Protein 2 (YTHDF2).

Methods of Identifying RBPs Implicated in MYC-driven Breast Cancer

In some embodiments, the present disclosure provides methods of identifying RNA binding proteins (RBPs) implicated in Myc-driven breast cancer. Provided herein are methods of identifying RBPs implicated in a Myc-dependent cancer in a patient in need thereof, the method including administering a therapeutically effective amount of a nucleic acid targeting YTH N-6 Methyladenosine RNA Binding Protein 2 (YTHDF2), thereby treating a Myc-dependent cancer in a subject in need thereof. In some embodiments, the nucleic acid comprises CRISPR/Cas9 components. In some embodiments, the nucleic acid comprises a single guide RNA (sgRNA), wherein the sgRNA is targeted to an individual gene of a cell. In some embodiments, the sgRNA targets a RNA binding protein.

As used herein, the term "CRISPR/Cas9" refers to a technique of sequence specific genetic manipulation relying on the clustered regularly interspaced short palindromic repeats (CRISPR) pathway, which unlike RNA interference regulates gene expression at a transcriptional level. The term "Cas9" refers to a Cas-associated endonuclease and "CRISPR/Cas9" is a system that has been repurposed or engineered to target RNA instead of DNA in living cells, wherein the engineered Cas9 polypeptide-comprising nucleoprotein complex binds to RNA. In some embodiments, CRISPR/Cas9 can be used as a means to target RNA. In some embodiments, nucleoprotein complexes as provided herein comprise a Cas9 protein, a single guide RNA (sgRNA), and optionally an (chemically-modified or synthetic) antisense PAMmer oligonucleotide. The PAMmer is an antisense oligonucleotide that serves to simulate a DNA substrate for recognition by Cas9 via hybridization to the target RNA.

As used herein, the term "gRNA" or "guide RNA" as used herein refers to the guide RNA sequences used to target specific genes for correction employing the CRISPR technique. Techniques of designing gRNAs and donor therapeutic polynucleotides for target specificity are well known in the art. For example, Doench, J., et al. Nature biotechnology 2014; 32(12):1262-7 and Graham, D., et al. Genome Biol. 2015; 16: 260. The term "Single guide RNA" or "sgRNA" is a specific type of gRNA that combines tracrRNA (transactivating RNA), which binds to Cas9 to activate the complex to create the necessary strand breaks, and crRNA (CRISPR RNA), comprising complimentary nucleotides to the tracrRNA, into a single RNA construct. Together, the Cas9 protein and sgRNA components allow recognition of hypothetically any RNA sequence.

In some embodiments, the single guide RNA can recognize a target RNA, for example, by hybridizing to the target RNA. In some embodiments, the single guide RNA comprises a sequence that is complementary to the target RNA. In some embodiments, the sgRNA can include one or more modified nucleotides. In some embodiments, the sgRNA has a length that is about 10 nt (e.g., about 20 nt, about 30 nt, about 40 nt, about 50 nt, about 60 nt, about 70 nt, about 80 nt, about 90 nt, about 100 nt, about 120 nt, about 140 nt, about 160 nt, about 180 nt, about 200 nt, about 300 nt, about 400 nt, about 500 nt, about 600 nt, about 700 nt, about 800 nt, about 900 nt, about 1000 nt, or about 2000 nt).

In some embodiments, a single guide RNA can recognize a variety of RNA targets. For example, a target RNA can be messenger RNA (mRNA), ribosomal RNA (rRNA), signal recognition particle RNA (SRP RNA), transfer RNA (tRNA), small nuclear RNA (snRNA), small nucleolar RNA (snoRNA), antisense RNA (aRNA), long noncoding RNA (lncRNA), microRNA (miRNA), piwi-interacting RNA (piRNA), small interfering RNA (siRNA), short hairpin RNA (shRNA), retrotransposon RNA, viral genome RNA, or viral noncoding RNA. In some embodiments, a target RNA can be an RNA involved in pathogenesis of conditions such as cancers, neurodegeneration, cutaneous conditions, endocrine conditions, intestinal diseases, infectious conditions, neurological conditions, liver diseases, heart disorders, or autoimmune diseases. In some embodiments, a target RNA can be a therapeutic target for conditions such as cancers, neurodegeneration, cutaneous conditions, endocrine conditions, intestinal diseases, infectious conditions, neurological conditions, liver diseases, heart disorders, or autoimmune diseases.

In some embodiments, CRISPR/Cas9 systems are used to screen for RBP dependencies in Myc-dependent breast cancer. In some embodiments, the CRISPR/Cas9 systems include a sgRNA, wherein the sgRNA targets a Myc-dependent cancer-related gene encoding a RBP. In some embodiments, the sgRNA targets a RNA binding protein. In some embodiments, the sgRNA targets YTH N-6 Methyladenosine RNA Binding Protein 2 (YTHDF2) (**FIG. 9**).

In some embodiments, a method of identifying RBPs in Myc-driven breast cancer can include using "enhanced crosslinking and immunoprecipitation (eCLIP)" as a method to profile RNAs bound by an RNA binding protein of interest. In some embodiments, the method can further include using Ribo-STAMP as a method to assess translation by directing C-to-U base editing of ribosome-bound transcripts using the cytidine deaminase enzyme APOBEC1 fused to the C-terminus of the 40S ribosomal protein S2 (RPS2).

Enhanced crosslinking and immunoprecipitation (eCLIP) is a method to profile RNAs bound by an RNA binding protein of interest that showed thousand-fold improved recovery of protein-bound RNA. This technique can be modified and used to profile RNAs bound by specific ribosomal subunit proteins (Ribo-eCLIP). In some embodiments, enhanced crosslinking and immunoprecipitation (eCLIP) recovers protein-coding mRNAs (with a particular enrichment for coding sequence regions), and the normalized Ribo-eCLIP enrichment correlates with translation rate estimates from independent approaches. In some embodiments, Ribo-eCLIP enables mapping translation rate from a variety of cell lines and tissue models.

Surveying targets by APOBEC mediated profiling (STAMP) is a method of efficiently detecting RBP-RNA interaction, and identifying RBP- and cell type-specific RNA-protein interactions, by using a chimeric protein including an RNA binding protein and RNA editing protein. STAMP is an integrated experimental and computational framework which demonstrates the discovery of RBP-RNA binding sites, including isoform-specific binding sites, at single-cell resolution. In some embodiments, STAMP is performed with computational methods that de-multiplex multiple RBPs by clustering cells using only edit signatures, allowing deconvolution of targets for multiplexed RBPs, and the cell-type specific binding of an RBP in a heterogeneous mixtures of cell-types. STAMP allows for reproducible and quantitative identification of RBP-RNA binding sites, including isoform-specific binding sites. Further, STAMP can be used to determine a relative translation rate of an mRNA at single-cell resolution and in a heterogeneous mixture of cell-types. In some embodiments, STAMP can be used to examine translational landscapes at a single cell resolution. In some embodiments, STAMP can be used with specific ribosome subunits, wherein gene expression can be measured simultaneously with detection of ribosome association.

In some embodiments, STAMP can identify cell-type specific RBP binding sites. In some embodiments, STAMP can identify multiple RBP binding sites for different RBPs in a single cell type. In some embodiments, STAMP can identify multiple RBP binding sites for different RBPs in multiple cell types. In some embodiments, STAMP can identify isoform-specific RBP binding sites. In some embodiments, STAMP and long-read sequencing can be used to identify isoform-specific RBP target sites. In some embodiments, STAMP can identify binding sites of full-length RBPs by C-to-U RNA editing. In some embodiments, STAMP can identify binding sites on single-stranded RNA targets. In some embodiments, STAMP provides a method for cell-type specific and multiplexed-RBP target identification in single cells. In some embodiments, STAMP can identify mammalian cell-type specific RBP

binding sites. In some embodiments, STAMP can identify plant cell-type specific RBP binding sites. In some embodiments, STAMP can identify bacterial cell-type specific RBP binding site.

In some embodiments, STAMP is performed using with ribosome subunits. As used herein, "ribosome-subunit STAMP" (Ribo-STAMP) refers to a chimeric protein, wherein the chimeric protein includes an RNA binding protein, and a ribosome subunit, wherein the ribosome subunit is fused to the RNA editing protein. In some embodiments, Ribo-STAMP uses small ribosomal subunits to measure transcriptome-wide ribosome association in single cells. In some embodiments, Ribo-STAMP can be used to simultaneously measure ribosome association and gene expression. In some embodiments, ribosome association and gene expression can be examined in a single-cell, in a homologous cell population, or in a heterologous cell population. In some embodiments, Ribo-STAMP allows mRNA editing while identifying ribosome association with the mRNA, and also distinguishes genes with varying levels of ribosome occupancy. In some embodiments, Ribo-STAMP uses edited and non-edited reads to reflect ribosome-associated and input gene expression values simultaneously. In some embodiments, the simultaneous readouts can be used in complex and heterogeneous cellular or in vivo models to address cell identity or disease states.

Methods of Treating a Myc-dependent cancer

Provided herein are methods of treating a Myc-dependent cancer in a patient in need thereof, the method including administering a therapeutically effective amount of a nucleic acid targeting YTH N-6 Methyladenosine RNA Binding Protein 2 (YTHDF2), thereby treating a Myc-dependent cancer in a subject in need thereof.

Also provided herein are methods of treating a Myc-dependent cancer in a subject in need thereof, the method comprising: (a) determining that the subject has a Myc-dependent cancer; and (b) administering to the subject a therapeutically effective amount of a nucleic acid targeting YTH N-6 Methyladenosine RNA Binding Protein 2 (YTHDF2), wherein administering the agent treats a Myc-dependent cancer in a subject in need thereof.

Also provided herein are in vitro methods of inducing apoptosis in a Myc-dependent cancer cell, the method comprising administering a therapeutically effective amount of a nucleic acid targeting YTH N-6 Methyladenosine RNA Binding Protein 2 (YTHDF2), thereby inducing apoptosis in a Myc-dependent cancer cell.

Also provided herein are methods of weakening triple negative breast cancer cells, the method comprising administering to the triple negative breast cancer cells a therapeutically

effective amount of a nucleic acid targeting YTH N-6 Methyladenosine RNA Binding Protein 2 (YTHDF2), thereby weakening triple negative breast cancer cells.

In some embodiments, administering the nucleic acid can result in a decreased expression of an RNA binding protein. In some embodiments, the decreased expression of the RNA binding protein inhibits the RNA binding protein interaction with an RNA. In some embodiments, the RNA binding protein binds to a modified site on the RNA. In some embodiments, the modified site is an m^6A modified site. In some embodiments, the modified site is located on a 3' untranslated region (UTR) of the RNA. In some embodiments, the inhibition of the interaction between the RNA binding protein and the RNA results in apoptosis in Myc-dependent cancer cells. In some embodiments, the Myc-dependent cancer cell is a Myc-dependent breast cancer cell. In some embodiments, the decreased expression of the RNA binding protein increases expression of the RNA. In some embodiments, the increased expression of the RNA results in an increased number of unfolded proteins.

In some embodiments, the determining step (a) includes performing a physical exam, a lab test, an imaging test, a biopsy, or any combination thereof. In some embodiments, a physical exam can include examining a patient for abnormalities, changes in skin color, or enlargement of an organ. In some embodiments, a lab test can include a urine test, or a blood test. In some embodiments, an imaging test can include a computerized tomography (CT) scan, a bone scan, a magnetic resonance imaging (MRI), a positron emission tomography (PET) scan, an ultrasound, or an x-ray. In some embodiments, a biopsy can include obtaining a sample of cells from a patient and imaging the cells to determine the presence or absence of cancerous cells. In some embodiments, the determining step (a) can include any of the methods disclosed herein and other methods as known in the art.

EXAMPLES

Example 1 - Identification of critical RBPs in MYC-driven breast cancer

To screen for RBP dependencies in cancer, a CRISPR/Cas9 lentiviral library was used containing 10 single-guide RNAs (sgRNAs) for each of 1,078 RBPs, 628 sgRNAs targeting essential genes as positive controls, and 1,058 non-targeting sgRNAs as negative controls. The small library size and specific focus on RBPs provides higher confidence hits and therefore higher reproducibility than whole-genome approaches typically using more shallow coverage of 3 or 4 sgRNAs per gene. High-throughput sequencing confirmed that the plasmid library maintained sgRNA coverage and that aliquots were tightly correlated (less than 0.065% of sgRNAs received undetectable normalized read counts.

MYC-ER HMECs were transduced with the CRISPR library in biological duplicate, selected for transduced cells with puromycin, treated half of the cells with tamoxifen (TAM) to induce MYC activity, and isolated genomic DNA (gDNA) 8 and 16 days after puromycin removal (**FIG. 1A**). The representation of randomly integrated sgRNAs was tightly correlated with their frequencies in the original plasmid library, and replicate libraries were highly correlated. A significant reduction was observed in sgRNA diversity in surviving cells on days 8 and 16 in both MYC-induced and uninduced HMECs, indicating dropout of cells transduced with sgRNAs targeting essential genes (positive controls) compared with cells transduced with non-targeting sgRNAs (negative controls) (**FIG. 1B**).

sgRNAs targeting 57 RBP candidates ($p < 0.05$) were depleted in MYC-induced cell populations compared with uninduced control cells (**FIG. 1C**). Analysis revealed RBPs that have been implicated in gene regulation downstream of MYC, including PTBP1, PCBP2, ELAVL1, and TRA2B and identified ~40 RBPs previously unknown in this context. Enrichment was observed for genes that negatively regulate macromolecule assembly, including several genes that repress exon inclusion (HNRNPA2B1, PTBP1, SRSF9), repress transcription (ZGPAT, SLTM), promote mRNA turnover (YTHDF2, UPF3B, UPF3A, XRN1, DCP2, AGO2), and prevent translation initiation (EIF4ENIF1, EIF4E2) (**FIG. 1C**). This suggests vulnerabilities in MYC-hyperactive cells by RBPs that reduce the stability of mRNAs for translation, or RBPs that reduce protein translation rates.

Next, public data was cross-referenced from The Cancer Genome Atlas (TCGA) pan-cancer clinical data resource and found that 67% of the RBP candidates are highly expressed in typically MYC-amplified basal-like TNBC tumors, compared with luminal A/luminal B, hormone receptor positive (HR+; estrogen receptor [ER] positive, progesterone receptor [PR] positive) or human epidermal growth factor receptor 2 positive (HER2+) breast tumors (**FIG. 1D**). Together, the results indicate that several RBPs controlling various stages of the RNA life cycle are aberrantly expressed in TNBC. As MYC-amplified cells typically contain increased quantities of mRNA, caused in part by 30 untranslated region (UTR) shortening, RBP candidates that regulate RNA stability and turnover were further examined. It was found that the overall survival of patients with TNBC tumors containing above median MYC expression levels was significantly improved when tumors contained below median expression levels of mRNA decay factors AGO2, EXOSC7, FUS, YTHDF2, and ZFP36L2.

Example 2 - Depleting YTHDF2 induces apoptosis of TNBC tumors in vivo

Results show that the m^{6}A reader protein YTHDF2 is significantly upregulated in TNBC compared with HR+ and HER2+ breast cancers (**FIG. 1E**). YTHDF2 mediates mRNA turnover by recruiting the CCR4-NOT deadenylase complex to initiate deadenylation and decay of m^{6}A-containing transcripts before localizing with bound targets to processing (P) bodies for committed degradation. However, the role of YTHDF2-mediated turnover of methylated

RNA in cancer is not clear because of conflicting findings regarding its function. Moreover, the direct and functionally relevant YTHDF2 target RNAs have yet to be defined in the mammary epithelium or in human breast cancer.

It was first verified that loss of YTHDF2 expression causes cell death in MYC-induced HMECs using two independent short hairpin RNA (shRNA)-mediated knockdowns of YTHDF2 (shYTHDF2-1 and shYTHDF2-2) (**FIG. 1F**). After 24 h of MYC induction, a significant increase was observed in apoptotic, Annexin V-positive cells and early cell death in MYC-induced HMECs compared with uninduced controls (**FIGs. 1G-1H**). Epistasis between YTHDF2 and m^{6}A-modified RNA targets was also confirmed using shRNA-mediated knockdown of m^{6}A writer, METTL3 (shMETTL3) (**FIG. 1F**), which similarly triggered apoptotic cell death (**FIGs. 1G-1H**). In addition, using propidium iodide (PI) staining, it was found that after 3 days of MYC induction, significantly more YTHDF2-depleted HMECs were assigned to sub-G1 cell cycle phase, and significantly fewer were assigned to G0/G1 phase, suggesting G1 checkpoint arrest. Uninduced HMECs did not show significant changes in fractions of cells assigned to G0/G1, S, or G2/M phases following YTHDF2 depletion (**FIG. 1I**). It was also found that proliferation rates of TNBC cell lines (MDA-MB-231 and secondary lung metastatic MDA-MB-231-LM2) were significantly reduced following YTHDF2 depletion, while HR+ and HER2+ breast cancer cell lines (MCF-7 and SKBR3, respectively) were not (**FIG. 1J**). To determine the importance of genes encoding regulators of mRNA turnover on MYC-driven tumor growth in vivo, a pool of MDA-MB-231-LM2 cells were generated, transduced with various doxycycline (DOX)-inducible, TurboRFP-tagged shRNAs targeting several proteins mediating RNA stability, three of which target YTHDF2, and dropout of shRNAs was assessed both in vitro cultured cells and in vivo by subcutaneous mouse xenograft (**FIG. 2A**). A YTHDF2-targeting hairpin that was significantly depleted in resected tumors and in cells cultured in vitro ($p < 0.001$) was identified, indicating a growth disadvantage in TNBC cells upon silencing of YTHDF2 (**FIGs. 2B–2D**). To verify that YTHDF2 inhibition negatively affects tumor growth in vivo, stable MDA-MB-231-LM2 cells transduced with the DOX-inducible shRNA identified by

the screen were generated. Following DOX treatment, it was confirmed that cells expressing the highest levels of the YTHDF2-targeting shRNA became depleted over time when cultured in vitro, suggesting death of cells with sufficient YTHDF2 depletion. After initial tumor engraftment, reduced growth rates and significantly smaller final tumor volumes were observed from DOX-treated mice compared with tumors from vehicle-treated mice (**FIGs. 2E–2G**). In addition to fewer proliferating cells, increased caspase-3 cleavage and a reduction in host angiogenic vascular endothelial cell markers were observed in tumors from DOX-treated mice (**FIGs.2H-2I**).

Next, inducible multi-tissue CAG-CreERT; Ythdf2fl/fl mice were generated by crossing CAG-CreERT mice with previously generated Ythdf2fl/fl mice to expose any effects on the viability of healthy cells in other organs. Systemic genetic depletion of Ythdf2 resulted in no gross physiological abnormalities or changes in body weight for at least 4 weeks following TAM administration, nor did it induce programmed cell death in female reproductive tissues known to rely on m^6A regulation by YTHDF2. This suggests that inhibition of Ythdf2 in an intact organism has no adverse effects in non-cancerous somatic tissues and that YTHDF2 depletion safely and specifically inhibits growth of cells predisposed to MYC addiction.

Example 3 - YTHDF2 targets are enriched for genes regulating growth factor signaling

To identify transcript-specific functions of YTHDF2 targets in MYC-driven cancer, enhanced crosslinking and immunoprecipitation (eCLIP) and m^6A sequencing (m^6A-seq) was performed in MYC-induced and uninduced HMECs, MDA-MB-231-LM2 cells, MDA-MB-231 cells, MCF-7 cells, and SKBR3 cells in biological duplicate. In agreement with previous YTHDF2 CLIP and RNA immunoprecipitation (RIP) sequencing experiments, it was found that a majority of high-confidence YTHDF2 and m6A peaks map to the 30 end of transcripts in the coding sequence (CDS) and 30 UTR (**FIG. 3A**) and contain the DRACH (D = A, G, or U; R = A or G; H = A, C, or U) sequence motif (**FIG. 3B**). It was confirmed that YTHDF2 binding sites generally overlap with m^6A-modified sites using pairwise comparisons between eCLIP and m^6A-seq IP reads at each m^6A site and that eCLIP IP reads were enriched at m^6A sites over size-matched (SM) inputs. Collectively, epitranscriptomic analyses confirm binding of YTHDF2 at m^6A-modified sites on RNAs containing the consensus sequence.

To determine if MYC activity influences the m^6A landscape, high-confidence m^6A sites among MYC-induced and uninduced HMECs and among TNBC, HR+, and HER2+ breast cancer cell lines were compared. Interestingly, it was found that the secondary lung

metastatic MDA-MB-231-LM2 tumor cells appeared to acquire new m^6A modifications, as ~72% of m^6A sites (14,873 peaks) and ~46% modified genes (4,512 genes) were unique from the parental MDA-MB-231 cell line (**FIG. 3C**). This suggests that the m^6A landscape is modified during tumor evolution and metastasis, indicating that cancer cells become increasingly reliant on m^6A-dependent RNA regulation as they become more invasive. However, MYC-induced HMECs did not display robust differences in m^6A-modified sites compared with uninduced HMECs in either direction, and neither did HR+ or HER2+ breast cancer cell lines compared with MDA-MB-231 cells, suggesting that MYC activity does not determine the m^6A landscape in mammary tumors (**FIG. 3C**).

As RBP binding affinity is driven largely by RNA sequence and secondary structure, which are conserved across cell types and states, it was expected that differences in YTHDF2 binding targets among cancer cell lines result from differences in target RNA expression level and alterations in m^6A status. To understand YTHDF2's role in promoting MYC-driven cancer cell growth and survival and to pinpoint the targets that uniquely contribute to apoptosis, RNA expression data was analyzed for overlapping YTHDF2 targets in TNBC cell lines (**FIG. 3D**). Using hierarchical clustering of Z scores, two clusters were identified in which YTHDF2 targets are highly expressed in TNBC cells compared with HR+ and HER2+ cells (**FIG. 3E**). These clusters were enriched for genes that regulate wound healing, cell adhesion, ERK1/2 signaling, and EMT, while clusters including genes that are also highly expressed in MCF-7 cells generally lack enrichment for genes belonging to these ontology terms (**FIG. 3F**).

Example 4 - Depletion of YTHDF2 upregulates EMT-specific pathways

Next, TNBC cells were verified to undergo expression changes resembling EMT following YTHDF2 depletion by performing RNA sequencing (RNA-seq) in YTHDF2-depleted, MYC-induced HMECs in biological duplicate. It was found that transcripts that are bound by YTHDF2 are upregulated compared with transcripts lacking binding sites (**FIG. 4A**), but inspection of the individual upregulated mRNAs revealed that >50% of upregulated transcripts were not direct YTHDF2 targets. These include CPA4, HMOX1, and MMP3, which are known to contribute to or are transcribed in response to cell migration, wound healing, and metastatic phenotypes (**FIG. 4B**). These genes exhibited very low or undetectable RNA expression (transcripts per million [TPM] % 1) in nontargeting control (NTC) cells yet were dramatically increased (~30–85 TPM) in YTHDF2-depleted cells. Among expressed genes, 4.8% (Bonferroni-adjusted p [padj] < 0.001, log2 fold change > 1)

were differentially upregulated in YTHDF2-depleted, MYC-induced HMECs compared with NTC and were enriched for ontologies associated with mesenchymal cell transition (i.e., tissue morphogenesis, TGF-b receptor signaling, and signaling responses to growth factor stimuli), while downregulated transcripts were enriched for ontologies associated with epithelial cell processes (i.e., adhesion and junction organization, keratinization, and epidermis development) (**FIG. 4C**). In addition, results show that upregulated genes overlapping with those in YTHDF2-depleted MYC-induced HMECs over YTHDF2-depleted uninduced HMECs were enriched for ontologies associated with inflammatory and stress response, but not EMT-specific pathways, indicating that general inhibition of YTHDF2 promotes EMT and growth factor signaling, but only in conjunction with elevated MYC activity does YTHDF2 inhibition lead to apoptosis.

Supporting this hypothesis, it was observed that YTHDF2- depleted TNBC cells displayed a spindle-shape morphology denoted by high levels of vimentin localized to cell projections (**FIG. 4D**). Additionally, it was found that several upstream regulators of EMT are YTHDF2 targets (**FIG. 4E**) and that depletion of YTHDF2 resulted in upregulation of the downstream EMT TFs ZEB-1 and SNAIL (**FIG. 4F**). EMT is executed transcriptionally in response to the activation of the MAPK/ERK cascades, often leading to upregulation of MYC itself and increased expression of several translation initiation factors known to contribute to cancer progression. Following YTHDF2 depletion, ERK1/2 phosphorylation, increased expression of translation initiation factors, and elevated MYC protein expression was detected (**FIG. 4G**). To determine if YTHDF2 limits the activation of signaling pathways operating upstream or in parallel to MYC, it was next tested if YTHDF2 regulates MYC's transcriptional targets or the MYC transcript itself. Results show that YTHDF2 binding did not always correspond with MYC transcript abundance, and although MYC targets were significantly upregulated in YTHDF2-depleted MYC-induced HMECs, very few significantly upregulated

MYC targets were bound by YTHDF2. Furthermore, the adaptive endoplasmic reticulum stress pathway is typically engaged during EMT to alleviate metabolic and oxidative stress that accompanies cancer cell transformation and growth by facilitating protein folding and averting cell death. Consistently, activation of the adaptive unfolded protein response (UPR) was detected in all breast cancer subtypes, including upregulation of genes downstream of the serine/threonine

PERK kinase, ATF4, GADD34, and CHOP and splicing of XBP1 (sXBP1) downstream of the serine/threonine IRE1 kinase (**FIG. 4H**). In conclusion, it was found that depletion of

YTHDF2 generally increases the expression of EMT pathway genes in breast cancer cells, but only TNBC cells were highly sensitive to upregulation of these pathways.

Example 5 - Depletion of YTHDF2 sensitizes TNBC cells to proteotoxicity

Although it is well established that MYC can actuate both cell proliferation and apoptosis, evidence suggests that rather than inducing apoptosis directly, high levels of MYC expression may be responsible for sensitizing cells to apoptotic triggers. As depletion of YTHDF2 has recently been shown to sensitize MYC-amplified acute myeloid leukemia (AML) cells to TNF-induced apoptosis, the extrinsic and intrinsic apoptotic pathways driving this phenotype were dissected (**FIG. 5A**). Of the most significantly upregulated YTHDF2 target transcripts in YTHDF2-depleted, MYC-induced HMECs, with strong YTHDF2 binding signal centered on m^6A sites, TNF receptor superfamily member 10b (TNFRSF10B; i.e., DR5) was first observed by probing DR5-induced apoptotic activity through co-depletion of YTHDF2 and DR5. Although a reduction in caspase-8 cleavage was observed with co-depletion compared with YTHDF2-only depleted cells, surprisingly reduced cleavage of downstream caspase-3 was not observed, indicating that DR5 knockdown did not halt the apoptotic cascade in YTHDF2-depleted cells.

As activation of the adaptive UPR in all YTHDF2-depleted breast cancer cells was detected, it was hypothesized that the terminal UPR may be activated in YTHDF2-depleted TNBC cells leading to intrinsic apoptosis from excessive endoplasmic reticulum stress (**FIG. 5A**). Indeed, upregulated expression of ER chaperone and foldase proteins was observed, indicating unfolded protein accumulation, and activation of the c-Jun N-terminal kinase (JNK) was detected, resulting in caspase-3 cleavage in TNBC cell lines but not in HR+ or HER2+ cell lines (**FIG. 5B**). Furthermore, unfolded protein accumulation and apoptosis were reversed following treatment with 4-phenylbutyric acid (4-PBA), an endoplasmic reticulum stress inhibitor, confirming proteotoxicity as the underlying cause of cell death in YTHDF2-depleted TNBC cells. Additionally, cross reference of public mass spectrometry data for 83 tumor samples provided by the Clinical Proteomic Tumor Analysis Consortium (CPTAC) from TCGA's Cancer Proteome Study of Breast Tissue indicated that YTHDF2 expression is negatively correlated with MAPK activity and that tumor samples with lower YTHDF2 expression have higher levels of ASK1 (MAP3K5), JNK1/2 (MAPK8/9), and p38 (MAPK14) phosphorylation.

To substantiate that proteotoxicity is a result of disrupting YTHDF2-mediated regulation of its target mRNAs, the expression of the most significantly upregulated direct

YTHDF2 target upon YTHDF2 depletion, serine protease 23 (PRSS23), was identified and modulated (**FIG. 4B** and **5C**). PRSS23 is significantly downregulated in patients with TNBC tumors compared with patients with HR+ or HER2+ tumors (**FIG. 5D**) and codepletion of YTHDF2 and PRSS23 rescued cell proliferation rates in YTHDF2-depleted TNBC cells (**FIG. 5E**). Additionally, co-depletion of YTHDF2 and PRSS23 produced a substantial reduction in protein levels of translation initiation factors, eiF4E and eiF2a, MYC and caspase-3 cleavage compared with silencing of YTHDF2 alone (**FIG. 5F**). It was found that TCF12 targets identified in publicly available chromatin immunoprecipitation sequencing (ChIP-seq) data (ENCODE: ENCSR000BUN) are upregulated in YTHDF2- depleted, MYC-induced HMECs and that the majority of upregulated TCF12 targets are not YTHDF2 targets (**FIGs. 5G** and **5H**). Moreover, it was found that co-depletion of YTHDF2 and PRSS23 partially rescued heat shock protein family A member 5 (BiP) expression (**FIG. 5F**), alleviated reactive oxygen species (ROS) levels by ~50% (**Fig. 5I**), and dampened intrinsic apoptotic signaling. Moreover, a new facet of regulation by m^6A in MYC-driven breast cancer was identified where YTHDF2 binds to and targets several transcripts for degradation, including PRSS23, and in doing so safeguards cancer cells from proteotoxicity resulting from excessive endoplasmic reticulum stress.

Example 6 - Depletion of YTHDF2 boosts translation rates in single cells across tumors

To further test the hypothesis that apoptosis of YTHDF2-depleted TNBC cells is driven by accumulated unfolded proteins, rates of protein synthesis in these cells was measured using puromycin incorporation as a surrogate measure of protein translation. It was observed that YTHDF2-depleted cells contained higher levels of puromycin incorporation into nascent peptides, indicating increased levels of protein synthesis. To substantiate this observation in vivo, Ribo-STAMP (surveying targets by APOBEC-mediated profiling) was used, a method to assess translation by directing C-to-U base editing of ribosome-bound transcripts using the cytidine deaminase enzyme APOBEC1 fused to the C-terminus of the 40S ribosomal protein S2 (RPS2). A DOX-inducible, HA-tagged, RPS2- APOBEC1 (RPS2-STAMP), and APOBEC1-only (control-STAMP) expressing cell lines both in wild-type (WT) and in DOX-inducible shRNA-targeting YTHDF2 (TurboRFP-tagged) MDA-MB-231- LM2 cells were generated. After engraftment, mice were given DOX water for 3 days to induce both shRNA and STAMP transgene expression prior to tumor resection, dissociation, and single-cell RNA-seq (scRNA-seq) using 10X Chromium Single Cell capture. At this early time point, cells

harboring molecularly distinct translational signatures driven by both tumor heterogeneity and gene expression changes were uncovered reflected by C-to-U sequence changes in mRNA (**FIG. 6A**).

Next, mRNA expression level changes in YTHDF2-depleted single cells were tested if it resembled the bulk, in vitro observations. First, YTHDF2-depleted tumor cell populations (control-STAMP and RPS2-STAMP) contained cells with high raw read coverage in mitochondrial genes compared with WT samples, indicating higher fractions of apoptotic or lysed cells. Second, uniform manifold approximation and projection (UMAP) visualization of mRNA expression revealed clusters of YTHDF2-depleted tumor cells that were distinct from their WT counterpart (**FIG. 6B**) and cells expressing the TurboRFP tag ($TurboRFP^{High}$) generally had lower YTHDF2 mRNA expression on average compared with cells that did not ($TurboRFP^{Low}$). Third, UMAP visualization defined a cell group containing the majority of $TurboRFP^{High}$ cells (**FIG. 6C**), which also contained the highest expression of genes that were upregulated in bulk YTHDF2-depleted, MYC-induced HMECs (**FIG. 6D**). This group of cells corresponded to three Louvain mRNA expression clusters (**FIG. 6E**, clusters 1, 2, and 3), with enrichment of $TurboRFP^{High}$ cells in cluster 2 (**FIG. 6F**). Fourth, Gene Ontology (GO) analysis of genes from cells assigned to the different mRNA expression Louvain clusters confirmed enrichment for ontologies related to EMT and stress response such as cytokine-mediated signaling, response to wounding, blood vessel development, extracellular matrix (ECM) organization, and positive regulation of cell death in clusters 1 and 2, while clusters 3 and 4 were highly enriched for genes involved in cell cycle progression (**FIG. 6G**). Fifth, in agreement with in vitro studies, it was found that clusters 1 and 2 contained larger fractions of cells assigned to G1 phase of the cell cycle on the basis of their transcriptomic expression profiles, while cluster 3 was overrepresented for S phase and cluster 4 for G2M phase. From these analyses, it was concluded that the majority of $TurboRFP^{High}$ cells undergoing G1 arrest exist in clusters 1 (control-STAMP) and 2 (RPS2-STAMP) and that cluster 3 may contain fewer $TurboRFP^{High}$ cells that either have yet to undergo cell-cycle arrest or have not undergone sufficient YTHDF2 depletion to initiate apoptosis, as the mRNA expression profile in cluster 3 more closely resembles that of cluster 4 (**FIG. 6G**), which contains cells expressing proliferative and tumorigenic markers.

Next, the translatomes of single tumor cells were analyzed by detecting C-to-U edits on transcripts and assigning site coverage (edited reads per kilobase of transcript per million

mapped reads [EPKM]). EPKM from CDS correlated strongly with values from both CDS and 30 UTRs, consistent with the previous observation that 30 UTR signal is specific to RPS2-STAMP-mediated editing. UMAP visualization of EPKM across all tumor samples revealed distinct clustering of control-STAMP samples away from RPS2-STAMP samples (**FIGs. 6H** and **6I**), and using Louvain clustering by EPKM, the dataset was filtered by excluding cells assigned to the control-STAMP cluster that did not contain substantial editing (**FIG. 6J**). As transcriptomes and proteomes of individual tumor cells are known to be heterogeneous, Ribo-STAMP was expected to capture the full spectrum of translational states in tumors regardless of YTHDF2 modulation. Indeed, the distribution of EPKM values for filtered cells revealed a full range of edits throughout the TurboRFP^{Low} population (**FIG. 6K**). Generally, more edits per gene in the YTHDF2-depleted, TurboRFP^{High} population were found, suggesting increased rates of protein synthesis (**FIG. 6K**).

Example 7 - scRibo-STAMP identifies unique translation profiles for single YTHDF2-depleted cells within heterogeneous tumors

Tumors are composed of subpopulations of cells that differ at both the genomic and proteomic levels. Interestingly, it was found that in addition to increased rates of protein synthesis, TurboRFP^{High} cells also contained edits on more genes per cell on average, suggesting that YTHDF2 depletion may initiate distinct translation programs. To identify differentially translated mRNAs, a subpopulation of cells containing the highest number of TurboRFP^{High} cells with high EPKM was observed. This group comprised enrichment for cells assigned to cluster
2 (**FIG. 7A**), confirming that many of these cells originated from the shYTHDF2 RPS2-STAMP tumor. Re-visualizing the UMAP space by Louvain clustering on EPKM produced very similar clusters with substantial overlap of mRNA expression-defined cluster 2 with EPKM-defined cluster A (**FIGs. 7A** and **7B**). This supports the observation that modulation of m^{6}A-modified transcripts on the RNA level incites widespread mRNA translation changes. Next, GO analysis of genes from cells assigned to the different EPKM Louvain clusters was performed. Clusters A and C contained the highest number of differentially edited transcripts (R99 genes) and enrichment for TurboRFP^{High} cells (**FIG. 7B**), and each cluster respectively corresponded to mRNA expression-defined cluster 2 and clusters 3 and 4 (**FIG. 7A**). Both clusters had high levels of editing within transcripts encoding genes known to contribute globally to translation (**FIG. 7C**). Uniquely, cluster A (‘‘pro-apoptotic’’ cluster) was enriched for edits within genes involved in apoptosis and antigen presentation, while cluster C (“pro-

tumorigenic" cluster) was enriched for edits within genes involved in preventing cell-cycle arrest, homotypic cell adhesion, and dampening oxidative stress, all of which are all associated with tumor progression (**FIG. 7C**). Twenty-six percent of the top 100 differentially edited genes ($p < 0.05$) between EPKM clusters A and C overlapped, while ~74% were unique to each cluster (**FIG. 7D**). The most highly edited genes in each cluster included cystatin C (CST3) in cluster A ("pro-apoptotic" cluster), cofilin 1 (CFL1) in cluster C ("protumorigenic" cluster), and 60S ribosomal protein L24 (RPL24) among overlapping genes (**FIGs. 7D** and **7E**). CST3 is a cysteine protease inhibitor that is secreted in response to hypoxia. While being an attractive biomarker in several types of cancers, CST3 is also involved in caspase-mediated cell death. Conversely, RPL24 is required for polysome assembly and is known to be upregulated in MYC-driven cancers, and CFL1 is known to drive invasiveness in basal breast cancers. Accordingly, it was found that TNBC tumors generally express significantly higher levels of CFL1 and RPL24 protein and less CST3 protein compared with HR+ and HER2+ tumors, supporting a role for CST3 in promoting MYC-driven apoptosis (**FIG. 7F**). In conclusion, Ribo-STAMP data corroborated the findings that YTHDF2-depleted tumor cells contain unique translatomes displaying increased translation of tumorigenic and apoptotic transcripts while lacking translation of cell cycle regulators important for maintaining oncogenic proliferation.

OTHER EMBODIMENTS

It is to be understood that while the invention has been described in conjunction with the detailed description thereof, the foregoing description is intended to illustrate and not limit the scope of the invention, which is defined by the scope of the appended claims. Other aspects, advantages, and modifications are within the scope of the following claims.

WHAT IS CLAIMED IS:

1. A method of treating a Myc-dependent cancer in a subject in need thereof, the method comprising administering a therapeutically effective amount of a nucleic acid targeting YTH N-6 Methyladenosine RNA Binding Protein 2 (YTHDF2), thereby treating a Myc-dependent cancer in a subject in need thereof.

2. A method of treating a Myc-dependent cancer in a subject in need thereof, the method comprising:
   (a) determining that the subject has a Myc-dependent cancer; and
   (b) administering to the subject a therapeutically effective amount of a nucleic acid targeting YTH N-6 Methyladenosine RNA Binding Protein 2 (YTHDF2), wherein administering the agent treats a Myc-dependent cancer in a subject in need thereof.

3. An *in vitro* method of inducing apoptosis in a Myc-dependent cancer cell, the method comprising administering a therapeutically effective amount of a nucleic acid targeting YTH N-6 Methyladenosine RNA Binding Protein 2 (YTHDF2), thereby inducing apoptosis in a Myc-dependent cancer cell.

4. A method of weakening triple negative breast cancer cells, the method comprising administering to the triple negative breast cancer cells a therapeutically effective amount of a nucleic acid targeting YTH N-6 Methyladenosine RNA Binding Protein 2 (YTHDF2), thereby weakening triple negative breast cancer cells.

5. The method of any one of claims 1 to 4, wherein the nucleic acid comprises RNA, DNA, or combinations thereof.

6. The method of claim 5, wherein the RNA comprises shRNA, miRNA, siRNA, or combinations thereof.

7. The method of claim 6, wherein the RNA comprises shRNA.

8. The method of claim 7, wherein the shRNA further comprises a lentiviral vector.

9. The method of claim 8, wherein the lentiviral vector comprises The RNAi Consortium (TRC) lentiviral shRNA vector YTHDF2.

10. The method of claim 7, wherein the shRNA further comprises an adenoviral vector (AAV).

11. The method of any one of claims 1 to 10, wherein the Myc-dependent cancer comprises ovarian cancer, breast cancer, colorectal cancer, pancreatic cancer, gastric cancer, uterine cancer, leukemia, or combinations thereof.

12. The method of claim 3, wherein the Myc-dependent cancer cell is a Myc-dependent breast cancer cell.

13. The method of any one of claims 1 to 4, wherein the administration of a nucleic acid targeting N-6 Methyladenosine RNA Binding Protein 2 (YTHDF2) induces unfolded protein accumulation in a Myc-dependent cancer cell.

14. The method of any one of claims 1 to 4, wherein the administration of a nucleic acid targeting N-6 Methyladenosine RNA Binding Protein 2 (YTHDF2) induces apoptosis in a Myc-dependent cancer cell.

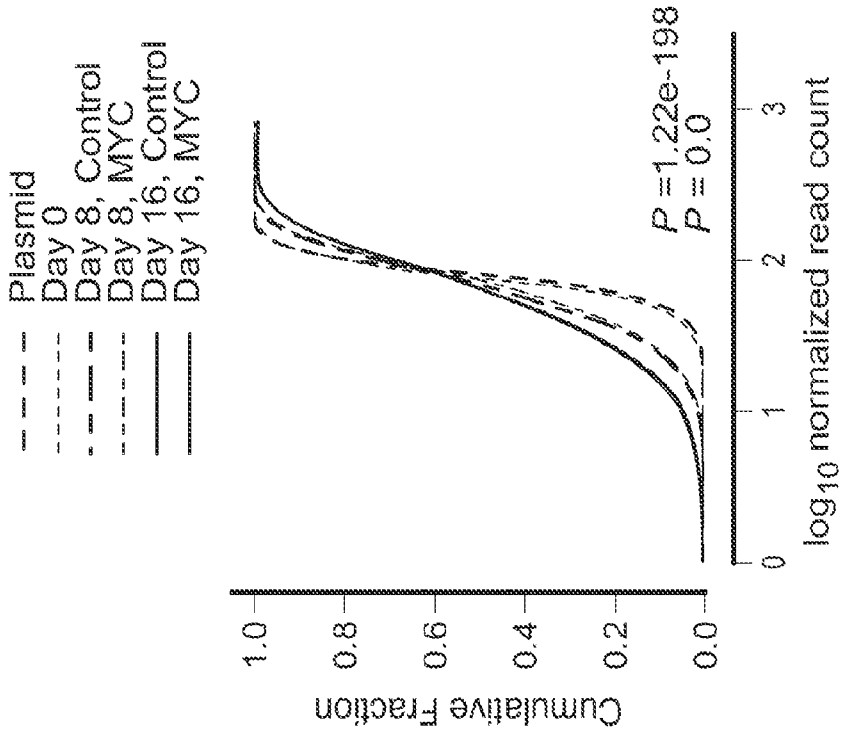

Plasmid
Day 0
Day 8, Control
Day 8, MYC
Day 16, Control
Day 16, MYC
P =1.22e-198
P = 0.0
log10 normalized read count
Cumulative Fraction
1.0
0.8
0.6
0.4
0.2
0.0
0
1
2
3

FIG. 1B

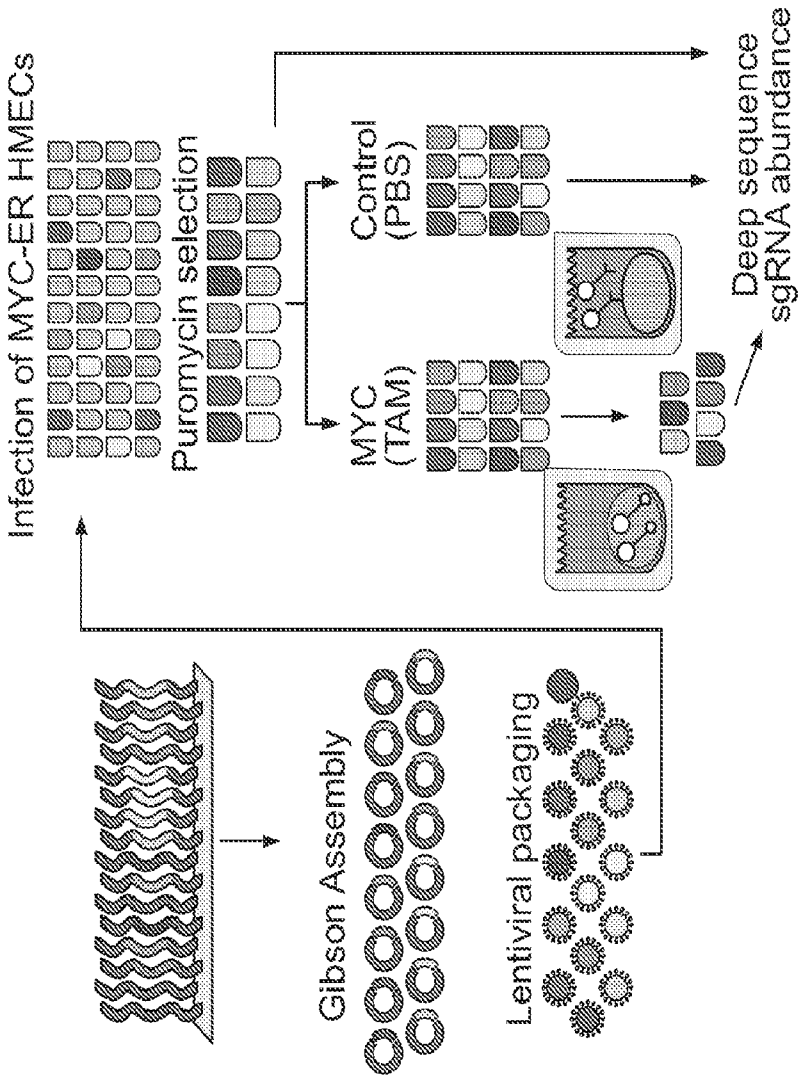

Infection of MYC-ER HMECs
Puromycin selection
Control (PBS)
MYC (TAM)
Deep sequence sgRNA abundance
Gibson Assembly
Lentiviral packaging

FIG. 1A

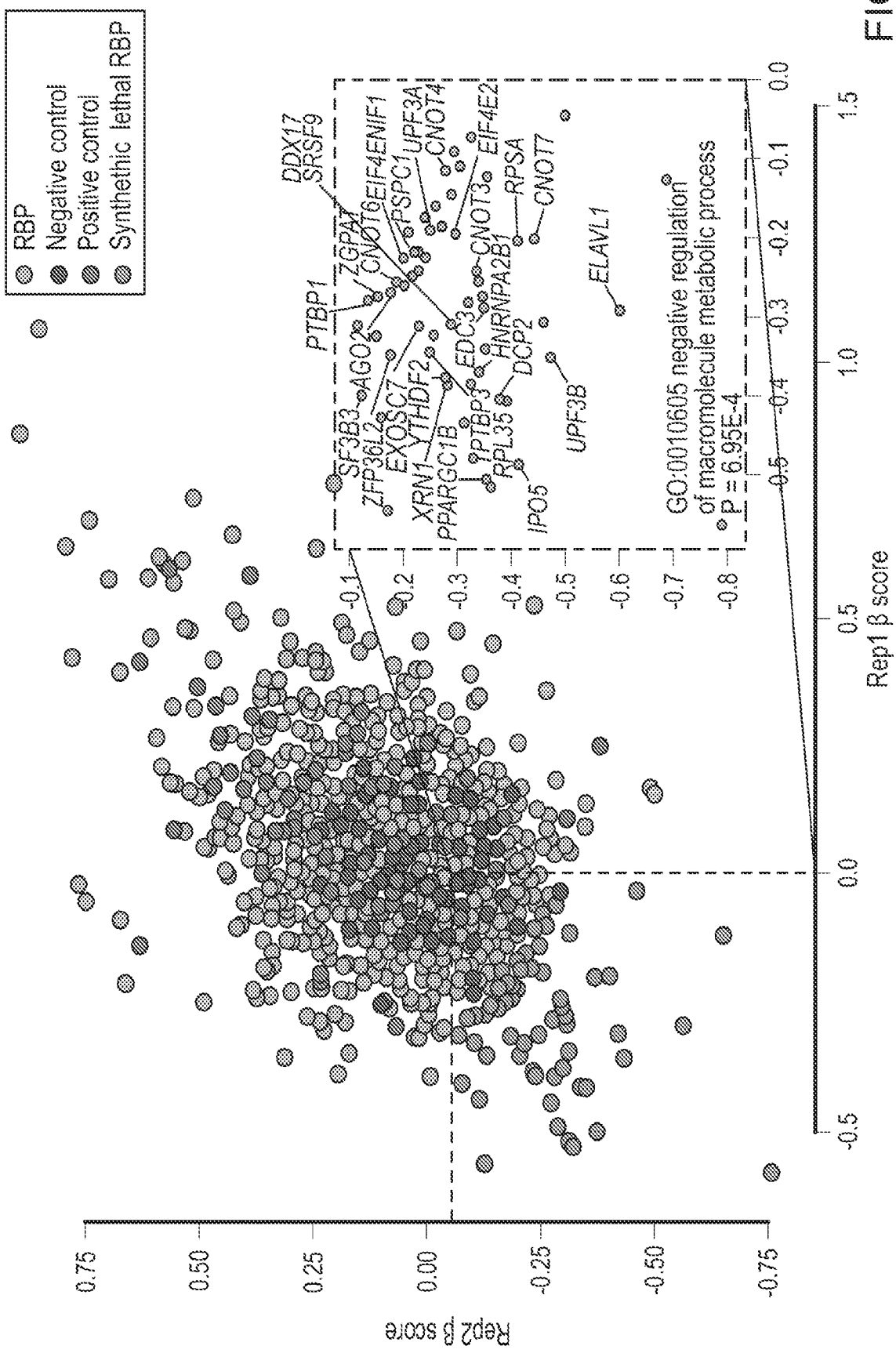

RBP
Negative control
Positive control
Synthethic lethal RBP
Rep2 β score
Rep1 β score
GO:0010605 negative regulation of macromolecule metabolic process
P = 6.95E-4
DDX17
SRSF9
PTBP1
ZGPAT
CNOT6
EIF4ENIF1
PSPC1
UPF3A
CNOT4
EIF4E2
AGO2
CNOT3
RPSA
CNOT7
SF3B3
ZFP36L2
EXOSC7
YTHDF2
EDC3
HNRNPA2B1
ELAVL1
XRN1
PPARGC1B
PTBP3
DCP2
RPL35
IPO5
UPF3B

FIG. 1C

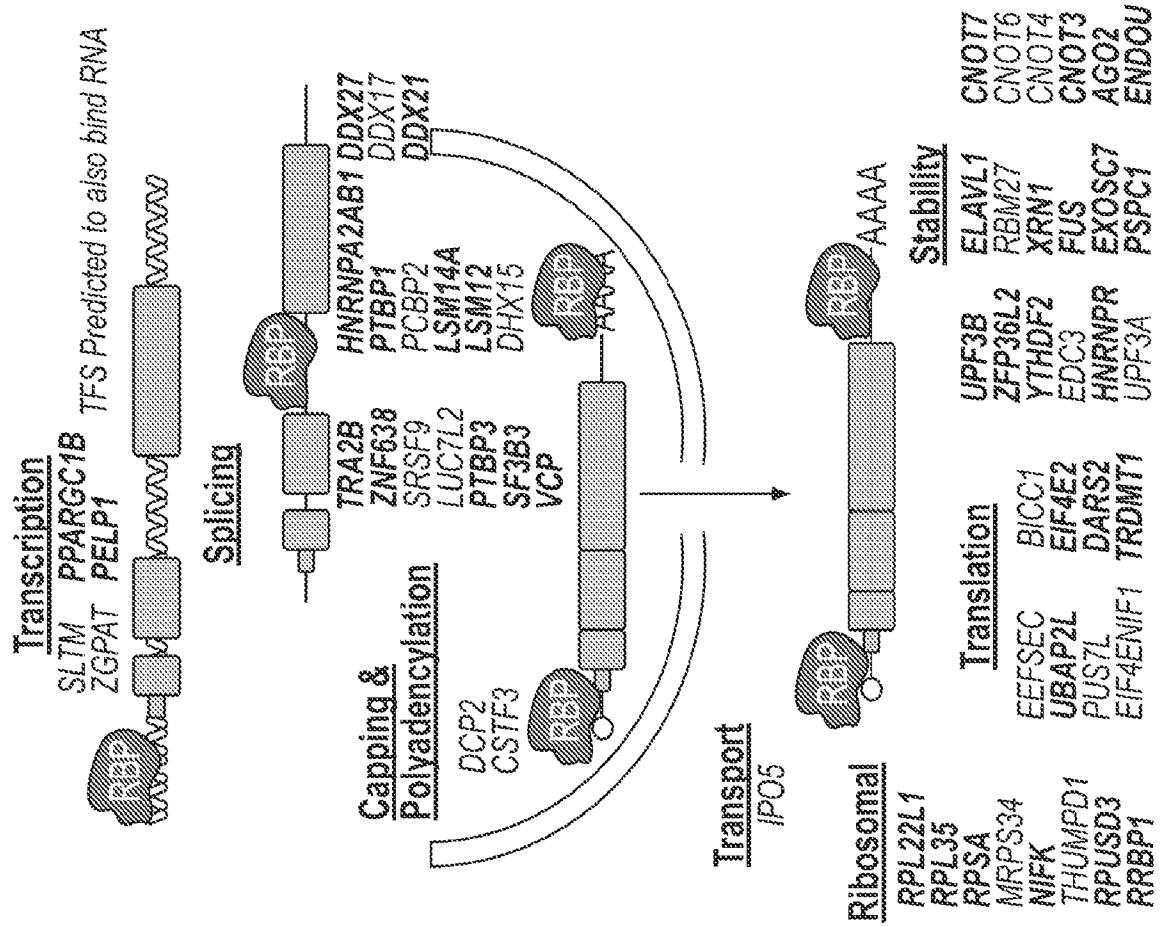

Transcription
SLTM PPARGC1B
ZGPAT PELP1
TFS Predicted to also bind RNA
Splicing
Capping & Polyadenylation
DCP2
CSTF3
TRA2B ZNF638 SRSF9 LUC7L2 PTBP3 SF3B3 VCP
HNRNPA2AB1 DDX27
PTBP1 DDX17
PCBP2 DDX21
LSM14A
LSM12
DHX15
AAAA
Transport
IPO5
Ribosomal
RPL22L1
RPL35
RPSA
MRPS34
NIFK
THUMPD1
RPUSD3
RRBP1
Translation
EEFSEC BICC1
UBAP2L EIF4E2
PUS7L DARS2
EIF4ENIF1 TRDMT1
UPF3B ZFP36L2 YTHDF2 EDC3 HNRNPR UPF3A
AAAA
Stability
ELAVL1 CNOT7
RBM27 CNOT6
XRN1 CNOT4
FUS CNOT3
EXOSC7 AGO2
PSPC1 ENDOU

FIG. 1D

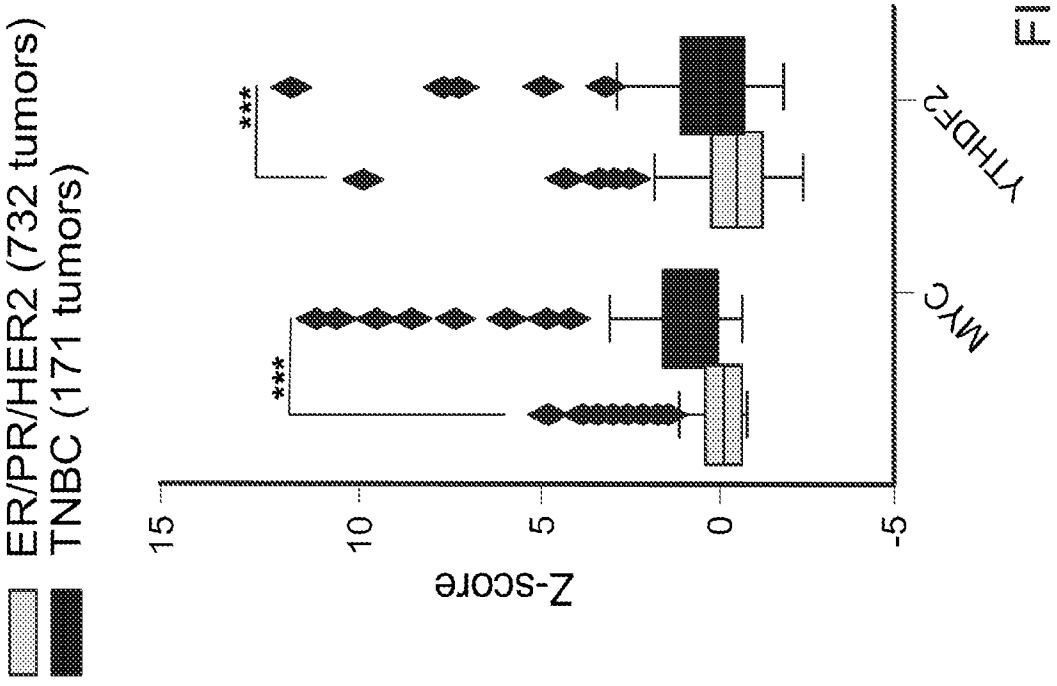

ER/PR/HER2 (732 tumors)
TNBC (171 tumors)
Z-score
15
10
5
0
-5
***
***
MYC
YTHDF2

FIG. 1E

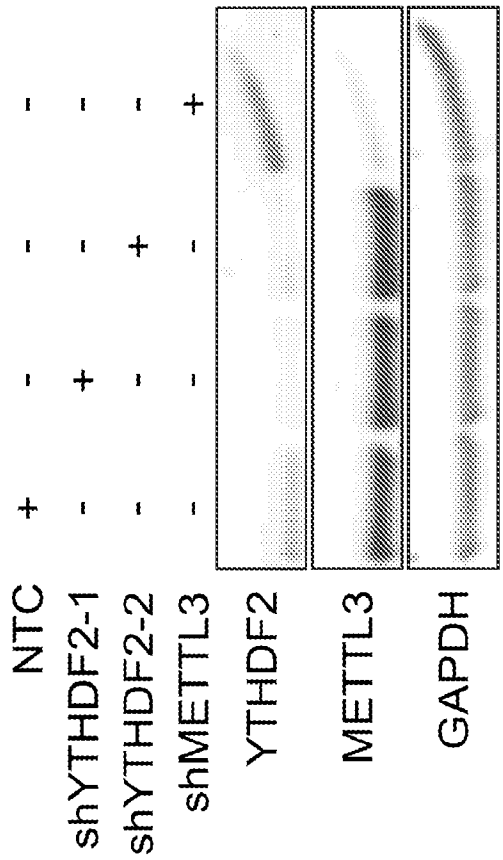

NTC
shYTHDF2-1
shYTHDF2-2
shMETTL3
YTHDF2
METTL3
GAPDH

FIG. 1F

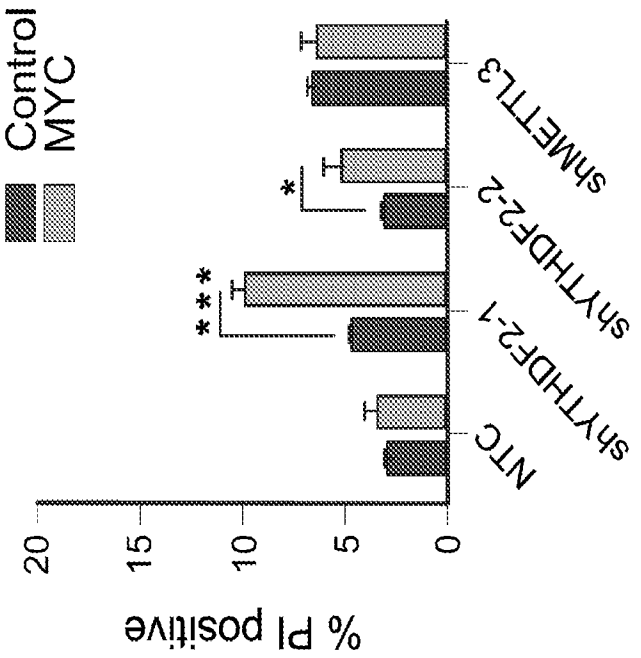

Control
MYC
% PI positive
0
5
10
15
20
NTC
shYTHDF2-1
shYTHDF2-2
shMETTL3
***
*

FIG. 1H

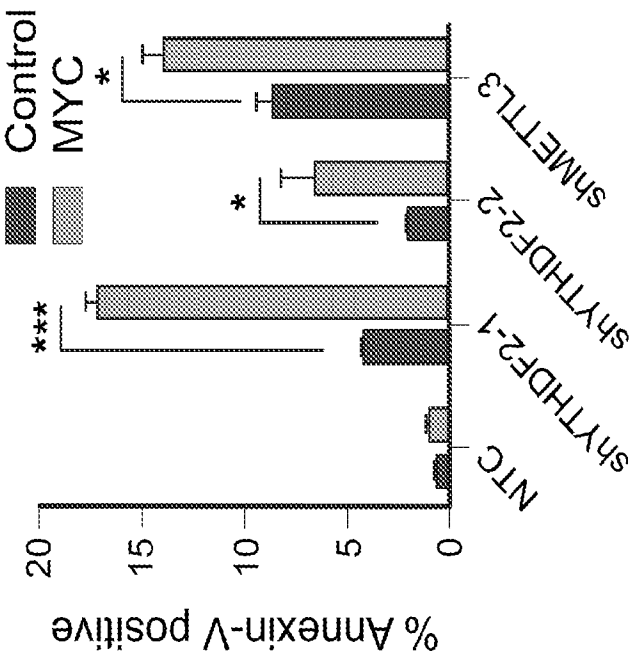

Control
MYC
% Annexin-V positive
0
5
10
15
20
NTC
shYTHDF2-1
shYTHDF2-2
shMETTL3
***
*
*

FIG. 1G

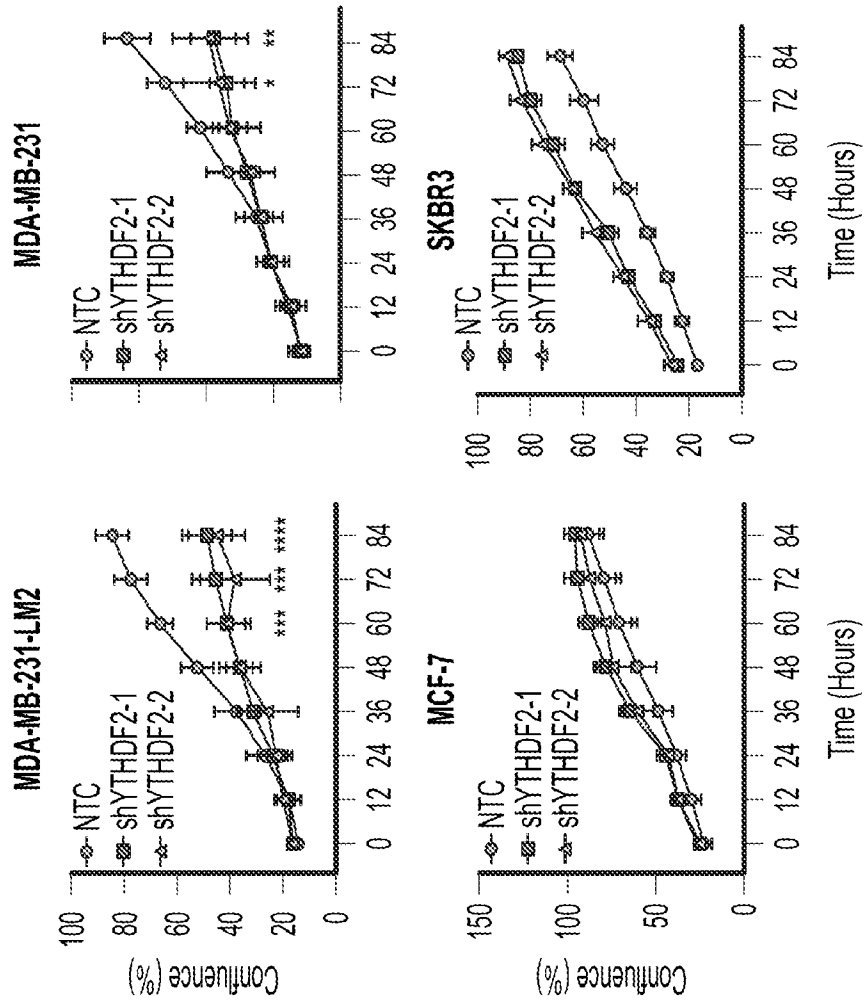

MDA-MB-231
MDA-MB-231-LM2
SKBR3
MCF-7
NTC
shYTHDF2-1
shYTHDF2-2
Confluence (%)
Time (Hours)
0 12 24 36 48 60 72 84
0 20 40 60 80 100
0 50 100 150

FIG. 1J

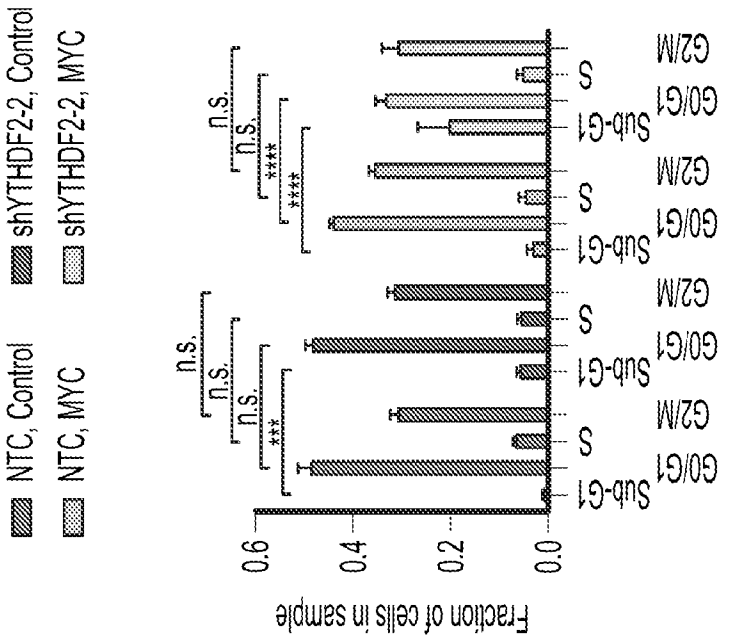

NTC, Control
NTC, MYC
shYTHDF2-2, Control
shYTHDF2-2, MYC
Fraction of cells in sample
0.0 0.2 0.4 0.6
n.s.
***
****
Sub-G1
S
G2/M
G0/G1
Cell cycle phase

FIG. 1I

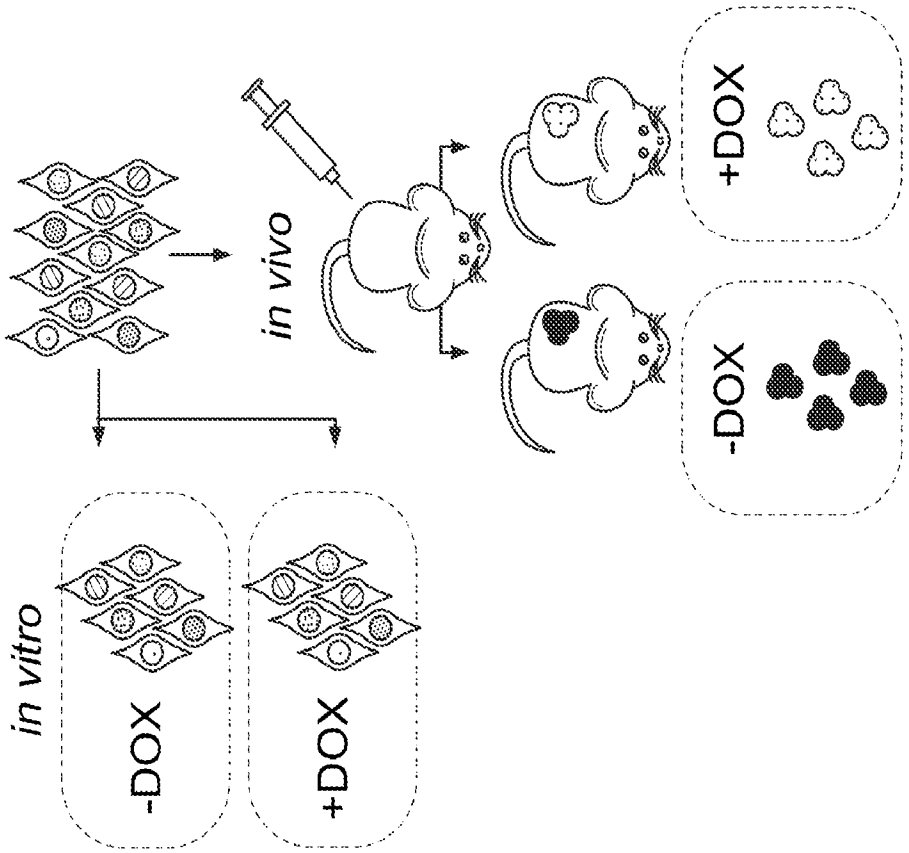


FIG. 2A

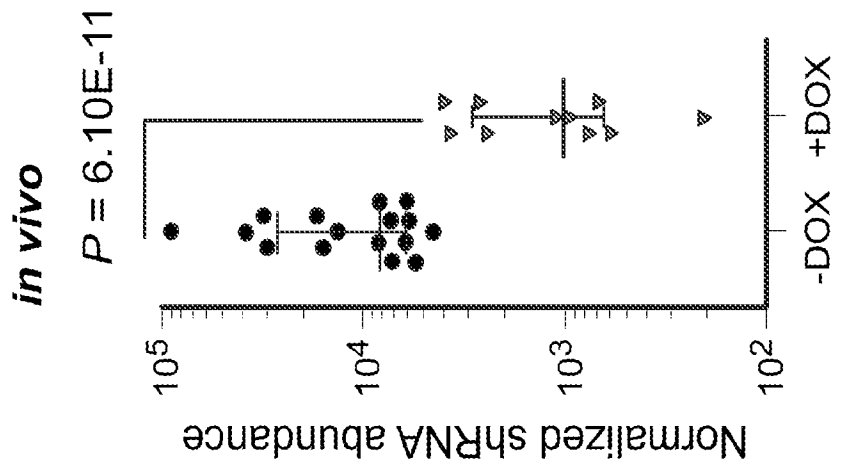


FIG. 2D

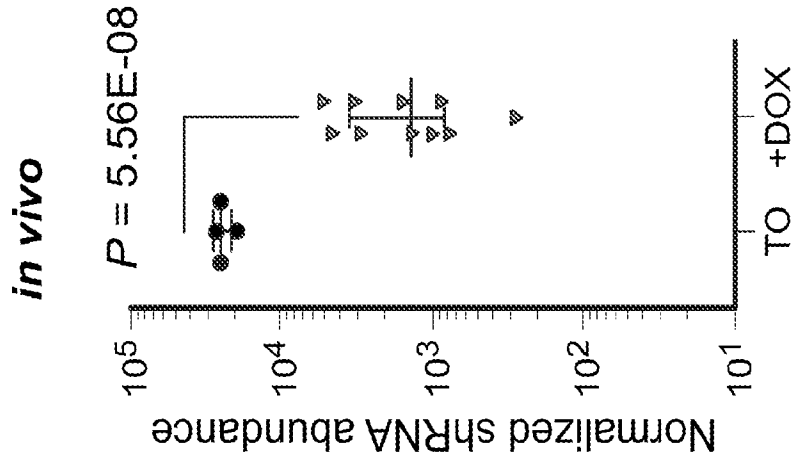


FIG. 2C

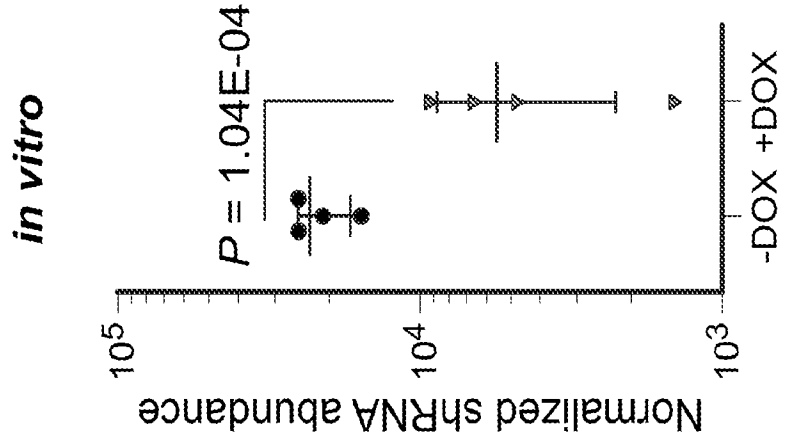


FIG. 2B

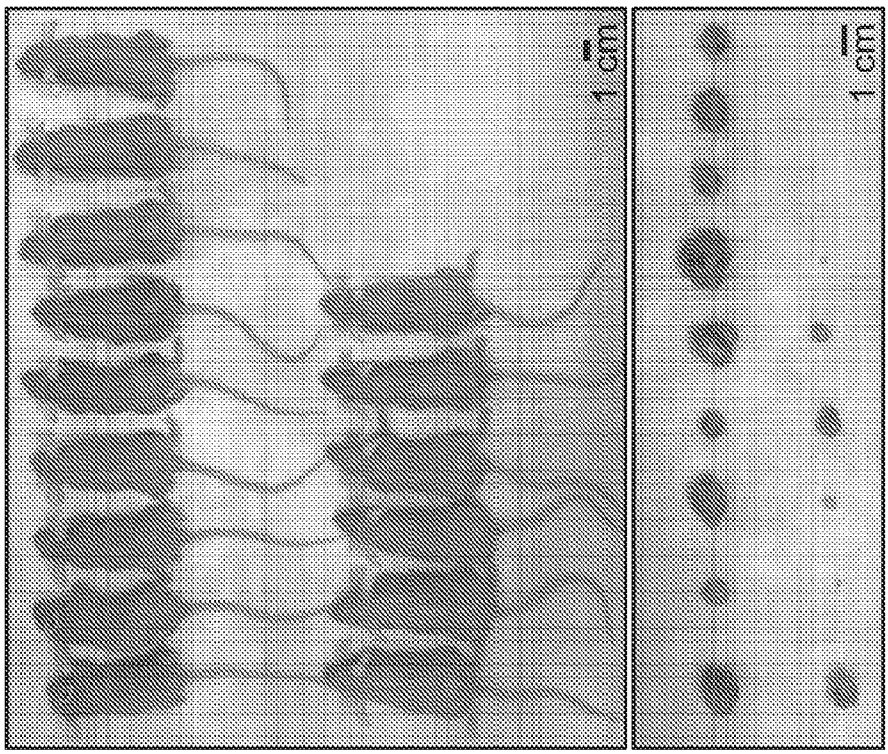

1 cm
1 cm
-DOX
+DOX
-DOX
+DOX

FIG. 2F

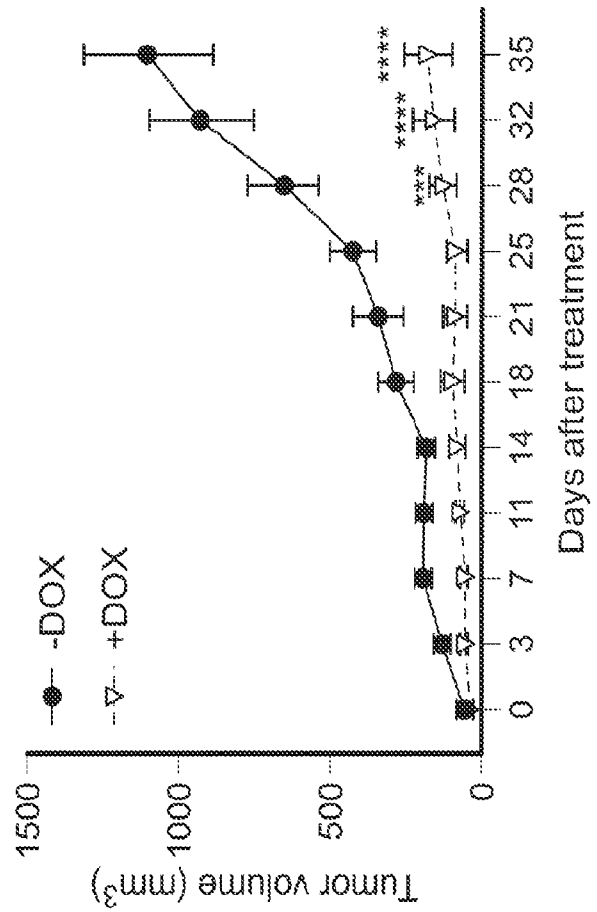

Tumor volume (mm3)
1500
1000
500
0
-DOX
+DOX
0
3
7
11
14
18
21
25
28
32
35
Days after treatment
***
****
****

FIG. 2E

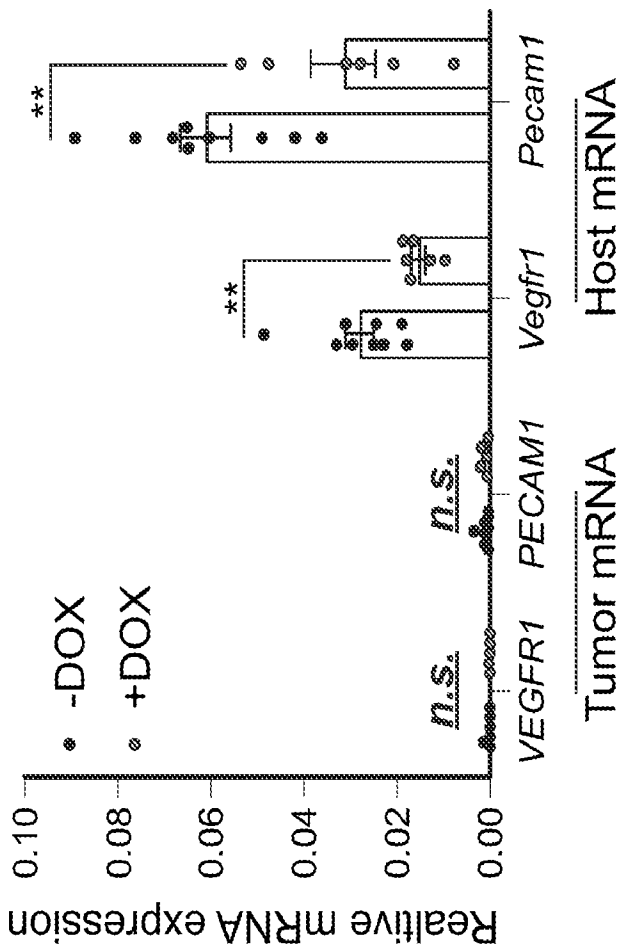

Realtive mRNA expression
0.10
0.08
0.06
0.04
0.02
0.00
-DOX
+DOX
n.s.
n.s.
**
**
VEGFR1
PECAM1
Vegfr1
Pecam1
Tumor mRNA
Host mRNA

FIG. 2H

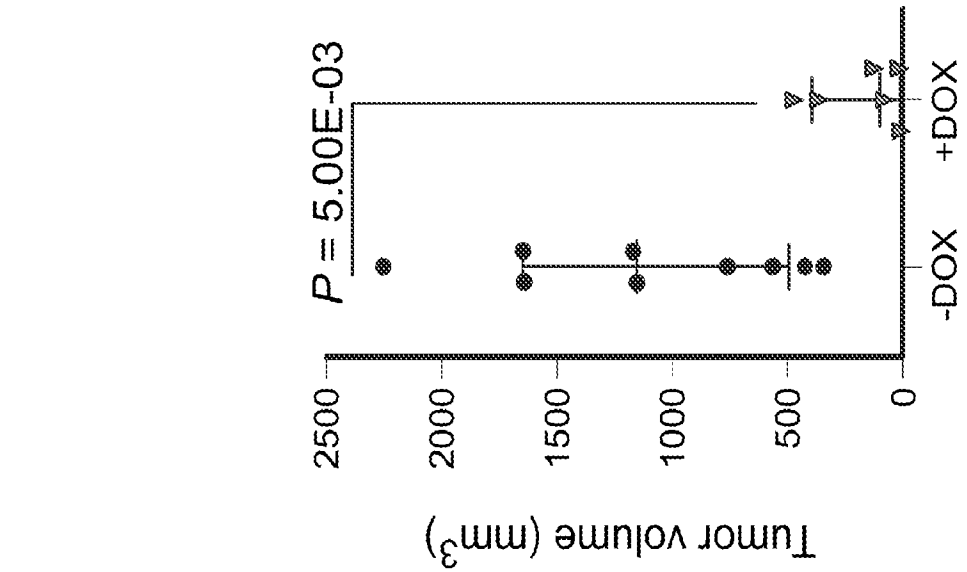

Tumor volume (mm3)
2500
2000
1500
1000
500
0
P = 5.00E-03
-DOX
+DOX

FIG. 2G

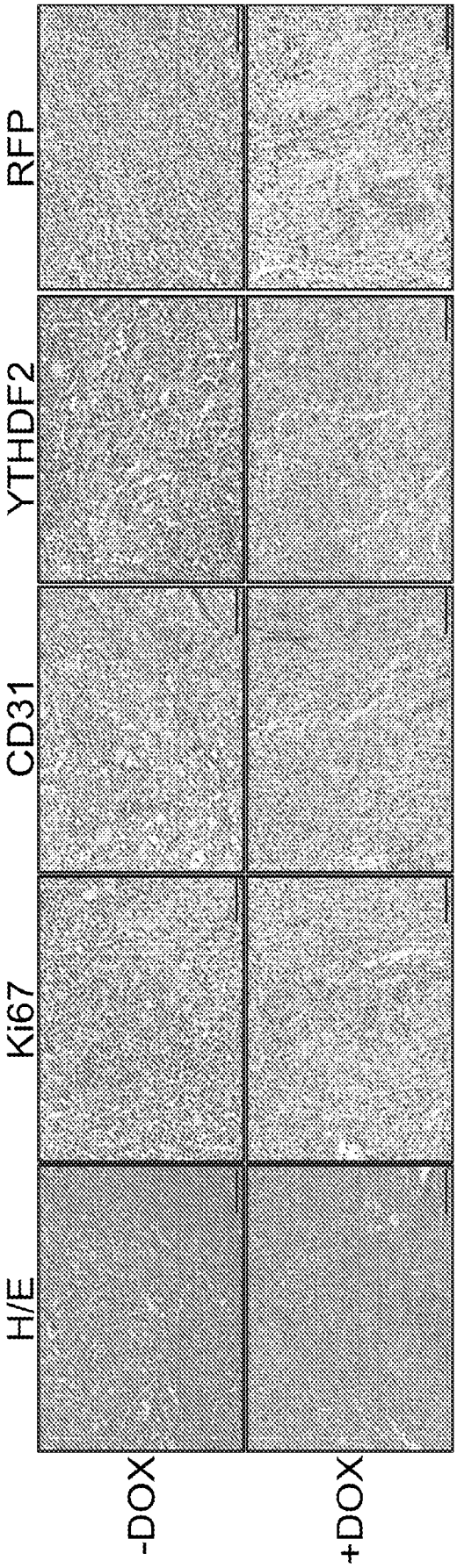


FIG. 2I

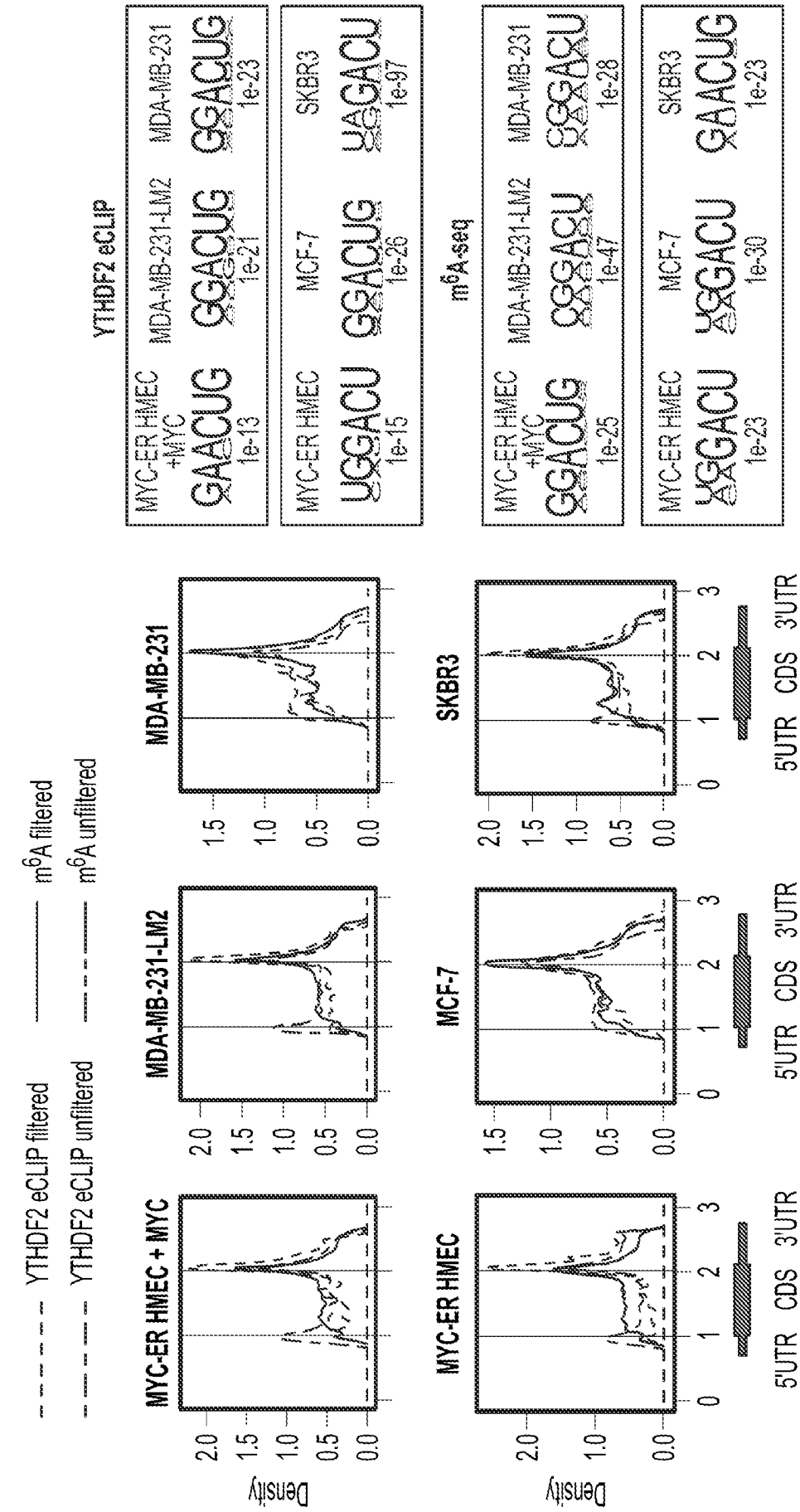

YTHDF2 eCLIP filtered
YTHDF2 eCLIP unfiltered
m6A filtered
m6A unfiltered
MYC-ER HMEC + MYC
MDA-MB-231-LM2
MDA-MB-231
MYC-ER HMEC
MCF-7
SKBR3
Density
5'UTR CDS 3'UTR
YTHDF2 eCLIP
m6A-seq
MYC-ER HMEC +MYC
MDA-MB-231-LM2
MDA-MB-231
MYC-ER HMEC
MCF-7
SKBR3
1e-13
1e-21
1e-23
1e-15
1e-26
1e-97
1e-25
1e-47
1e-28
1e-23
1e-30
1e-23

FIG. 3A

FIG. 3B

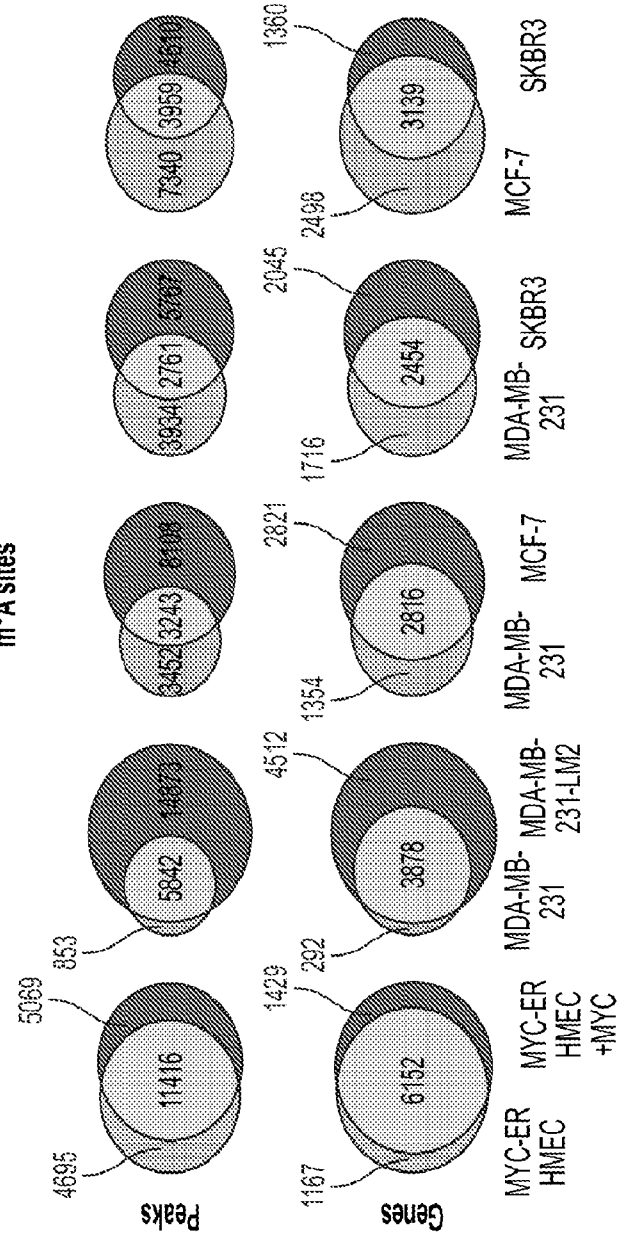

m6A sites
Peaks
Genes
MYC-ER HMEC
MYC-ER HMEC +MYC
MDA-MB-231
MDA-MB-231-LM2
MCF-7
SKBR3
4695
11416
5069
853
5842
14873
6152
1167
1429
292
3878
4512
3452
3243
8108
1354
2816
2821
3934
2761
6767
1716
2454
2045
7340
3959
8510
2496
3139
1360

FIG. 3C

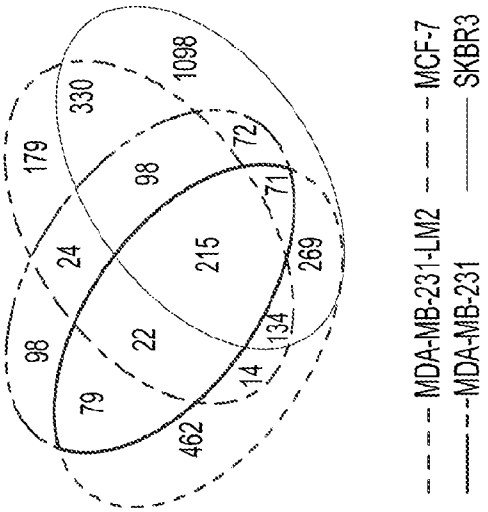

eCLIP target genes
MDA-MB-231-LM2
MCF-7
MDA-MB-231
SKBR3
98
79
462
22
24
14
215
134
98
71
269
179
72
330
1098

FIG. 3D

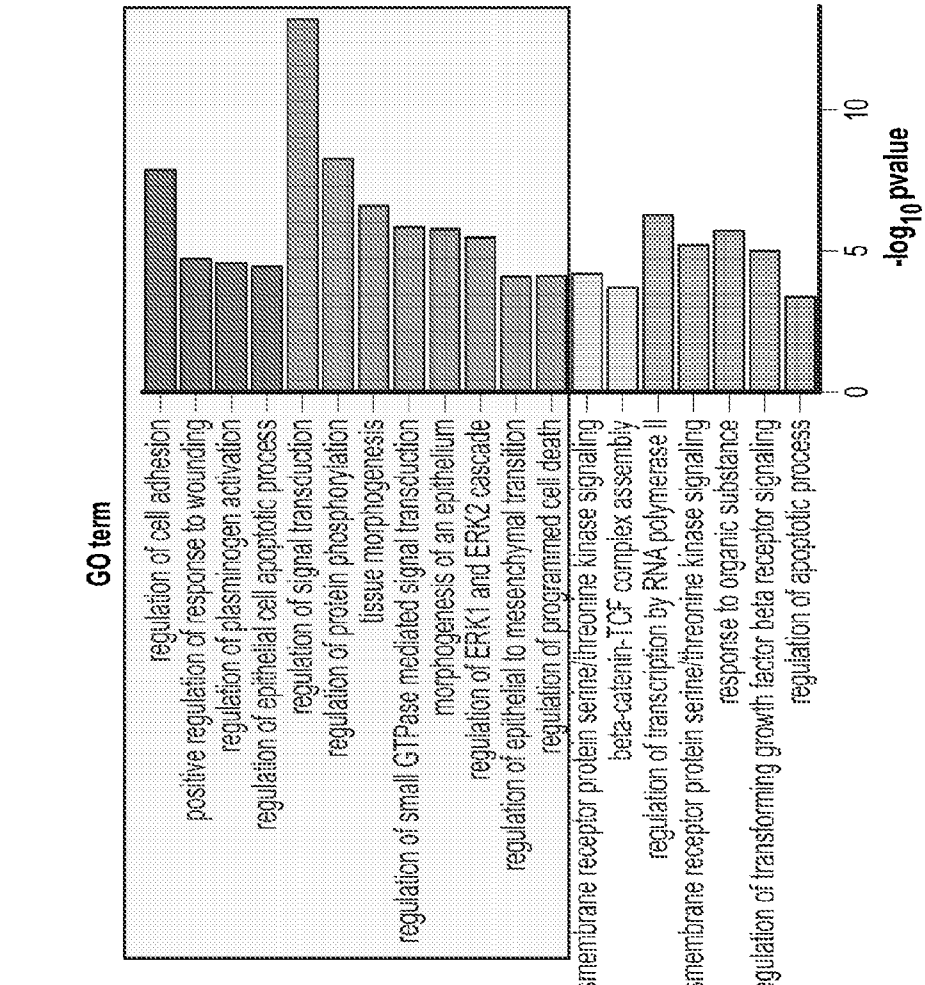

GO term
regulation of cell adhesion
positive regulation of response to wounding
regulation of plasminogen activation
regulation of epithelial cell apoptotic process
regulation of signal transduction
regulation of protein phosphorylation
tissue morphogenesis
regulation of small GTPase mediated signal transduction
morphogenesis of an epithelium
regulation of ERK1 and ERK2 cascade
regulation of epithelial to mesenchymal transition
regulation of programmed cell death
regulation of transmembrane receptor protein serine/threonine kinase signaling
beta-catenin-TCF complex assembly
regulation of transcription by RNA polymerase II
regulation of transmembrane receptor protein serine/threonine kinase signaling
response to organic substance
regulation of transforming growth factor beta receptor signaling
regulation of apoptotic process
0
5
10
-log10pvalue

FIG. 3F

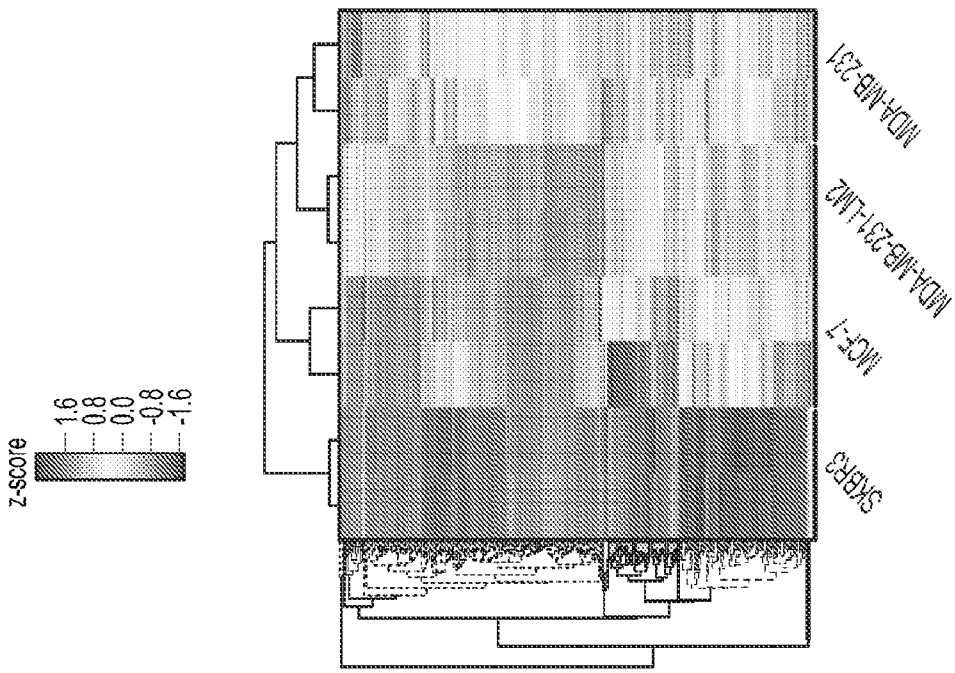

z-score
1.6
0.8
0.0
-0.8
-1.6
SKBR3
MCF-7
MDA-MB-231-LM2
MDA-MB-231

FIG. 3E

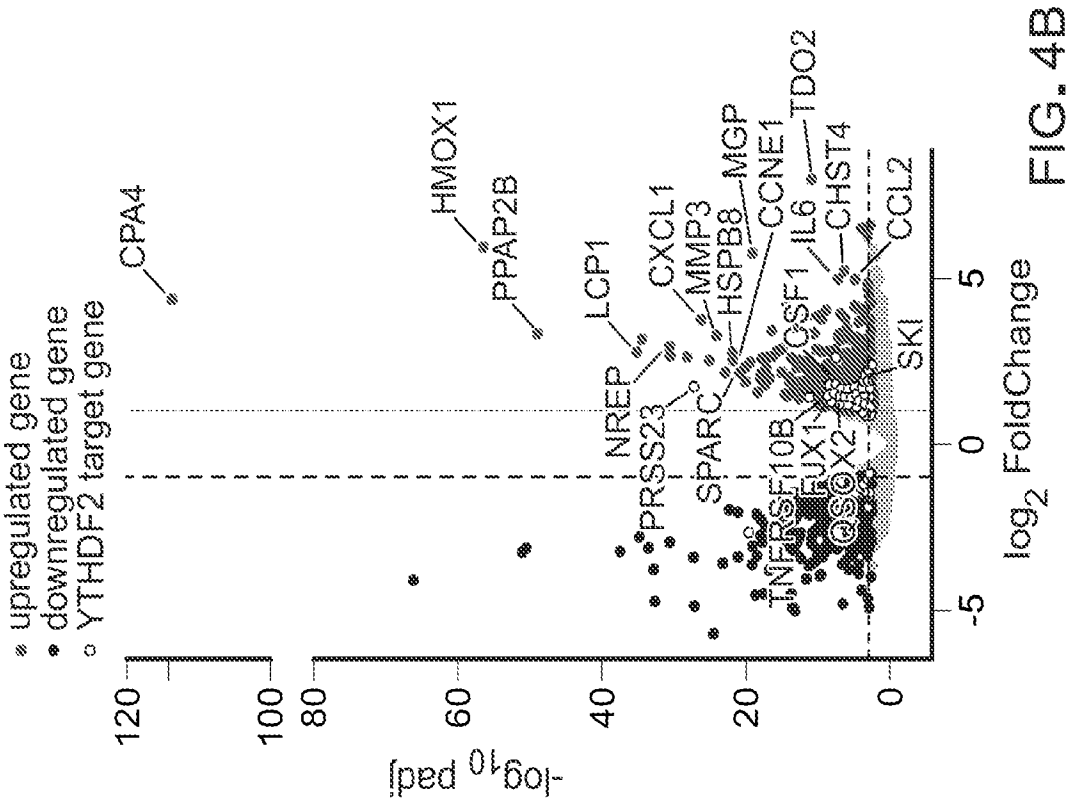

upregulated gene
downregulated gene
YTHDF2 target gene
CPA4
HMOX1
PPAP2B
LCP1
CXCL1
MMP3
HSPB8
MGP
CCNE1
TDO2
IL6
CHST4
CCL2
CSF1
SKI
NREP
PRSS23
SPARC
FUX1
TNFRSF10B
-log10 padj
log2 FoldChange

FIG. 4B

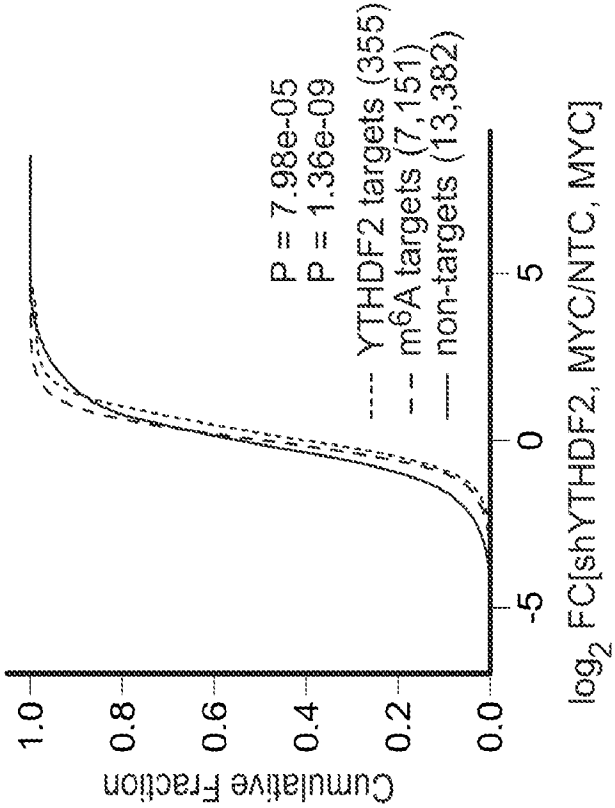

P = 7.98e-05
P = 1.36e-09
YTHDF2 targets (355)
m6A targets (7,151)
non-targets (13,382)
Cumulative Fraction
log2 FC[shYTHDF2, MYC/NTC, MYC]

FIG. 4A

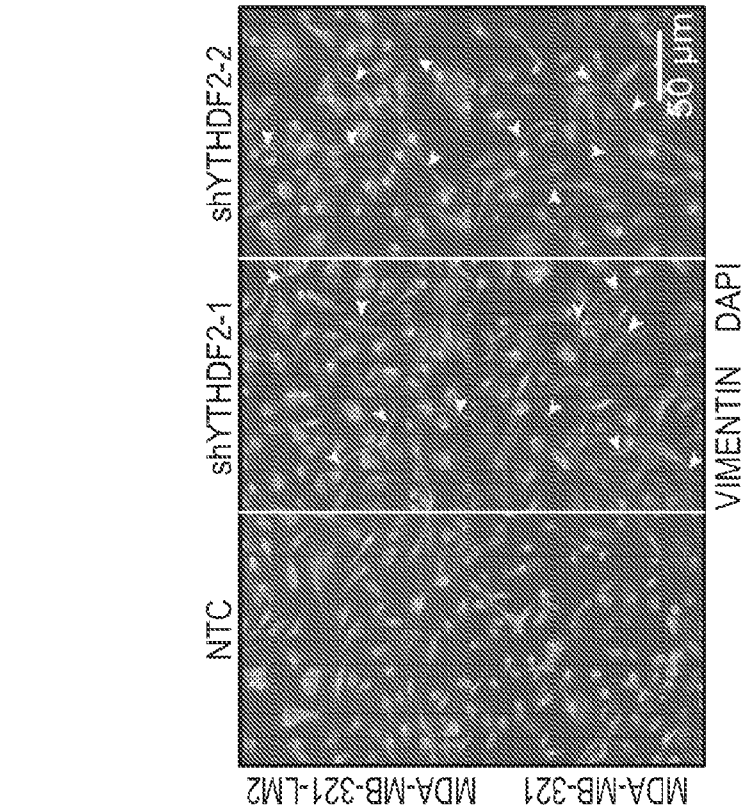

NTC
shYTHDF2-1
shYTHDF2-2
50 μm
VIMENTIN DAPI
MDA-MB-321
MDA-MB-321-LM2

FIG. 4D

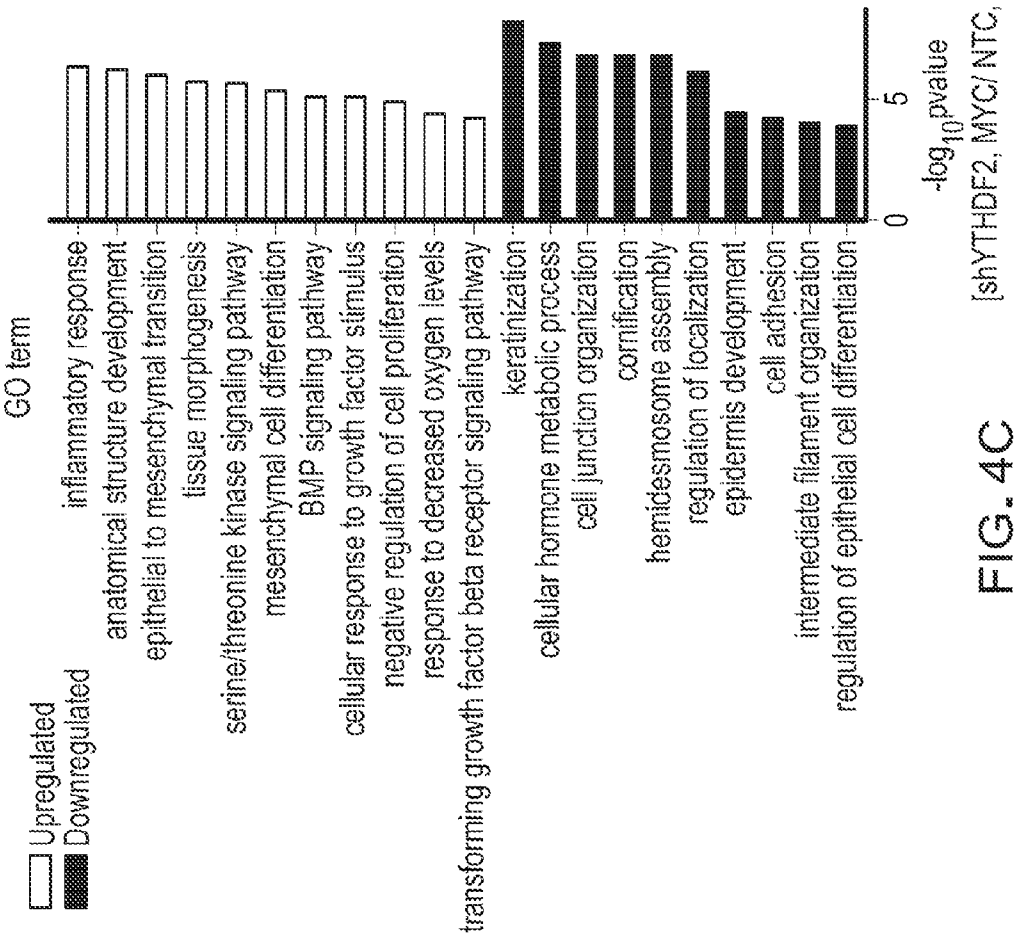

GO term
Upregulated
Downregulated
inflammatory response
anatomical structure development
epithelial to mesenchymal transition
tissue morphogenesis
serine/threonine kinase signaling pathway
mesenchymal cell differentiation
BMP signaling pathway
cellular response to growth factor stimulus
negative regulation of cell proliferation
response to decreased oxygen levels
transforming growth factor beta receptor signaling pathway
keratinization
cellular hormone metabolic process
cell junction organization
cornification
hemidesmosome assembly
regulation of localization
epidermis development
cell adhesion
intermediate filament organization
regulation of epithelial cell differentiation
0
5
-log10pvalue
[shYTHDF2, MYC/ NTC, MYC]

FIG. 4C

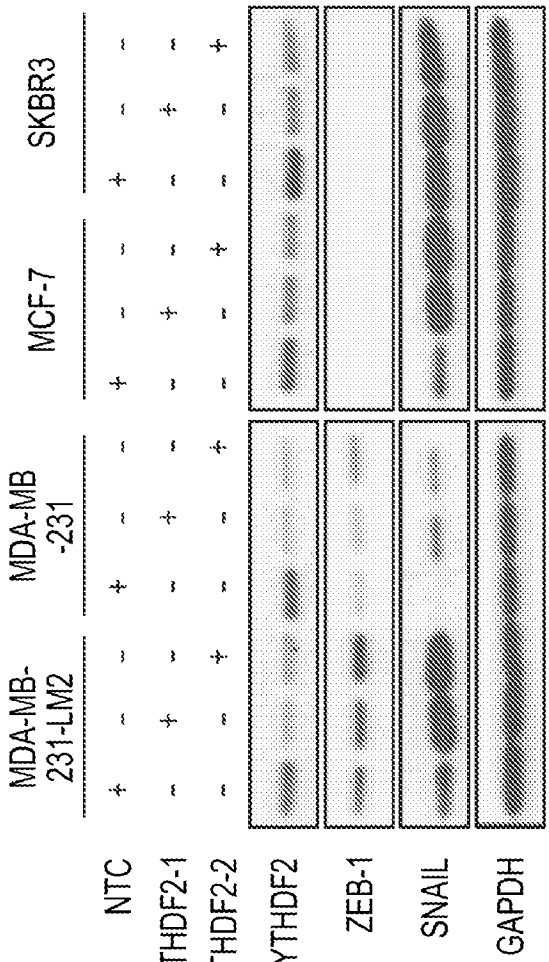

MDA-MB-231-LM2
MDA-MB-231
MCF-7
SKBR3
NTC
shYTHDF2-1
shYTHDF2-2
YTHDF2
ZEB-1
SNAIL
GAPDH

FIG. 4F

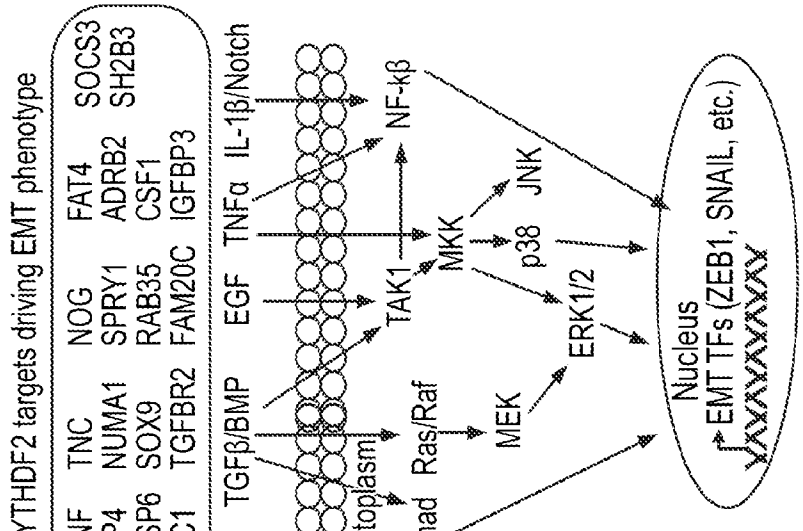

YTHDF2 targets driving EMT phenotype
BDNF TNC NOG FAT4 SOCS3
BMP4 NUMA1 SPRY1 ADRB2 SH2B3
DUSP6 SOX9 RAB35 CSF1
GPC1 TGFBR2 FAM20C IGFBP3
TGFβ/BMP
EGF
TNFα
IL-1β/Notch
Cytoplasm
Smad
Ras/Raf
MEK
TAK1
MKK
p38
JNK
ERK1/2
NF-kβ
Nucleus
EMT TFs (ZEB1, SNAIL, etc.)

FIG. 4E

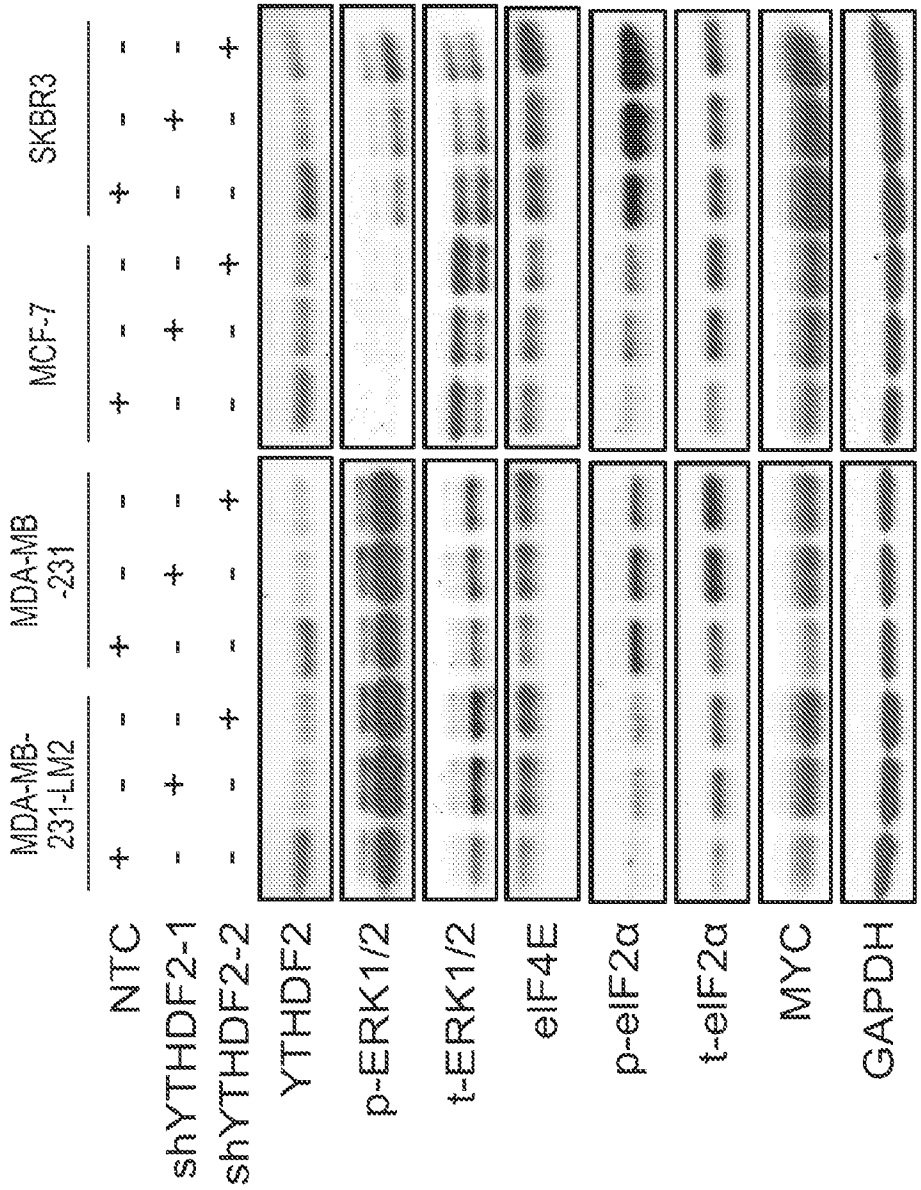

MDA-MB-231-LM2
MDA-MB-231
MCF-7
SKBR3
NTC
shYTHDF2-1
shYTHDF2-2
YTHDF2
p-ERK1/2
t-ERK1/2
eIF4E
p-eIF2α
t-eIF2α
MYC
GAPDH

FIG. 4G

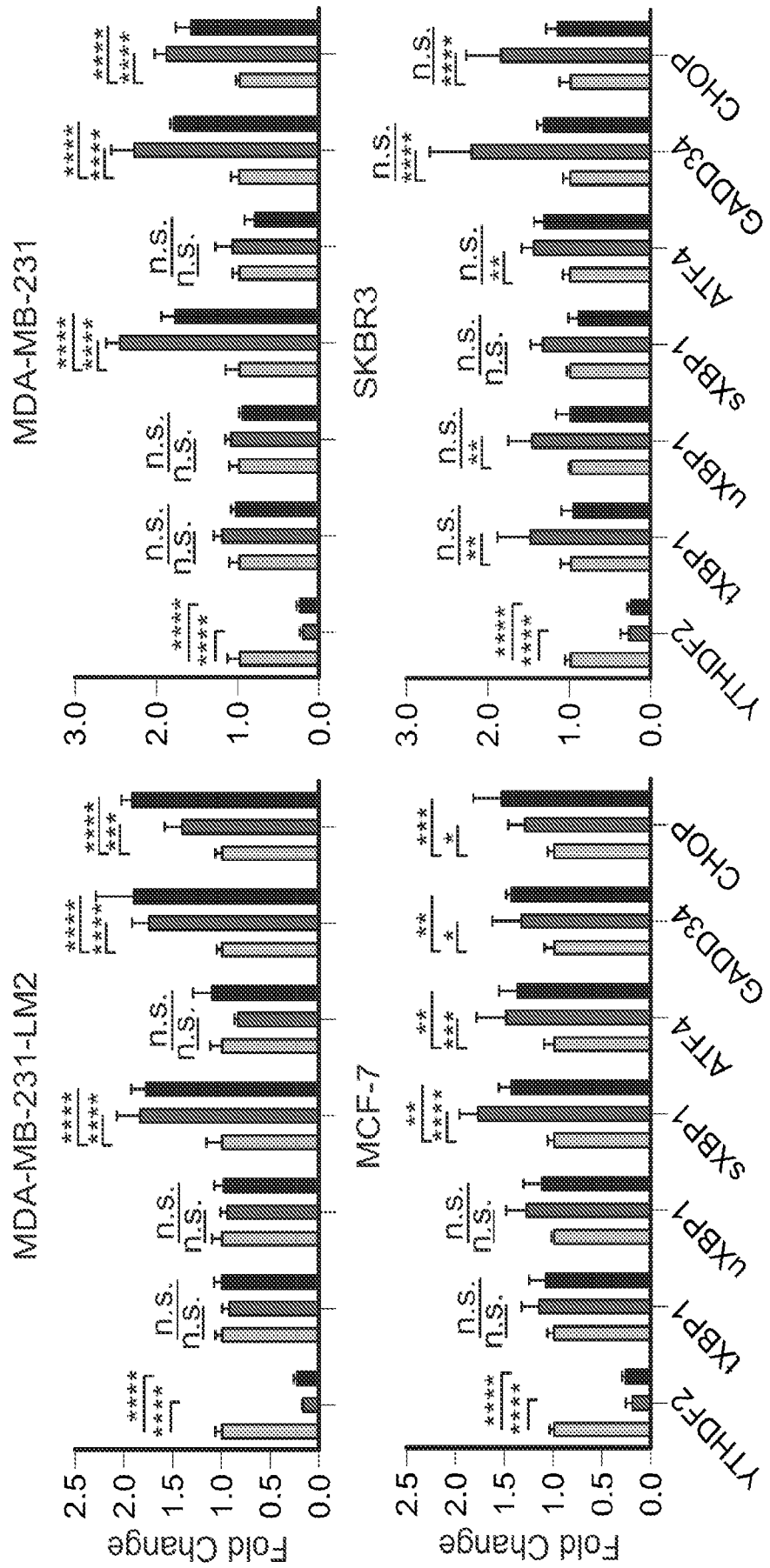

MDA-MB-231
SKBR3
MDA-MB-231-LM2
MCF-7
Fold Change
NTC
shYTHDF2-1
shYTHDF2-2
YTHDF2
UXBP1
UXBP1
SXBP1
ATF4
GADD34
CHOP

FIG. 4H

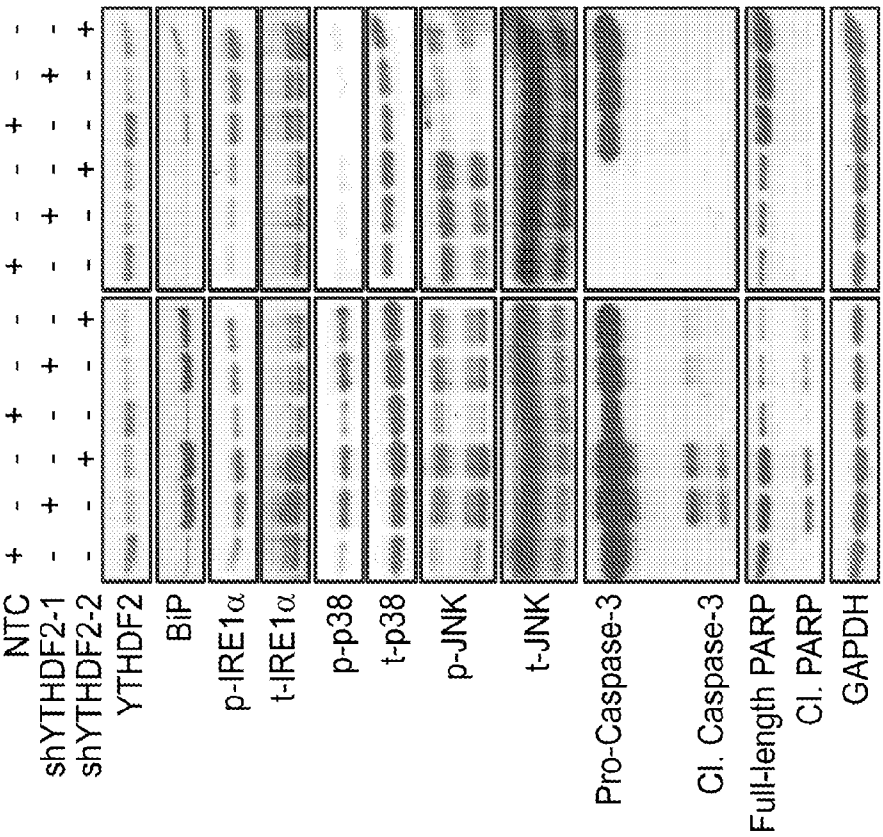

MDA-MB-231-LM2
MDA-MB-231
MCF-7
SKBR3
NTC
shYTHDF2-1
shYTHDF2-2
YTHDF2
BiP
p-IRE1α
t-IRE1α
p-p38
t-p38
p-JNK
t-JNK
Pro-Caspase-3
Cl. Caspase-3
Full-length PARP
Cl. PARP
GAPDH

FIG. 5B

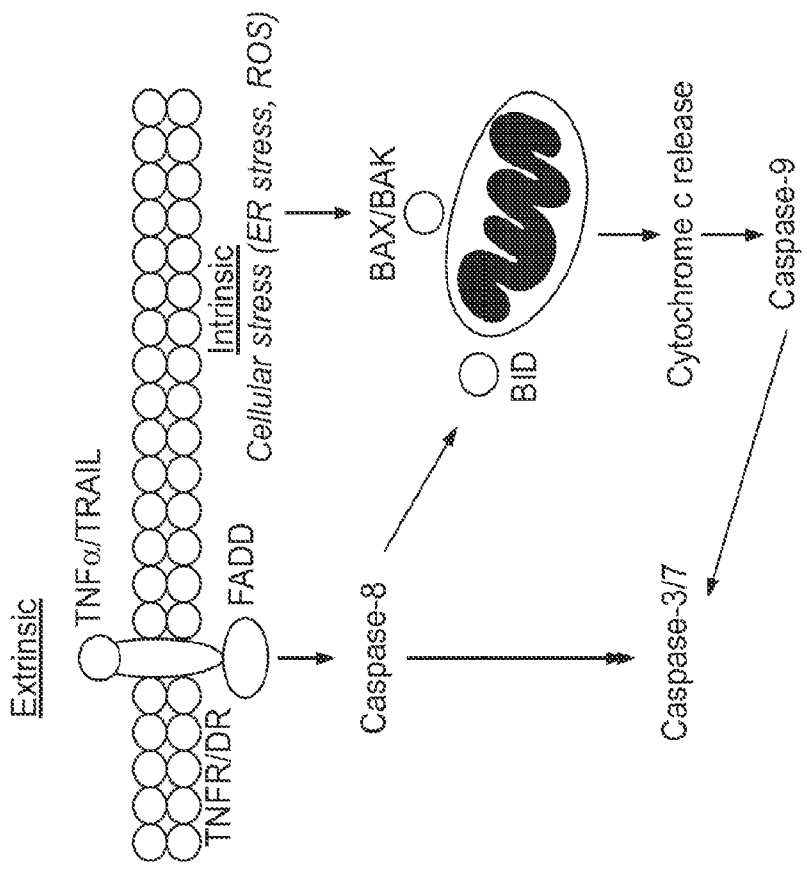

Extrinsic
TNFα/TRAIL
TNFR/DR
FADD
Caspase-8
Intrinsic
Cellular stress (ER stress, ROS)
BAX/BAK
BID
Cytochrome c release
Caspase-9
Caspase-3/7

FIG. 5A

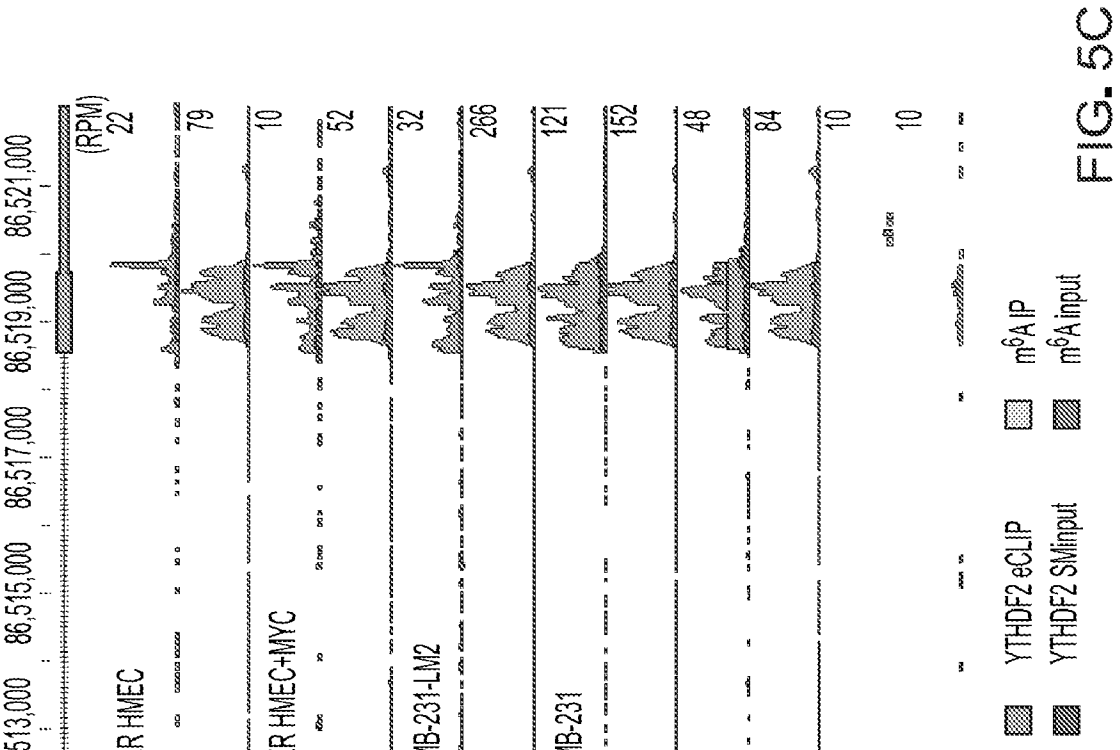

chr11:
PRSS23
86,513,000
86,515,000
86,517,000
86,519,000
86,521,000
(RPM)
MYC-ER HMEC
MYC-ER HMEC+MYC
MDA-MB-231-LM2
MDA-MB-231
MCF-7
SKBR3
22
79
10
52
32
266
121
152
48
84
10
10
YTHDF2 eCLIP
YTHDF2 SMinput
m6A IP
m6A input

FIG. 5C

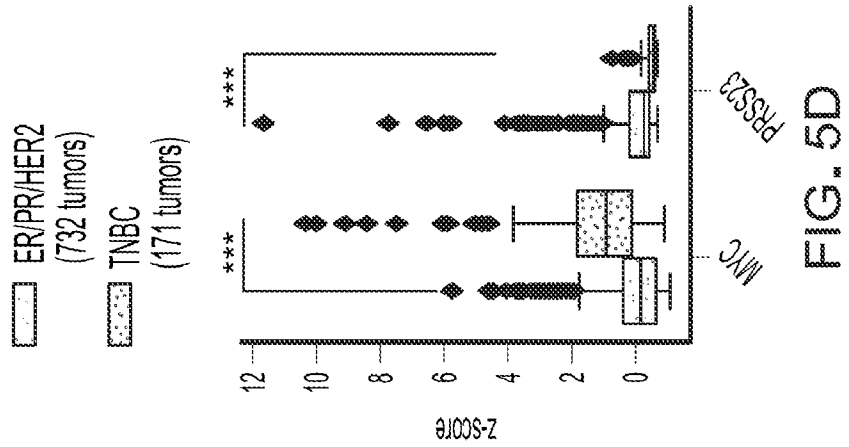

ER/PR/HER2
(732 tumors)
TNBC
(171 tumors)
***
***
Z-score
12
10
8
6
4
2
0
MYC
PRSS23

FIG. 5D

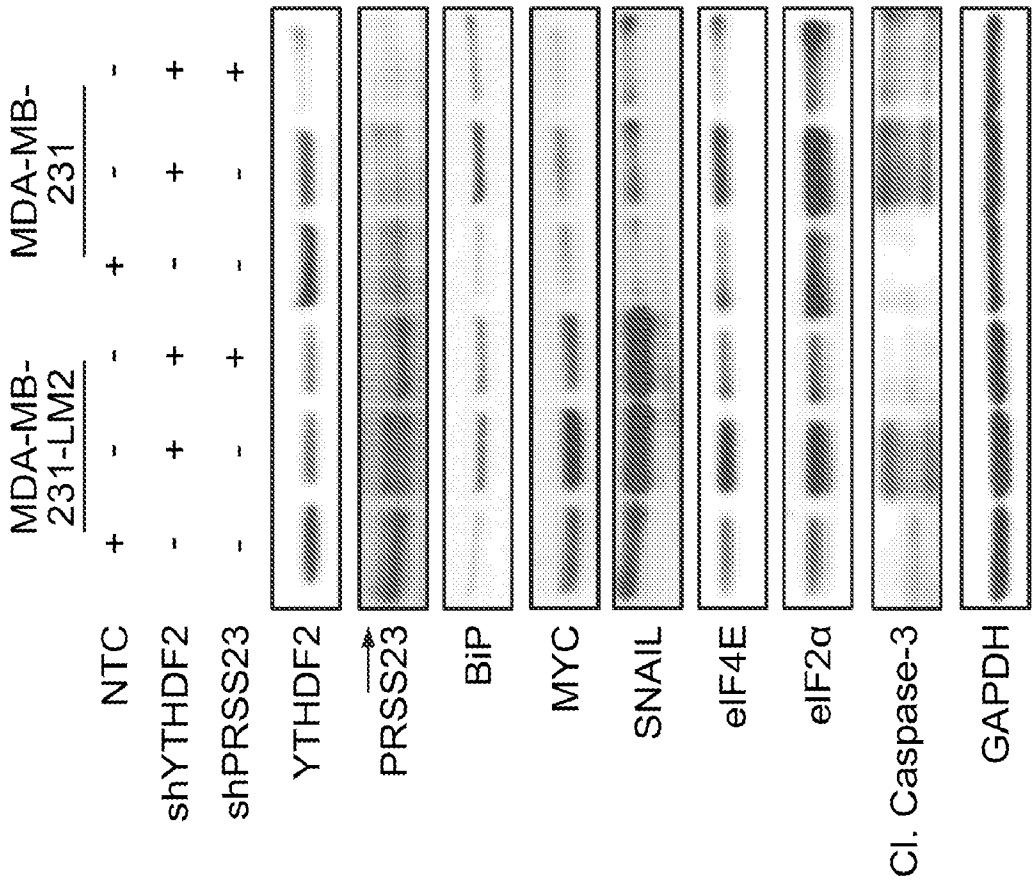

MDA-MB-231-LM2
MDA-MB-231
NTC
shYTHDF2
shPRSS23
YTHDF2
PRSS23
BiP
MYC
SNAIL
eIF4E
eIF2α
Cl. Caspase-3
GAPDH

FIG. 5F

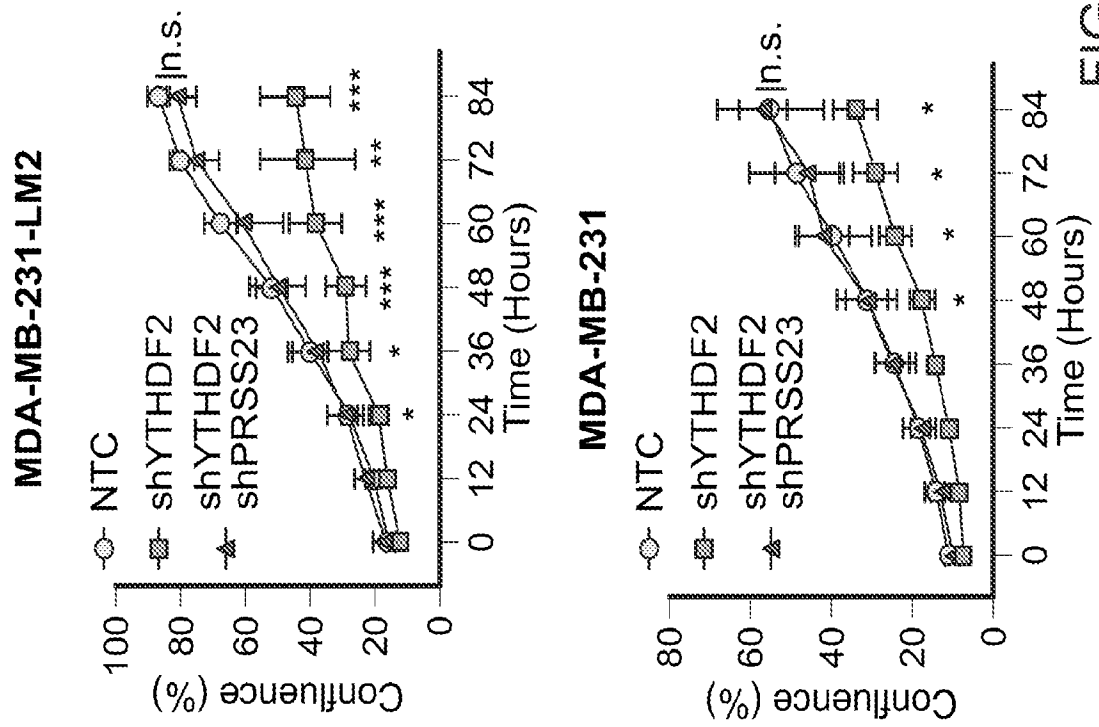

MDA-MB-231-LM2
MDA-MB-231
NTC
shYTHDF2
shPRSS23
n.s.
Confluence (%)
Time (Hours)
0 12 24 36 48 60 72 84

FIG. 5E

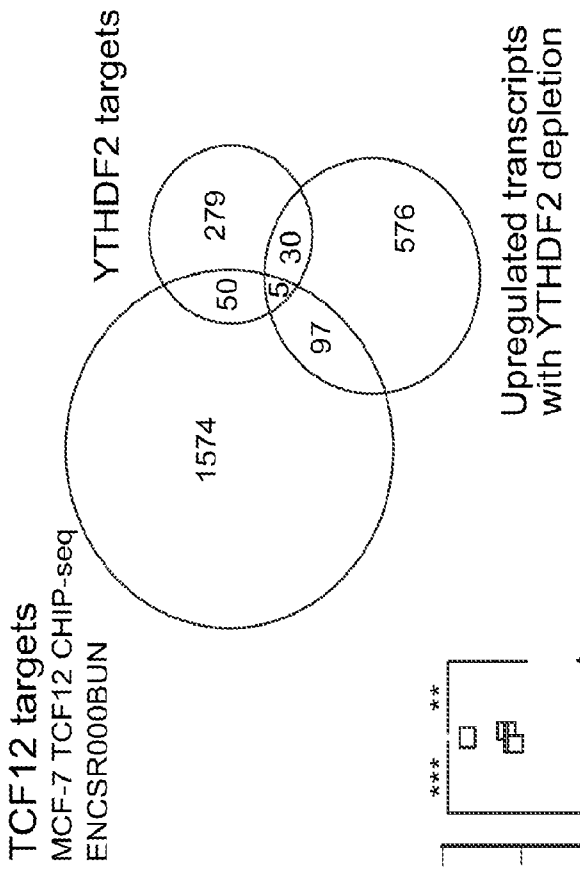


FIG. 5H

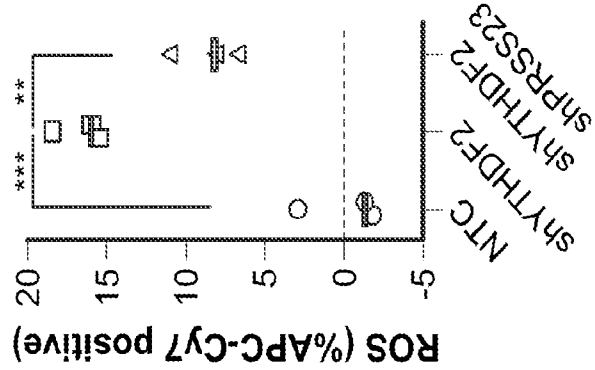


FIG. 5I

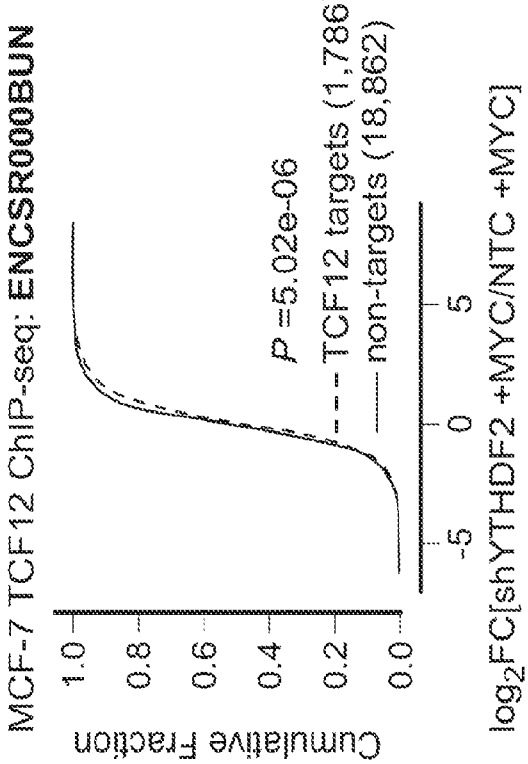


FIG. 5G

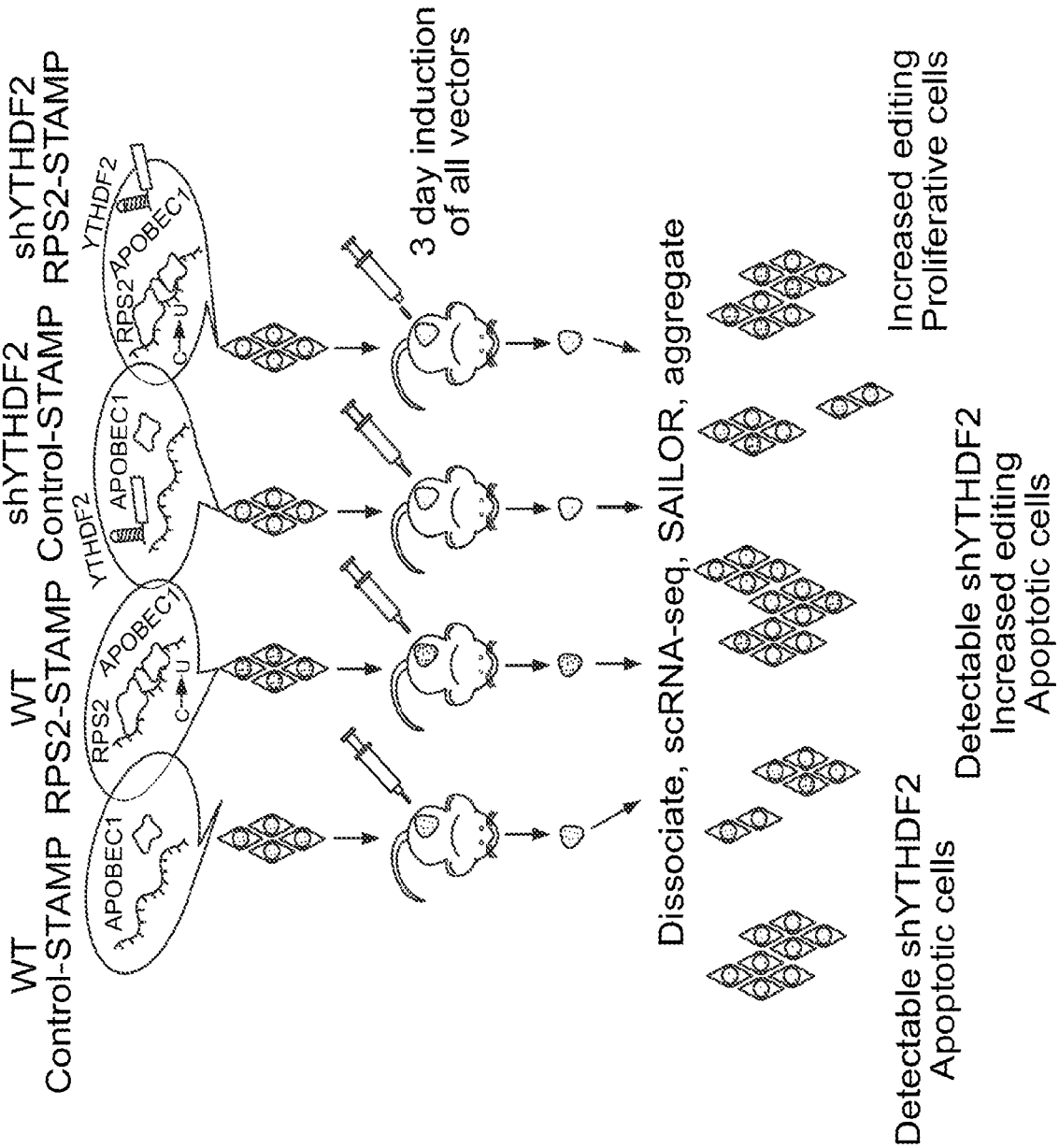
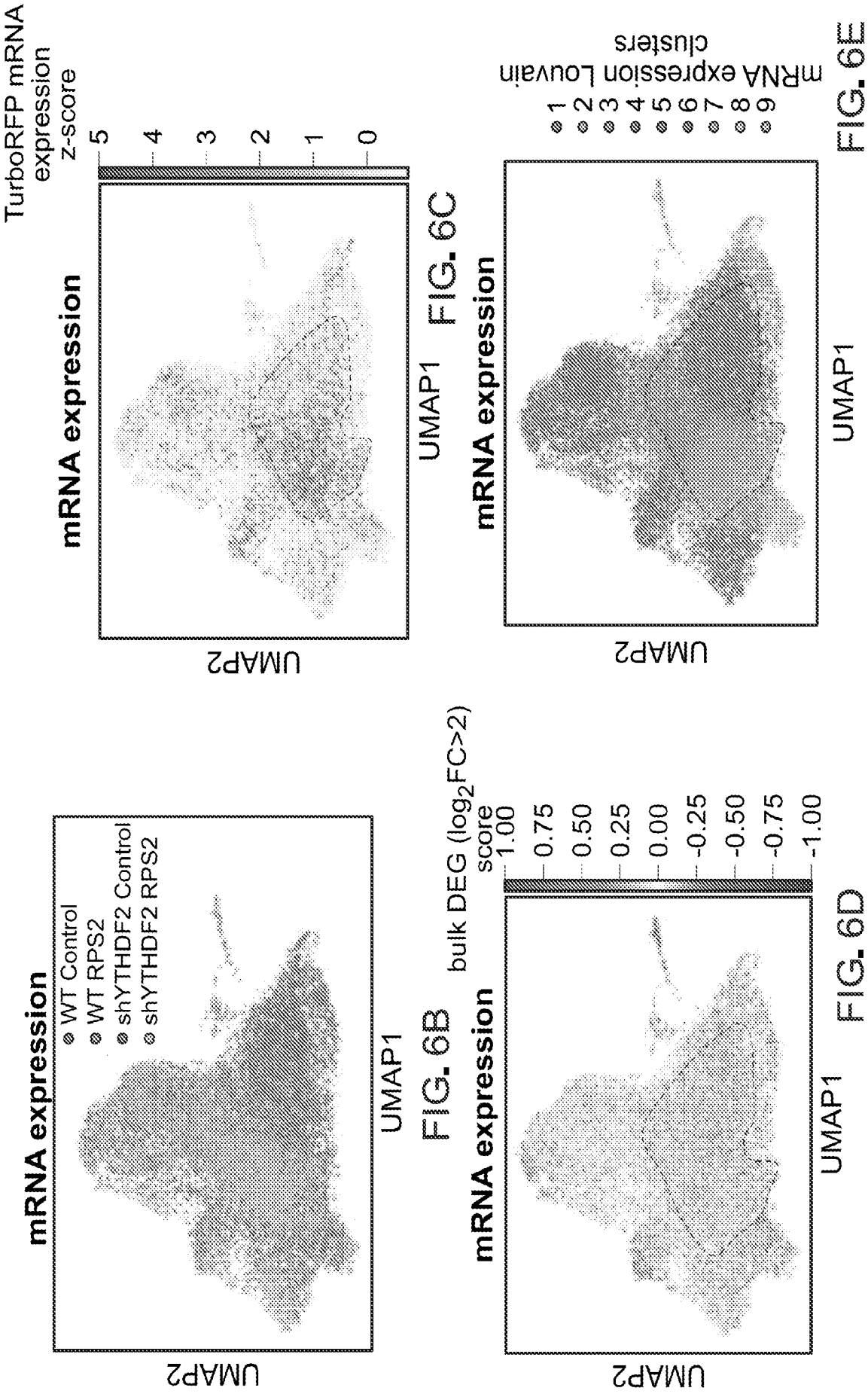

WT
Control-STAMP
WT
RPS2-STAMP
shYTHDF2
Control-STAMP
shYTHDF2
RPS2-STAMP
APOBEC1
RPS2
C→U
YTHDF2
3 day induction
of all vectors
Dissociate, scRNA-seq, SAILOR, aggregate
Increased editing
Proliferative cells
Detectable shYTHDF2
Apoptotic cells
Detectable shYTHDF2
Increased editing
Apoptotic cells

FIG. 6A


mRNA expression
WT Control
WT RPS2
shYTHDF2 Control
shYTHDF2 RPS2
UMAP1
UMAP2
FIG. 6B
mRNA expression
bulk DEG (log_2FC>2) score
1.00
0.75
0.50
0.25
0.00
-0.25
-0.50
-0.75
-1.00
UMAP1
UMAP2
FIG. 6D
mRNA expression
TurboRFP mRNA expression z-score
5
4
3
2
1
0
UMAP1
UMAP2
FIG. 6C
mRNA expression
mRNA expression Louvain clusters
1
2
3
4
5
6
7
8
9
UMAP1
UMAP2
FIG. 6E

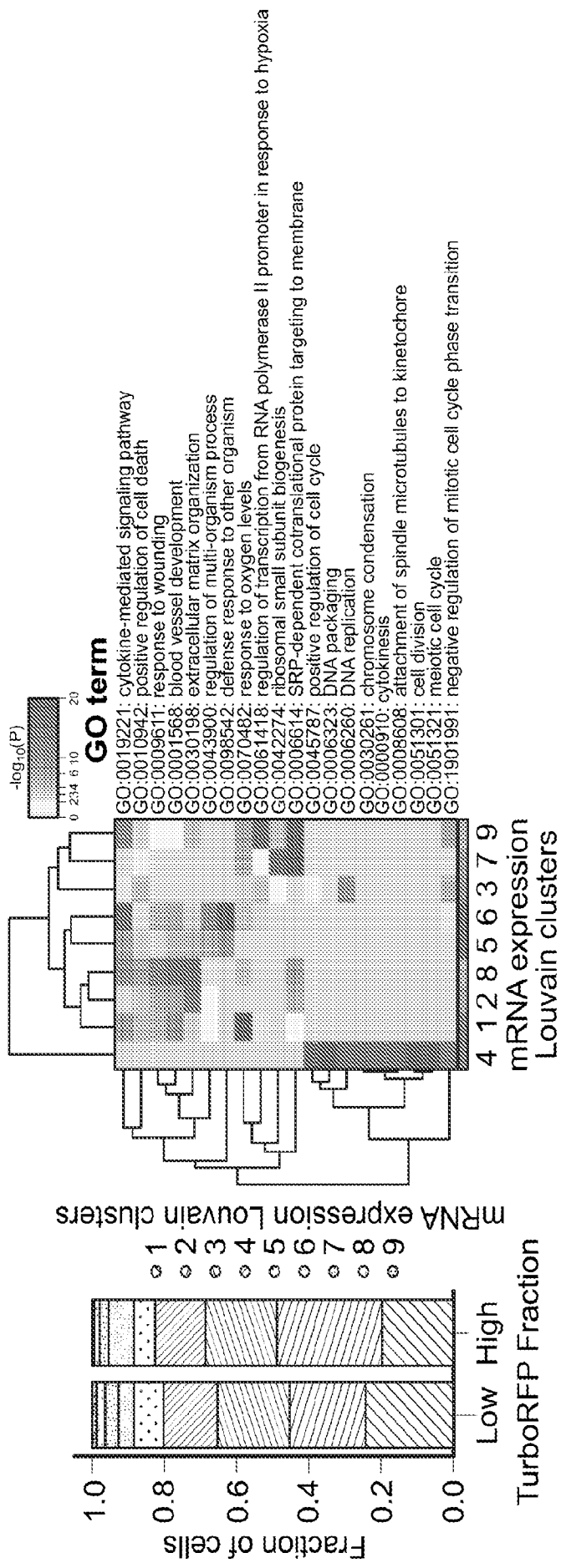

Fraction of cells
1.0
0.8
0.6
0.4
0.2
0.0
Low High
TurboRFP Fraction
mRNA expression Louvain clusters
1 2 3 4 5 6 7 8 9
mRNA expression Louvain clusters
4 1 2 8 5 6 3 7 9
GO term
-log10(P)
0 2 3 4 6 10 20
GO:0019221: cytokine-mediated signaling pathway
GO:0010942: positive regulation of cell death
GO:0009611: response to wounding
GO:0001568: blood vessel development
GO:0030198: extracellular matrix organization
GO:0043900: regulation of multi-organism process
GO:0098542: defense response to other organism
GO:0070482: response to oxygen levels
GO:0061418: regulation of transcription from RNA polymerase II promoter in response to hypoxia
GO:0042274: ribosomal small subunit biogenesis
GO:0006614: SRP-dependent cotranslational protein targeting to membrane
GO:0045787: positive regulation of cell cycle
GO:0006323: DNA packaging
GO:0006260: DNA replication
GO:0030261: chromosome condensation
GO:0000910: cytokinesis
GO:0008608: attachment of spindle microtubules to kinetochore
GO:0051301: cell division
GO:0051321: meiotic cell cycle
GO:1901991: negative regulation of mitotic cell cycle phase transition

FIG. 6F

FIG. 6G

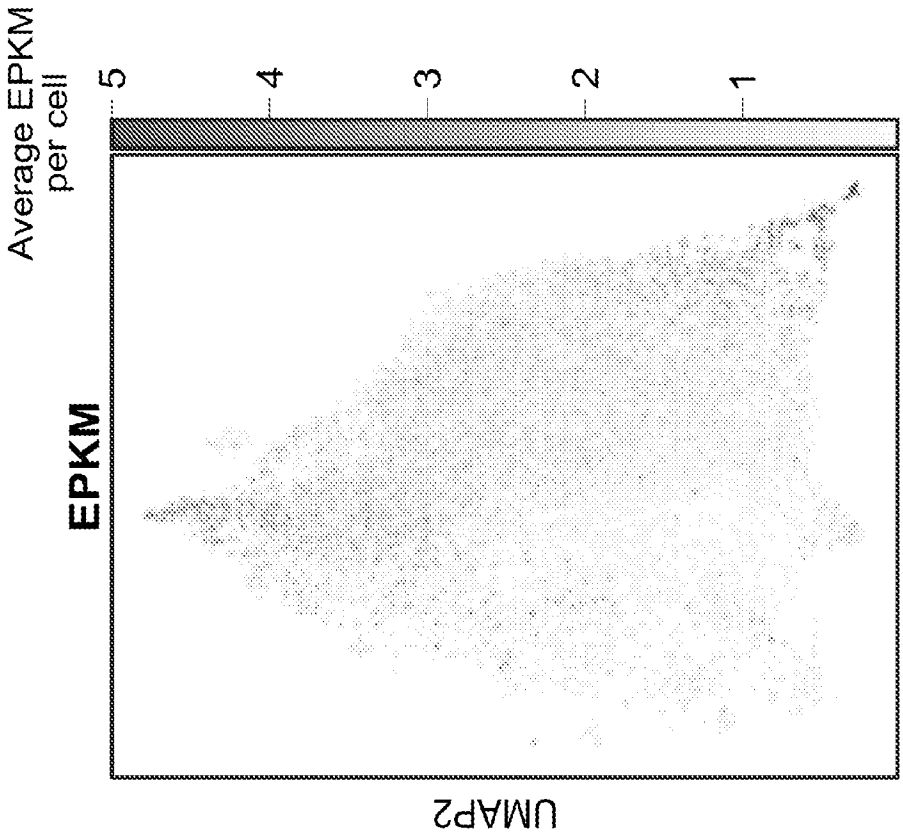

Average EPKM per cell
5
4
3
2
1
EPKM
UMAP1
UMAP2

FIG. 6I

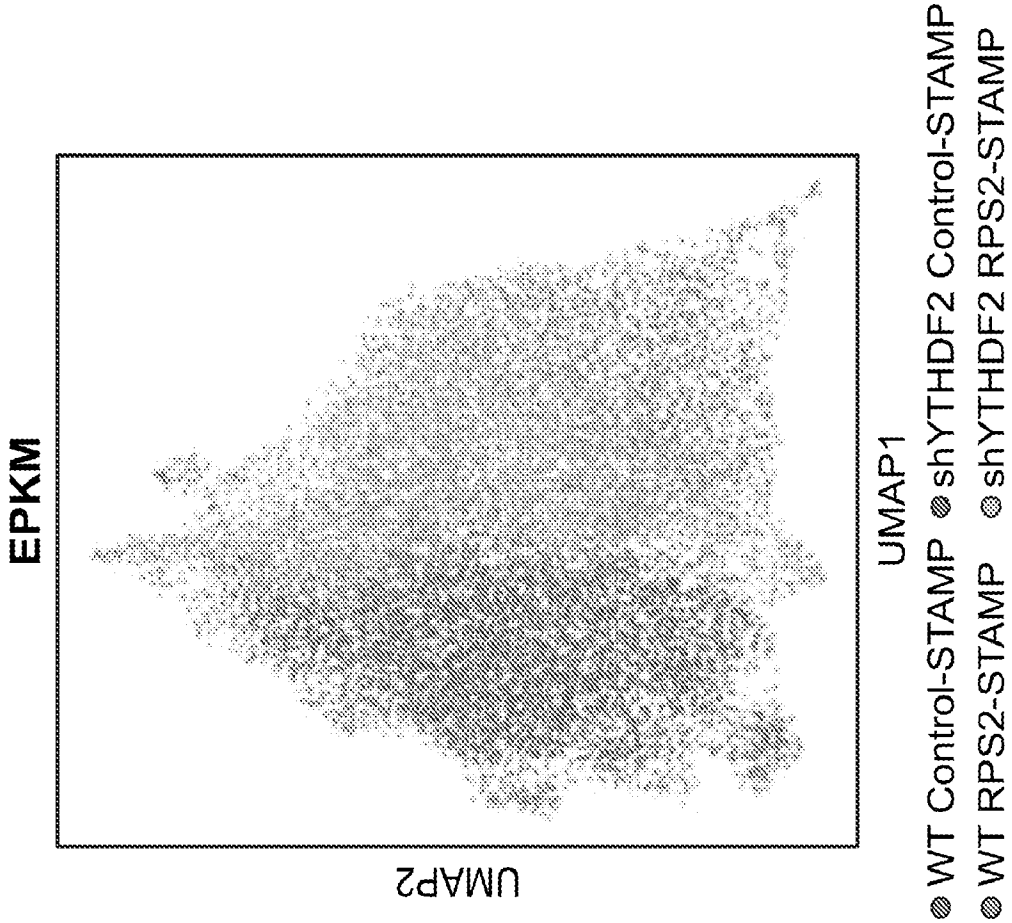

EPKM
UMAP1
UMAP2
WT Control-STAMP
shYTHDF2 Control-STAMP
WT RPS2-STAMP
shYTHDF2 RPS2-STAMP

FIG. 6H

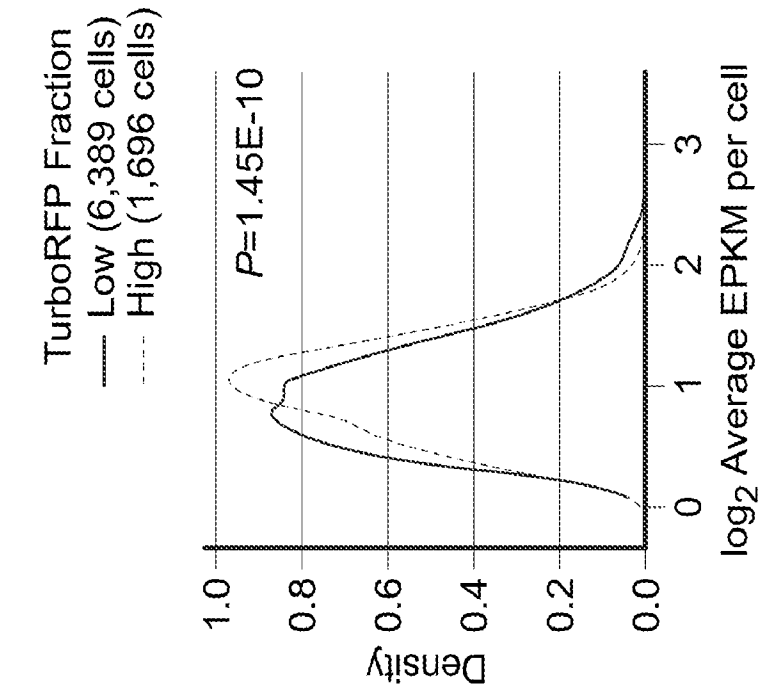

TurboRFP Fraction
Low (6,389 cells)
High (1,696 cells)
P=1.45E-10
Density
1.0
0.8
0.6
0.4
0.2
0.0
0
1
2
3
log2 Average EPKM per cell

FIG. 6K


Fraction of cluster in sample
1.0
0.8
0.6
0.4
0.2
0.0
WT Control-STAMP
WT RPS2-STAMP
shYTHDF2 Control-STAMP
shYTHDF2 RPS2-STAMP

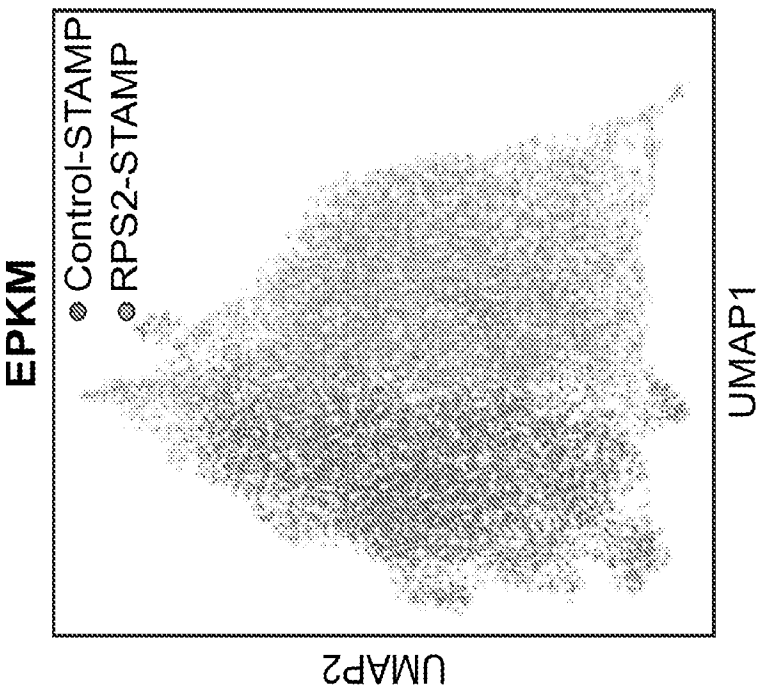

EPKM
Control-STAMP
RPS2-STAMP
UMAP1
UMAP2

FIG. 6J

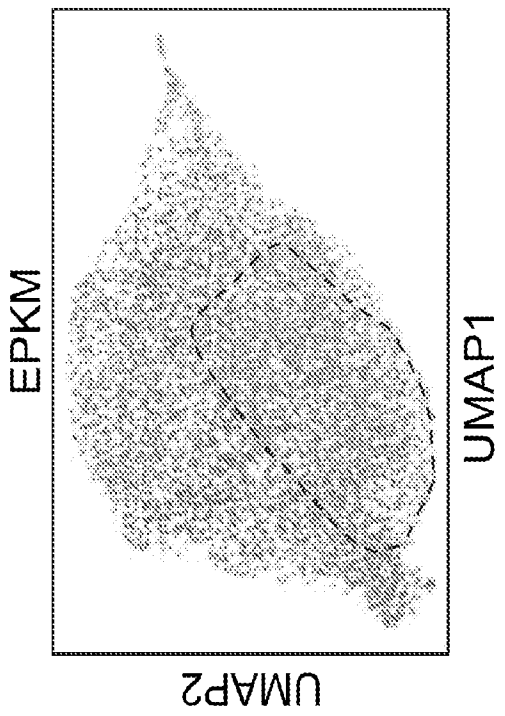
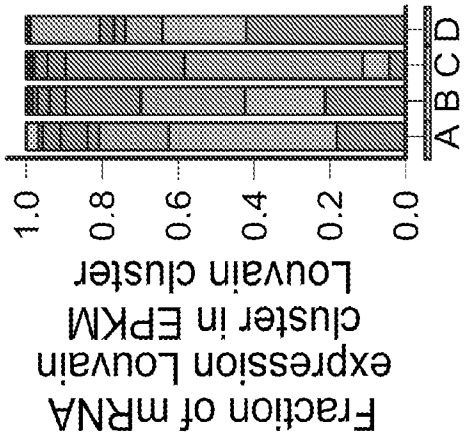
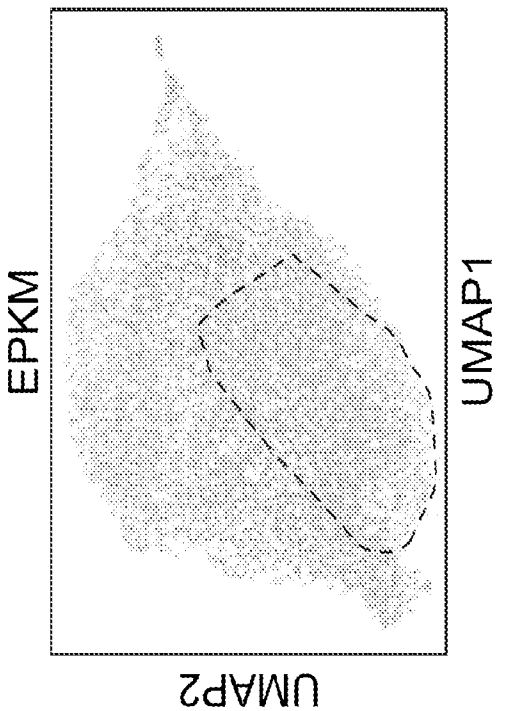

EPKM
UMAP1
UMAP2
mRNA expression
Louvain clusters
1
2
3
4
5
6
7
8
9

FIG. 7A


Fraction of mRNA
expression Louvain
cluster in EPKM
Louvain cluster
1.0
0.8
0.6
0.4
0.2
0.0
A
B
C
D


EPKM
UMAP1
UMAP2
EPKM
Louvain clusters
A
B
C
D

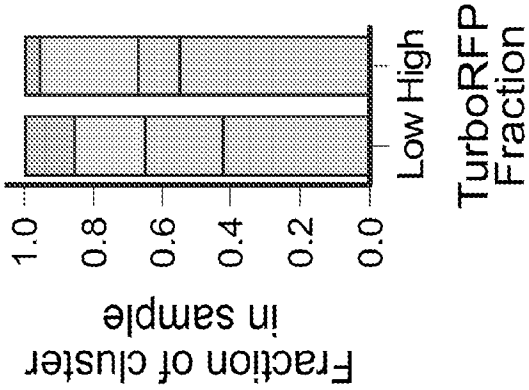

Fraction of cluster
in sample
1.0
0.8
0.6
0.4
0.2
0.0
Low
High
TurboRFP
Fraction

FIG. 7B

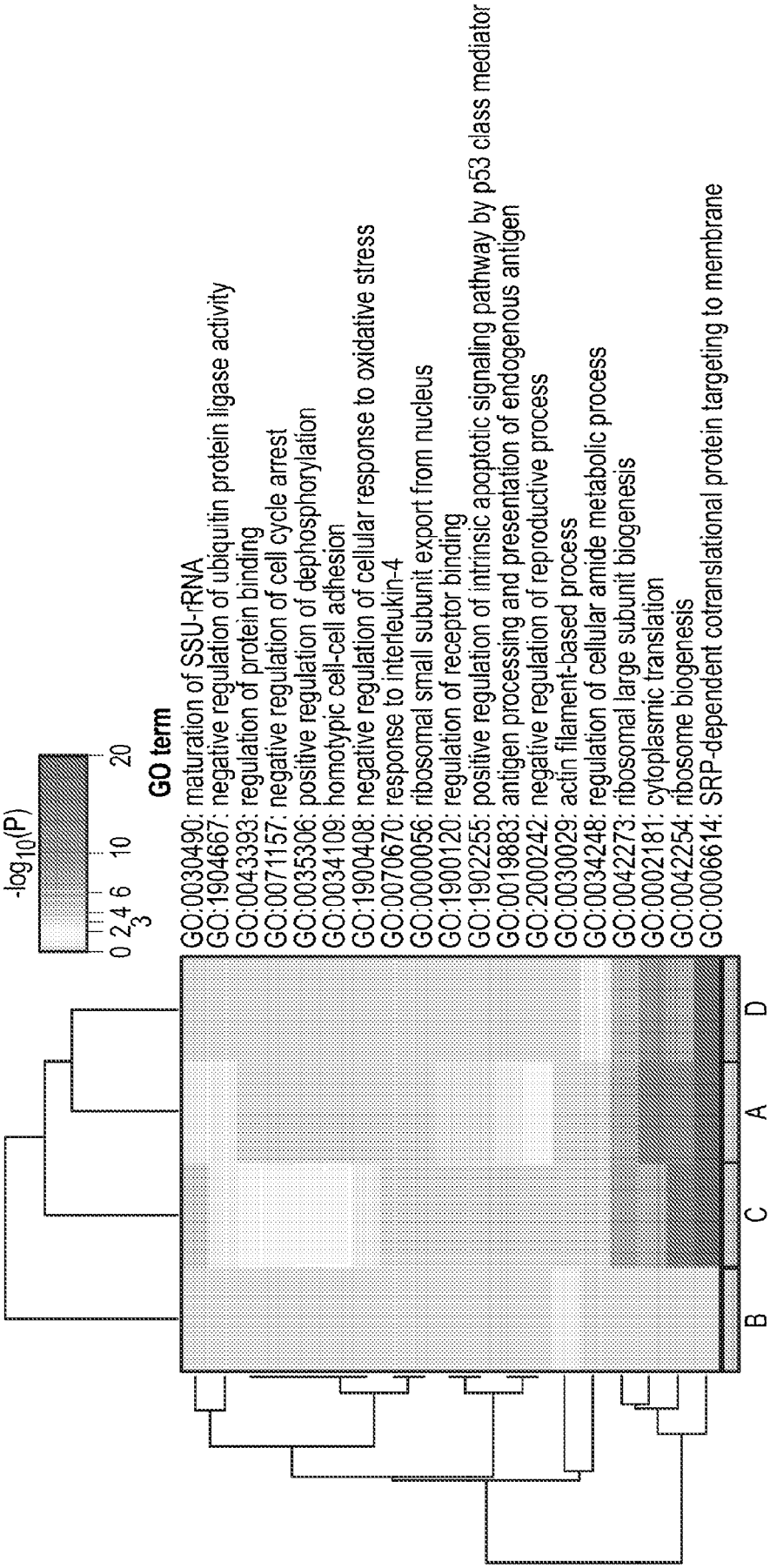

-log10(P)
0 2 4 6 10 20
3
GO term
GO:0030490: maturation of SSU-rRNA
GO:1904667: negative regulation of ubiquitin protein ligase activity
GO:0043393: regulation of protein binding
GO:0071157: negative regulation of cell cycle arrest
GO:0035306: positive regulation of dephosphorylation
GO:0034109: homotypic cell-cell adhesion
GO:1900408: negative regulation of cellular response to oxidative stress
GO:0070670: response to interleukin-4
GO:0000056: ribosomal small subunit export from nucleus
GO:1900120: regulation of receptor binding
GO:1902255: positive regulation of intrinsic apoptotic signaling pathway by p53 class mediator
GO:0019883: antigen processing and presentation of endogenous antigen
GO:2000242: negative regulation of reproductive process
GO:0030029: actin filament-based process
GO:0034248: regulation of cellular amide metabolic process
GO:0042273: ribosomal large subunit biogenesis
GO:0002181: cytoplasmic translation
GO:0042254: ribosome biogenesis
GO:0006614: SRP-dependent cotranslational protein targeting to membrane
B C A D
EPKM Louvin clusters

FIG. 7C

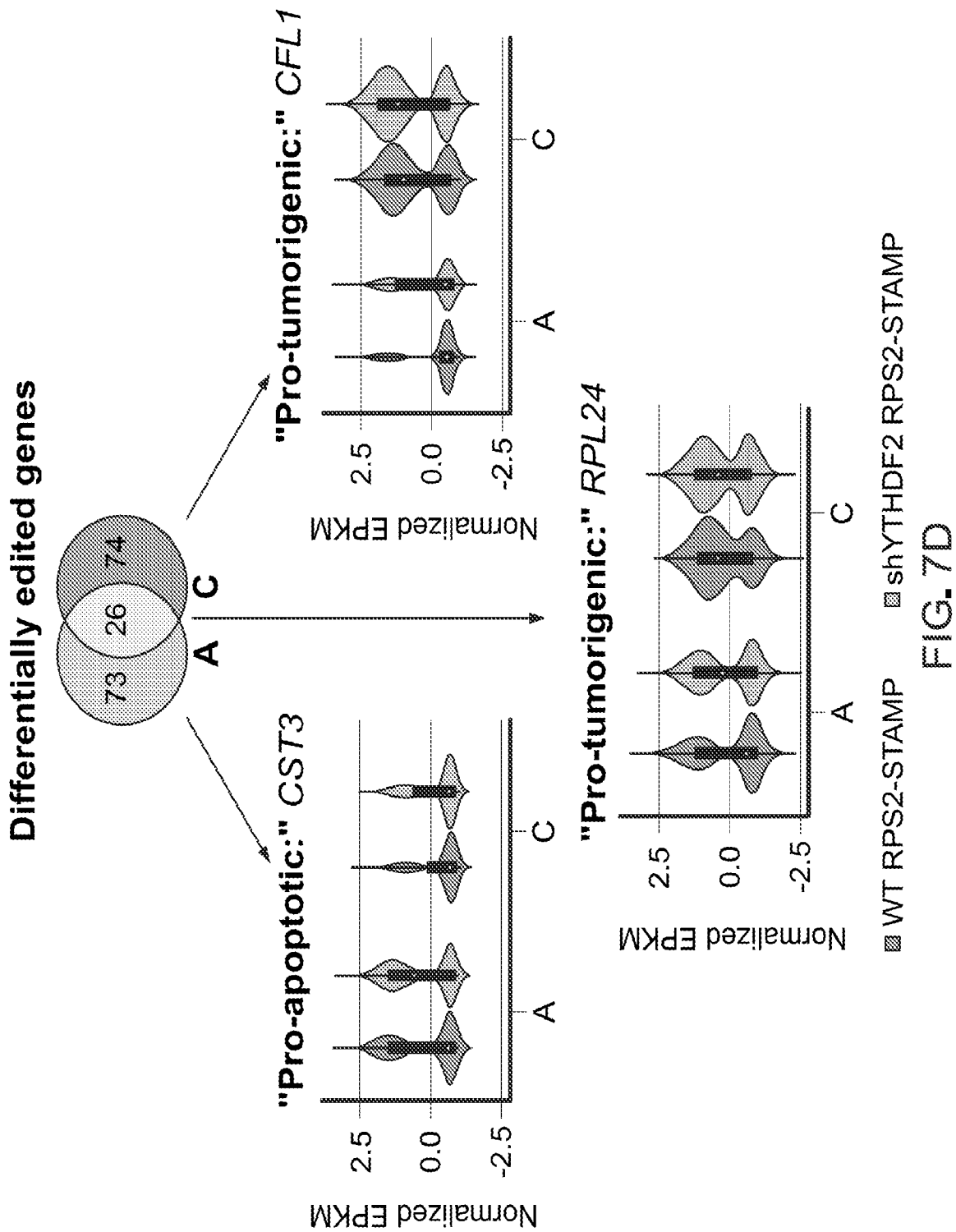

Differentially edited genes
73
26
74
A
C
"Pro-apoptotic:" CST3
"Pro-tumorigenic:" CFL1
"Pro-tumorigenic:" RPL24
Normalized EPKM
2.5
0.0
-2.5
A
C
WT RPS2-STAMP
shYTHDF2 RPS2-STAMP

FIG. 7D

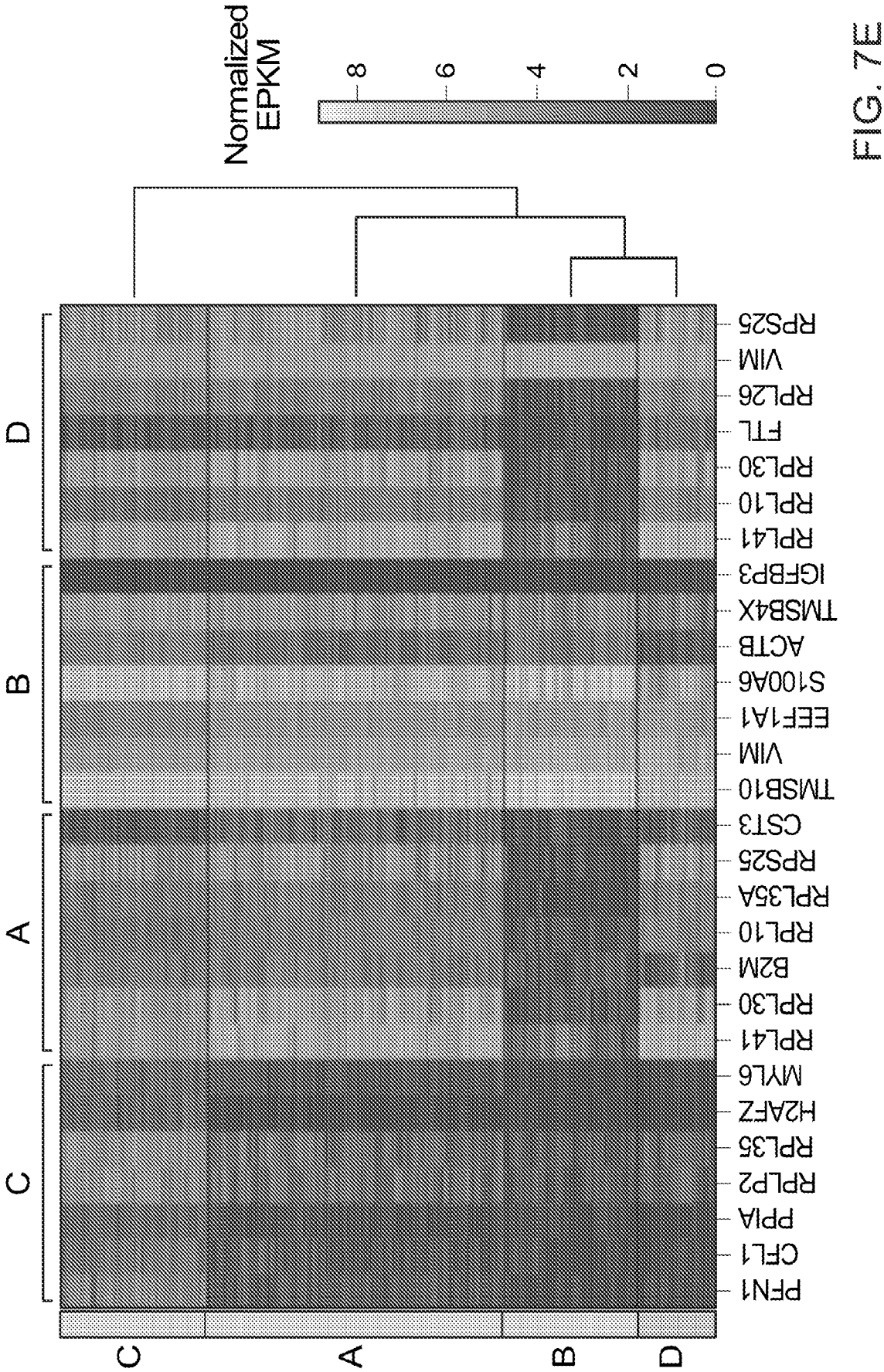

Normalized EPKM
8
6
4
2
0
C
A
B
D
PFN1
CFL1
PPIA
RPLP2
RPL35
H2AFZ
MYL6
RPL41
RPL30
B2M
RPL10
RPL35A
RPS25
CST3
TMSB10
VIM
EEF1A1
S100A6
ACTB
TMSB4X
IGFBP3
RPL41
RPL10
RPL30
FTL
RPL26
VIM
RPS25

FIG. 7E

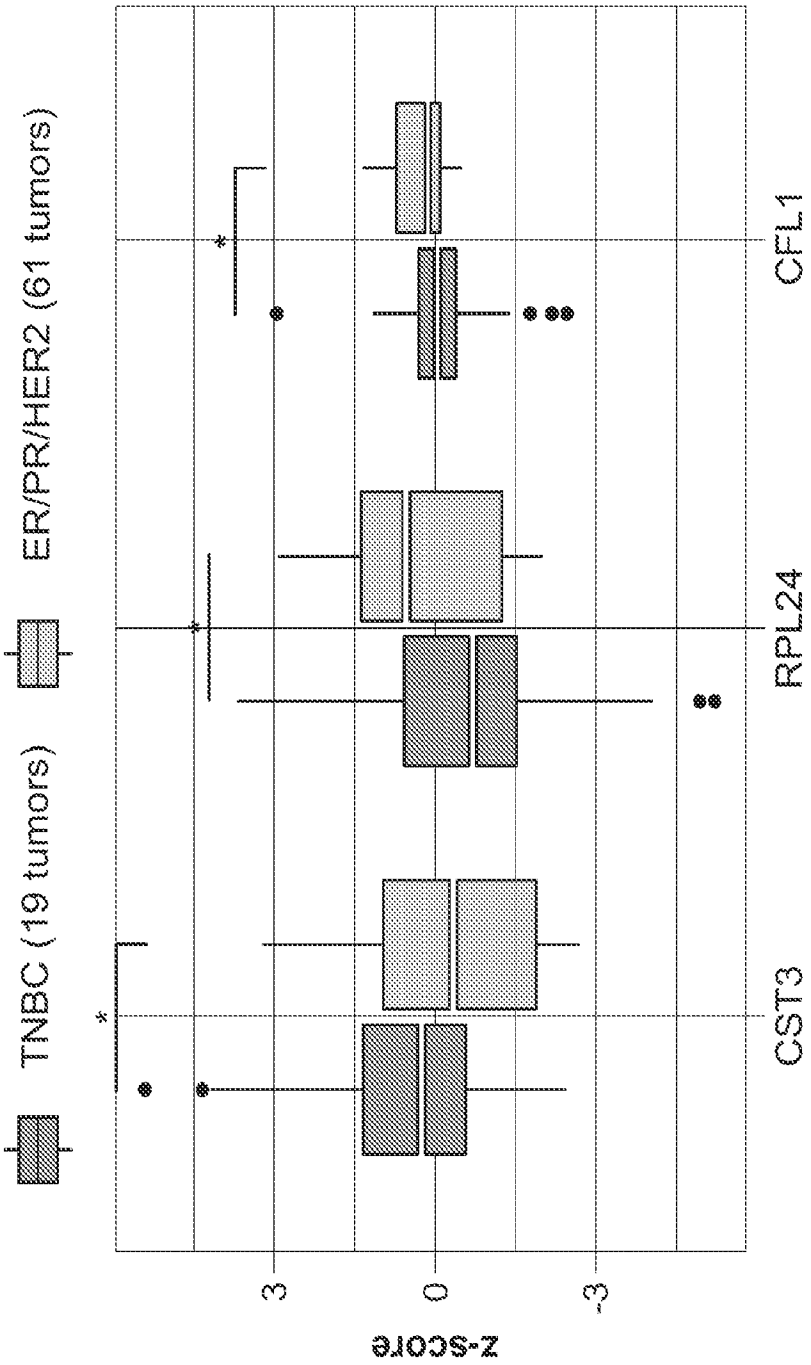

TNBC (19 tumors)
ER/PR/HER2 (61 tumors)
CFL1
RPL24
CST3
3
0
-3
z-score

FIG. 7F

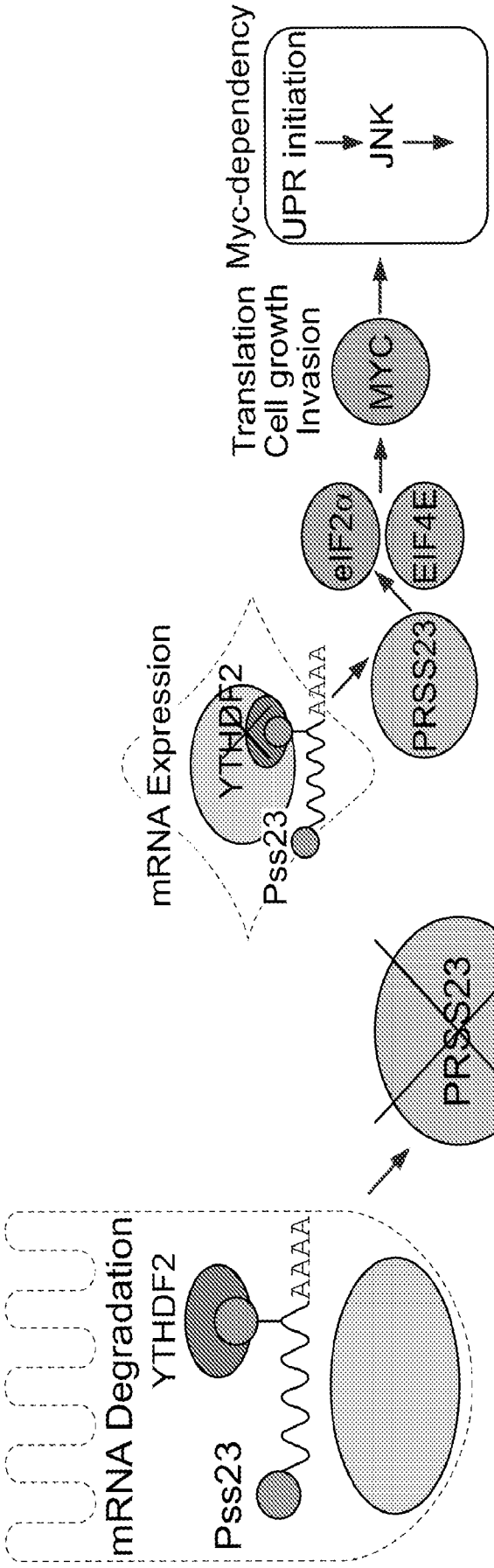

mRNA Degradation
YTHDF2
AAAA
Pss23
PRSS23
mRNA Expression
YTHDF2
AAAA
Pss23
PRSS23
eIF2α
EIF4E
Translation
Cell growth
Invasion
MYC
Myc-dependency
UPR initiation
JNK

FIG. 8A

FIG. 8B

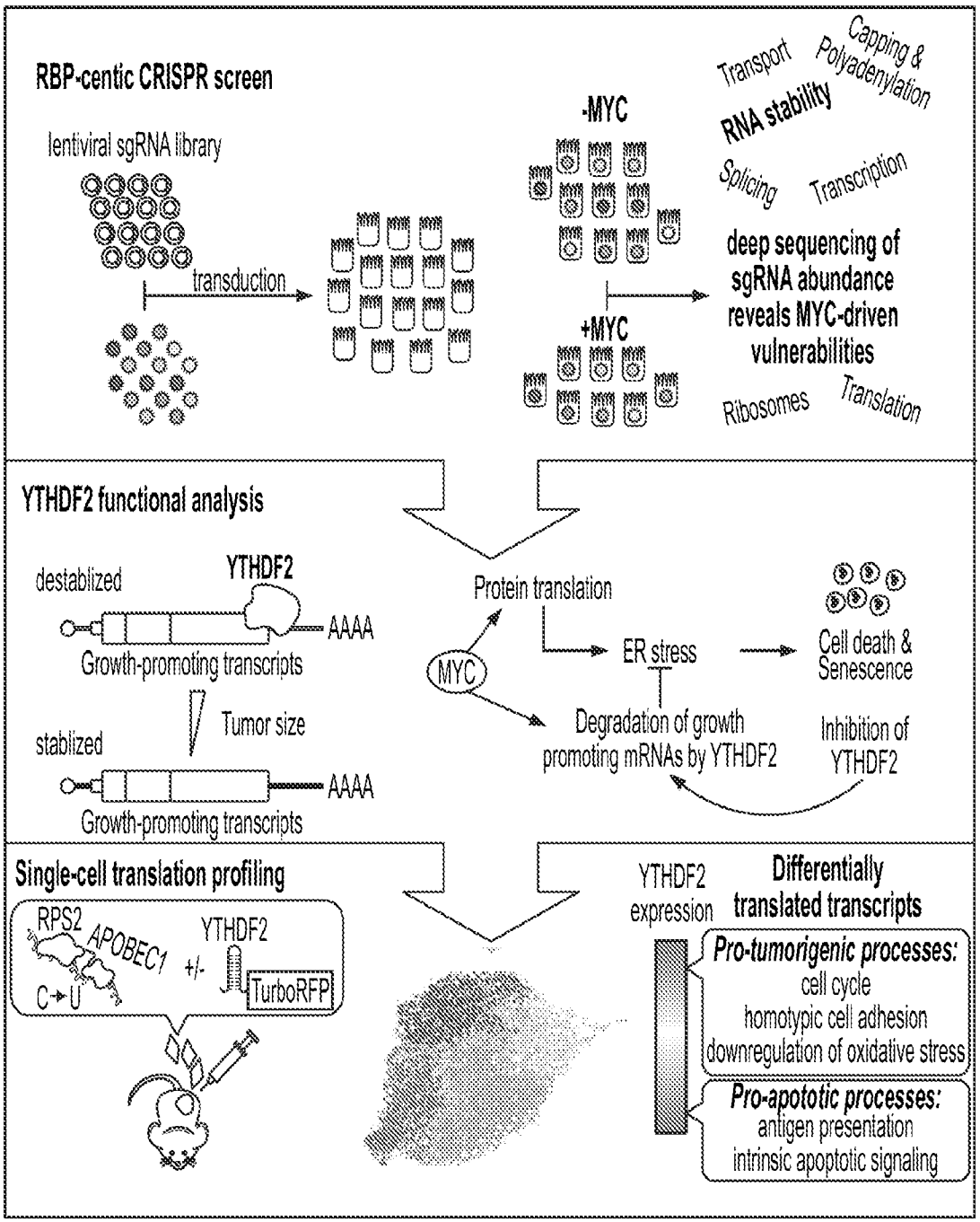

RBP-centic CRISPR screen
lentiviral sgRNA library
transduction
-MYC
+MYC
Transport
Capping & Polyadenylation
RNA stability
Splicing
Transcription
deep sequencing of sgRNA abundance reveals MYC-driven vulnerabilities
Ribosomes
Translation
YTHDF2 functional analysis
destablized
YTHDF2
AAAA
Growth-promoting transcripts
Tumor size
stablized
AAAA
Growth-promoting transcripts
Protein translation
MYC
ER stress
Cell death & Senescence
Degradation of growth promoting mRNAs by YTHDF2
Inhibition of YTHDF2
Single-cell translation profiling
RPS2
APOBEC1
C→U
YTHDF2
+/-
TurboRFP
YTHDF2 expression
Differentially translated transcripts
Pro-tumorigenic processes:
cell cycle
homotypic cell adhesion
downregulation of oxidative stress
Pro-apototic processes:
antigen presentation
intrinsic apoptotic signaling

FIG. 9

INTERNATIONAL SEARCH REPORT

International application No.
PCT/US2021/048208

A. CLASSIFICATION OF SUBJECT MATTER

IPC(8) - A61K 31/437; A61K 31/713; A61P 35/00; C07H 21/04; C12N 15/113 (2021.01)
CPC - A61P 35/00; C12N 2310/122; C12N 2310/14; C12N 2310/141; C12N 2310/531 (2021.08)

According to International Patent Classification (IPC) or to both national classification and IPC

B. FIELDS SEARCHED

Minimum documentation searched (classification system followed by classification symbols)
see Search History document

Documentation searched other than minimum documentation to the extent that such documents are included in the fields searched
see Search History document

Electronic data base consulted during the international search (name of data base and, where practicable, search terms used)
see Search History document

C. DOCUMENTS CONSIDERED TO BE RELEVANT

Category*	Citation of document, with indication, where appropriate, of the relevant passages	Relevant to claim No.
A	PARIS et al. "Targeting the RNA m6A Reader YTHDF2 Selectively Compromises Cancer Stem Cells in Acute Myeloid Leukemia," Cell Stem Cell, 25 April 2019 (02.04.2019), Vol. 25, No. 1, Pgs. 137-148. entire document	1-10, 12-14
A	US 2018/0195067 A1 (BETH ISRAEL DEACONESS MEDICAL CENTER) 12 July 2018 (12.07.2018) entire document	1-10, 12-14
P, A	WO 2021/076617 A1 (THE REGENTS OF THE UNIVERSITY OF CALIFORNIA et al) 22 April 2021 (22.04.2021) entire document	1-10, 12-14
P, A	DIXIT et al."The RNA m6A Reader YTHDF2 Maintains Oncogene Expression and Is a Targetable Dependency in Glioblastoma Stem Cells," Cancer Discovery, 06 October 2020 (06.10.2020), Vol. 11, No., 2, Pgs. 1-38. entire document	1-10, 12-14
P, A	EINSTEIN et al. "Inhibition of YTHDF2 triggers proteotoxic cell death in MYC-driven breast cancer," Molecular Cell, 02 July 2021 (02.07.2021), Vol. 81, No. 15, Pgs. 3048-3064. entire document	1-10, 12-14

☐ Further documents are listed in the continuation of Box C. ☐ See patent family annex.

* Special categories of cited documents:
"A" document defining the general state of the art which is not considered to be of particular relevance
"D" document cited by the applicant in the international application
"E" earlier application or patent but published on or after the international filing date
"L" document which may throw doubts on priority claim(s) or which is cited to establish the publication date of another citation or other special reason (as specified)
"O" document referring to an oral disclosure, use, exhibition or other means
"P" document published prior to the international filing date but later than the priority date claimed
"T" later document published after the international filing date or priority date and not in conflict with the application but cited to understand the principle or theory underlying the invention
"X" document of particular relevance; the claimed invention cannot be considered novel or cannot be considered to involve an inventive step when the document is taken alone
"Y" document of particular relevance; the claimed invention cannot be considered to involve an inventive step when the document is combined with one or more other such documents, such combination being obvious to a person skilled in the art
"&" document member of the same patent family

Date of the actual completion of the international search	Date of mailing of the international search report
10 November 2021	DEC 20 2021
Name and mailing address of the ISA/US Mail Stop PCT, Attn: ISA/US, Commissioner for Patents P.O. Box 1450, Alexandria, VA 22313-1450 Facsimile No. 571-273-8300	Authorized officer Harry Kim Telephone No. PCT Helpdesk: 571-272-4300

INTERNATIONAL SEARCH REPORT

International application No.
PCT/US2021/048208

Box No. II Observations where certain claims were found unsearchable (Continuation of item 2 of first sheet)

This international search report has not been established in respect of certain claims under Article 17(2)(a) for the following reasons:

1. ☐ Claims Nos.:
because they relate to subject matter not required to be searched by this Authority, namely:

2. ☐ Claims Nos.:
because they relate to parts of the international application that do not comply with the prescribed requirements to such an extent that no meaningful international search can be carried out, specifically:

3. ☒ Claims Nos.: 11
because they are dependent claims and are not drafted in accordance with the second and third sentences of Rule 6.4(a).

Box No. III Observations where unity of invention is lacking (Continuation of item 3 of first sheet)

This International Searching Authority found multiple inventions in this international application, as follows:

1. ☐ As all required additional search fees were timely paid by the applicant, this international search report covers all searchable claims.

2. ☐ As all searchable claims could be searched without effort justifying additional fees, this Authority did not invite payment of additional fees.

3. ☐ As only some of the required additional search fees were timely paid by the applicant, this international search report covers only those claims for which fees were paid, specifically claims Nos.:

4. ☐ No required additional search fees were timely paid by the applicant. Consequently, this international search report is restricted to the invention first mentioned in the claims; it is covered by claims Nos.:

Remark on Protest

☐ The additional search fees were accompanied by the applicant's protest and, where applicable, the payment of a protest fee.

☐ The additional search fees were accompanied by the applicant's protest but the applicable protest fee was not paid within the time limit specified in the invitation.

☐ No protest accompanied the payment of additional search fees.